106

EVALUATION OF PRECIPITATION MODIFICATION EXPERIMENTS FROM PRECIPITATION RATE MEASUREMENTS

Prepared by

F. A. Huff, W. L. Shipp, and P. T. Schickedanz
Illinois State Water Survey
Urbana, Illinois

FINAL REPORT

Contract INT 14-06-D-6575

Sponsored by

U. S. Department of Interior
Bureau of Reclamation
Office of Atmospheric Water Resources

April 30, 1969

CONTENTS

ILLUSTRATIONS

TABLES

ACKNOWLEDGMENTS

This research program was carried out under the general direction of G. E. Stout, Head, Atmospheric Sciences Section. Robert Sinclair merits special credit for development of numerous computer programs used in the various studies. Marvin Clevenger was responsible for computer processing of the data. Dr. J. C. Neill was consulted on statistical problems. Most of the routine analyses were accomplished by Marian Adair, Elmer Schlessman, and Donald Satterfield. Mrs. W. L. Busch assisted in the statistical analyses.

KEYWORDS AND DESCRIPTORS

1. Rainfall Rate
2. Weather Modification
3. Time Distribution of Rainfall Rates
4. Space Distribution of Rainfall Rates
5. Rainfall Rate Sampling
6. Rainfall Rate Climatology

ABSTRACT

An investigation of the natural time and space characteristics of 1-minute rainfall rates in warm season storms of the Midwest was made. The potential applicability of rate distributions in the verification of cloud seeding effects was evaluated from the analytical results within the limits permitted by the statistical sample. Analyses were based upon a 50-storm sample of 1-minute amounts collected with two dense networks of raingages on areas of 60 mi^2 and 100 mi^2 during 1951-1953. Attention was given to the effects of rain type, synoptic storm type, and other meteorological parameters on the time-space distributions. Time characteristics were defined primarily through the development of storm time distribution models, calculation of sequential variability, and determination of lag correlation relations. Spatial distribution characteristics were based largely upon studies of area-depth relations, spatial correlation patterns, and relative variability calculations. Statistical theory and testing were applied to the data to obtain estimates of sampling time required to verify cloud seeding effects through use of three experimental designs and two statistical tests, and based upon various assumed changes in rainfall rate resulting from seeding. Overall, it was concluded that rainfall rate may be one of several useful rainfall measurement tools in weather modification evaluations, but that, by itself, it is not very effective unless pronounced changes in the rate structure are produced by seeding.

INTRODUCTION

On May 1, 1968, the Illinois State Water Survey entered into a 12-month contract with the Bureau of Reclamation. Under this contract, research has been conducted on the natural space and time distribution of rainfall rates in warm season storms and the potential utilization of rainfall rate measurements in the verification of cloud seeding effects.

One of the key problems encountered in precipitation modification projects has been the evaluation of the seeding effects. A logical expectation in cloud seeding undertaken to stimulate the production of surface rainfall is substantial modification of the natural rainfall rate; that is, the rate that would have occurred in the given meteorological situation in the absence of artificial stimulation. Thus, the utilization of rainfall rate measurements in the verification of seeding effects is highly desirable. However, this cannot be done until a much better understanding of the space and time distribution characteristics of rainfall rate under natural conditions is achieved and the various rate parameters are evaluated with respect to their applicability in weather modification verification.

The 1-year research under this contract was undertaken specifically as a pilot study to obtain first approximations of the space-time properties of rainfall rate in midwestern storms and to determine their potential applicability in weather modification experiments. The pilot study was based upon an extensive set of 1-minute rainfall amounts obtained with two dense raingage networks. Although midwestern data were employed in the study, the methods, techniques and general findings should be applicable throughout the United States.

Data Used in Studies

The two dense networks are shown in Fig. 1. The upper illustration is a 33-gage network in 60 mi^2 operated on the Goose Creek watershed in 1951. A total of 21 storms during the warm season was sampled on this network in conjunction with the radar-rainfall studies being carried on at that time.

The lower illustration in Fig. 1 shows a 50-gage network on 100 mi^2 operated during 1952-1953. This was an expansion of the 1951 network and provided a sample of 29 storms in which 3142 minutes of rain were included. This network was subdivided to provide information on areas of 25 and 50 mi^2. Furthermore, data from the most central gage were used to develop point rainfall relations for comparison with the areal distribution relations. This 29-storm sample was used in the majority of the studies described in this report.

An enlarged (12.6-inch) orifice and 6-hour gears were used on the recording gages during 1951-1953. This provided measurement accuracy of point and areal mean rainfall rates, spatial patterns, and time distributions not attainable with standard orifice gages operating with daily or weekly recording charts (Huff and Neill, 1957).

In the time distribution studies, limited use was made also of data from the East Central Illinois Network of 49 standard-type recording gages in 400 mi^2. This network was operated in the 1955-1966 period and was located in the same general region as the Goose Creek Networks of Fig. 1 (Huff, 1967). All networks were located in flat rural areas.

In several studies described in this report, the data for the 60 mi^2 in 1951 and the 50 mi^2 subarea in 1952-1953 have been combined. In such cases, the sampling area is referred to as 50-60 mi^2.

Approach to Problem

Major emphasis was placed upon development of quantitative measures of the time and space distributions of 1-minute rainfall rates in warm season, convective storms. In these studies, the effects of rainfall type, synoptic storm type, storm mean rainfall, storm duration, and other factors upon the distribution of rates were evaluated to the extent permitted by the data.

In the time distribution studies, non-dimensional time distribution models of storm rainfall were developed in which cumulative percent of total storm rainfall was related to cumulative percent of storm time. These models were expressed in the form of families of probability curves to reveal both interstorm variability and individual storm characteristics under average and extreme conditions for basic storm types.

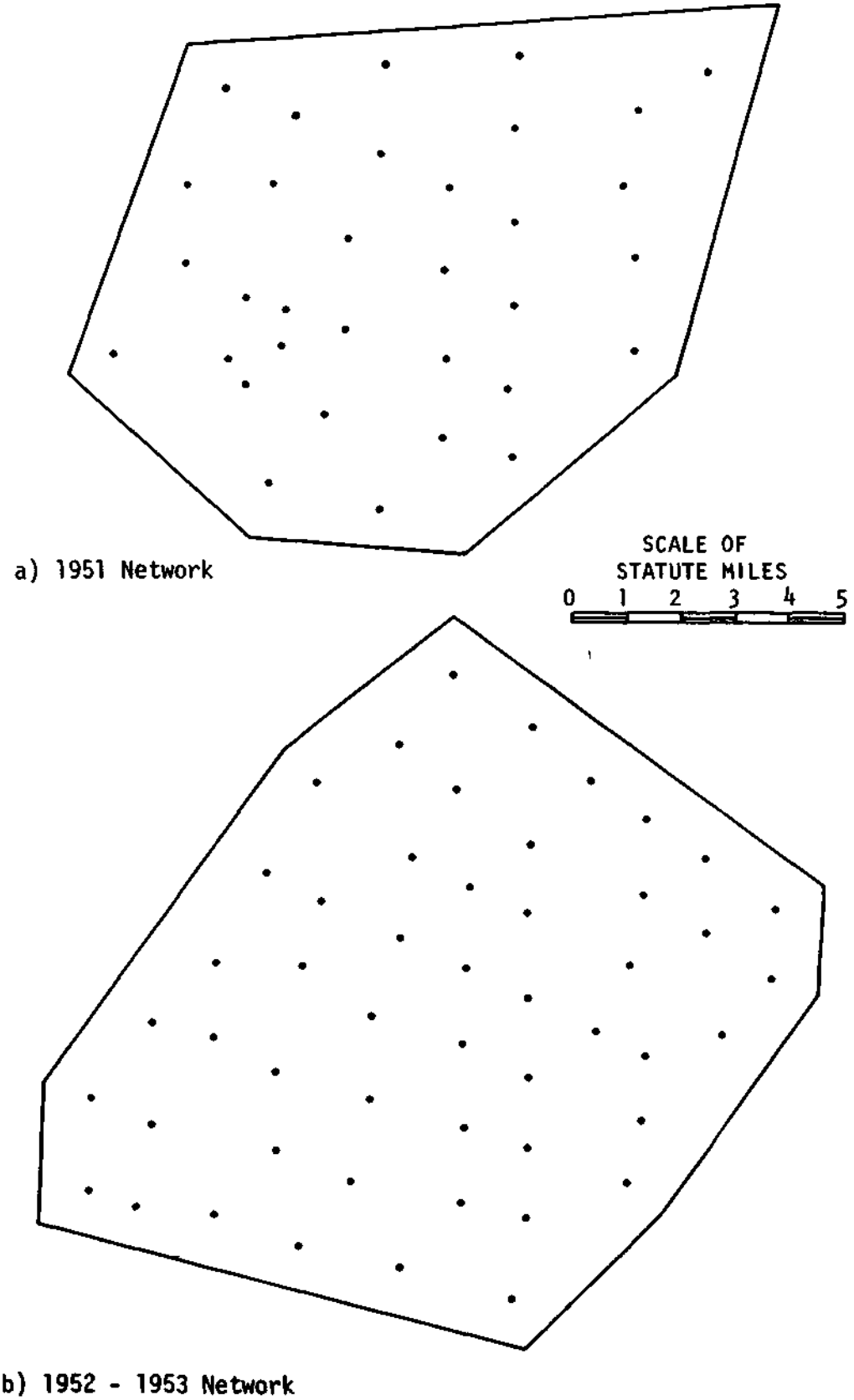

Figure 1. Raingage networks

Further definition of the time distribution of rainfall rates was obtained through determination of the sequential variability in storms and from lag correlation relations. The sequential variability provides a quantitative measure of the rate of change of rain intensity with time in storms, and takes into account both the magnitude and sequence of rates in characterizing the time distribution of rainfall intensity. Lag correlation analyses were performed to define further the time distribution characteristics and to ascertain whether the rainfall rate structure under natural conditions shows cyclic or oscillatory properties within storms.

In the spatial distribution studies, use was made of area-depth relations, spatial correlation patterns, rainfall rate variations with distance, and spatial relative variability calculations in defining spatial characteristics. Area-depth curves of average and enveloping rainfall rate, a basic tool in hydrology, were studied in considerable detail. These two types of curves provide a mathematical expression of the rainfall gradient, maximum point rainfall, volumetric distribution over the sampling region, and information relative to the type and degree of skewness in the rainfall distribution (Huff, 1968). The area-depth approach also provided a means of establishing models of areal rainfall rate distribution.

Spatial correlation patterns yielded pertinent information on the stability of the rate distribution with increasing distance and on sampling requirements for the definition of rate patterns. Analyses of the variation of point rainfall with distance provided a quantitative definition of spatial variability and additional information on sampling requirements. The spatial relative variability also provided a means of quantitatively expressing the spatial variability.

Rainfall rate profiles were studied to obtain additional quantitative measures of the space-time distribution characteristics of rainfall rate. A profile portrays the rate distribution along a line of sight through a storm. The profile for any minute provides a measure of the spatial variability, and the change along a profile from minute-to-minute aids in definition of the time variability.

Other investigations of rainfall rate characteristics resulted in the development of curves relating rate, percent of storm rainfall, and percent of

storms. In order to obtain information of sampling requirements for the measurement of areal mean rainfall rates with various degrees of accuracy, empirical relations were developed in which sampling error, gage density, and areal mean rate were related.

Representativeness of 29-Storm Sample

In a majority of the analyses performed in this research project, results were based upon the 29-storm sample obtained on the 100 mi^2 network in 1952-1953. This sample contained 3142 minutes having rainfall within the network. As stressed throughout this report, the 29-storm sample for 1952-1953 and the 50-storm sample on 50-60 mi^2 in 1951-1953 provide much-needed quantitative information on the space and time characteristics of rainfall rates, but the results must be considered first approximations in view of the sampling limitations.

Examination of the 29-storm sample for 1952-1953 indicated that it conformed quite well to the climatic distribution of warm season storms. This is illustrated by several comparisons with statistics obtained from a 12-year sample on 100 mi^2 in the same climatic area (Huff, 1969) during 1955-1966. Thus, the 1952-1953 sample shows 21% of the storms with 100 mi2 mean rainfall equalling or exceeding 0.50 inch, 42% with means in the range from 0.11 to 0.49 inch, and 38% with means equal to or less than 0.10 inch. Comparable statistics for the 12-year sample of 675 storms in the warm season (May-September) are 20%, 41%, and 40%, respectively. In the 12-year sample, 88% of the storms were thunderstorms and/or rainshowers compared with 93% in the 1952-1953 limited sample of 29 storms. Synoptically, 69% of the 1952-1953 storms were frontal or squall-line types compared with 66% in the 12-year sample. Air mass storms accounted for 25% of the cases in 1955-1966 and 21% in 1952-1953. Low center passages were associated with 10% of the 1952-1953 storms and 9% of the 12-year sample.

In an effort to obtain a more definite estimate of the representativeness of the 29-storm sample, two analyses were performed. In the first, standard randomization procedures were employed to select two samples of 14 storms each from the 29-storm sample. This selection procedure was repeated 10 times. Comparisons were then made between the frequency distributions of rainfall rate

in the 14-storm samples and those in the 29-storm sample. These comparisons were made for point rainfall rates at gage 29 near the network center and for the 100 mi^2 mean rates.

Results of this analysis are summarized in Tables 1 and 2. In these tables, equivalent frequency values are shown for the two 14-storm sets (Groups A and B) and the 29-storm sample. These values were obtained from frequency curves constructed from the data in each case. Comparisons are shown for (1) the first of the 10 random selections made when dividing the 29-storm sample into two 14-storm samples, and (2) 10-selection averages of the two 14-storm samples.

Interpretation of the results is illustrated by the following examples. In Table 1 for 100 mi^2, the frequency distribution of 1-minute rates for the 29-storm sample shows 92% of the total minutes with rainfall rates equalling or exceeding 0.01 inch/hour. This decreases gradually to 20% of the minutes for rates of 0.25 inch/hour or more and only 4% of the minutes for 1 inch or greater rates. Equivalent values obtained from the Group A curve in the first randomization were 91%, 19%, and 5%, respectively. For the 10-selection average in Group A, the equivalent percentages were 92, 20, and 5.

Table 1 shows only small differences between the 14-storm frequency distributions of rainfall rates and those for the 29 storms. Thus, the frequency distribution of rates became relatively stable after 14 randomly selected storms were sampled. This suggests that the quantitative estimates obtained from the 29-storm sample provide reasonably accurate definitions of the time distribution characteristics of rainfall rate in warm season storms.

Table 2 indicates larger differences between the 14-storm and 29-storm samples when point rainfall is the measurement considered. Consequently, point relationships developed from the 29-storm sample must be considered less reliable than the areal relations. However, at the relatively heavy rainfall rates, the 14—storm and 29-storm point differences are small.

In another examination of the representativeness of the 29-storm sample, spatial correlation patterns were compared between two 14-storm samples selected by randomization procedures and the 29-storm sample on 100 mi^2. This provides a measure of space distribution differences in these samples. Results

Table 1. Comparison of mean rainfall rate frequency distributions in 14- and 29-storm samples on 100 mi^2.

	Percentages of minutes in which given rate (inch/hour) was equalled or exceeded							
	0.01	0.05	0.10	0.25	0.50	0.75	1.00	1.50
29 storms	92	65	44	20	12	8	4	1+
14-storm groups								
Group A - first selection	91	63	44	19	11	8	5	3
Group B - first selection	93	69	46	20	11	7	4	1-
Group A - 10-selection average	92	65	45	20	12	8	5	1+
Group B - 10-selection average	92	66	46	19	11	8	4	1+

Table 2. Comparison of point rainfall rate frequency distributions in 14- and 29-storm samples.

	Percentages of minutes in which given rate (inch/hour) was equalled or exceeded							
	0.10	0.20	0.30	0.50	1.00	2.00	3.00	5.00
29 storms	76	40	28	17	12	6	3	0.5
14-storm groups								
Group A - first selection	80	50	39	28	19	8	4	0.6
Group B - First selection	77	38	26	20	12	4	2	0.3
Group A - 10-selection average	74	46	35	24	15	6	3	0.4
Group B - 10-selection average	78	43	32	22	13	5	2	0.3

are summarized in Table 3 which shows average correlation coefficients and variance explained (%) in each sample about the most central gage (No. 29).

Relatively small differences are shown between the 14-storm and 29-storm samples in Table 3. The variance explained by the correlation coefficients differs by less than 10% at all distances between the three samples. Thus, the correlation pattern changed very little between the 14-storm and 29-storm samples. This is evidence that the 29-storm sample provides reliable estimates of the spatial distribution characteristics of rainfall rates in convective storms.

Numerous other analyses could have been performed to test further the representativeness of the 29-storm sample, but time and personnel limitations prevented further concentration on this subject. The results of the two tests performed are encouraging with respect to the reliability of the 29-storm sample in characterizing the space and time distribution characteristics of rainfall rates in warm season storms.

Table 3. Comparison between 14-storm and 29-storm correlation patterns about network central gage.

Distance Distance (miles)	Correlation coefficient for given sample: 14 storms Group A	14 storms Group B	29 storms
1	0.73	0.75	0.78
2	0.54	0.59	0.60
3	0.42	0.50	0.48
4	0.36	0.44	0.40
5	0.32	0.39	0.35
6	0.30	0.33	0.31
	Variance explained (%)		
1	53	56	61
2	29	35	36
3	18	25	23
4	13	19	16
5	10	15	12
6	9	11	10

PART I

TIME DISTRIBUTION STUDIES

TIME DISTRIBUTION MODELS OF STORM RAINFALL

Previous Research

In an earlier study, Huff (1967) used data from 261 storms on a dense raingage network of 400 mi^2 in east central Illinois to derive time distribution relations. The time distributions were expressed as cumulative percentages of storm rainfall and storm duration to enable valid comparisons between storms and to simplify analyses and presentation of data. Relations were developed for point rainfall and for areal mean rainfall on areas of 50 to 400 mi^2. Rainfall distributions were grouped according to whether the heaviest rainfall occurred in the first, second, third, or fourth quarter of a storm.

Other analyses showed storm duration and storm mean rainfall explaining only a small portion of the variance between storms, when the time distributions were classified by quartile and expressed as percentages of total storm duration and rainfall. Part of the effects of duration and mean rainfall are absorbed in the quartile groupings, which showed a trend for the longer, heavier storms to dominate the fourth-quartile grouping, whereas short-duration storms accounted for a major portion of the first and second quartile groups. As a result of these analyses, it was considered more logical, as a first approximation, to determine average rainfall distributions for point and areal mean rainfall by quartile group only.

Areal groupings showed only small changes in the time distribution with increasing size of sampling area. Thus, an average relationship for areas of 50 to 400 mi^2 combined was determined, and specific areas distributions were expressed as departures from the average in presenting the results.

The time distributions were expressed in probability terms because of the great variability in the characteristics of the distribution from storm to storm. Numerous factors contribute to the storm variance, but no single parameter dictates the characteristics of the distribution. Among the factors are the stage of development of the storm, the size and complexity of the storm system, rainfall type, synoptic storm type, location of the sampling area with respect to the storm center, and the movement of the storm system across the sampling region. Probability distributions allow selection of a time distribution most appropriate for a particular application.

In the study discussed above, smoothed time distributions were obtained from 30-minute rainfall totals throughout each storm. Further, the relations were based upon heavy storms in which areal mean rainfall exceeded 0.50 inch and/or point amounts of 1 inch or more were recorded in the sampling area. Thus, the applicability of the results to storms of lesser intensity and to those in which the rainfall was accumulated over shorter intervals of time was questionable. Therefore, it was considered desirable to investigate the time distribution characteristics further through use of the 50-storm sample of 1-minute rainfall amounts available for the 1951-1953 period.

Rainfall Rate Distributions

Investigation showed 12, 22, 11, and 5 storms, respectively, in the first, second, third, and fourth quartile types. These data were used to calculate average time distributions for the 50-60 mi^2 sampling areas from the 1-minute rainfall amounts in each storm.

The 5-storm, fourth quartile sample was not considered adequate to derive an average distribution. The three average distributions derived from the 1-minute data on the Goose Creek Network were then compared with those for 50 mi^2 obtained from the 261-storm sample of 30-minute amounts on the East Central Illinois Network. Results are summarized in Table 4.

As shown in this table, time distributions for second quartile storms from both studies are almost identical, and except at the 10% value, are nearly equal in first quartile storms. With the third quartile storms, there are some significant differences in the middle parts of the storm models. Overall, however, there appears to be excellent agreement when one considers the relatively small sample of 1-minute storm data. Therefore, it was concluded that the results of the earlier study of 261 storms are applicable, as a first approximation, for deriving the time distribution characteristics of all types of storms in which unstable types of rain predominate. The large sample of 261 storms provides a more reliable determination of model time distributions with various probabilities of occurrence.

Time Distribution Models

Statistical models of time distributions for each quartile are shown in Figs. 2 to 5 for areas of 50 to 400 mi^2 combined. These are considered typical

Table 4. Comparison of average time distributions on Goose Creek and East Central Illinois Networks.

Network		Number of storms	Cumulative percent of mean rainfall for given percent of storm time										
			5	10	20	30	40	50	60	70	80	90	95
							First Quartile Storms						
East Central	Ill.	95	5	20	47	68	78	84	89	93	97	99	99+
Goose Creek		12	4	11	46	68	79	85	90	93	96	98	99
							Second Quartile Storms						
East Central	Ill.	69	1	4	13	29	51	71	83	92	96	99	99+
Goose Creek		22	1	4	12	29	55	71	83	90	95	98	99
							Third Quartile Storms						
East Central	Ill.	63	2	4	10	14	17	27	50	74	90	97	99
Goose Creek		11	1	2	5	10	20	37	63	83	92	97	99

of midwestern, warm season storms or cold season storms in which unstable rainfall types are the major rain producers. Combining all areas, 33%, 33%, 23%, and 11%, respectively, of the storms were classified as first, second, third, and fourth quartile storms. No distinct trend in quartile types was found with increasing area, although there was considerable fluctuation between areas. The statistical models are smooth curves reflecting the average rainfall distribution with time and, therefore, do not exhibit the burst characteristics of a mass rainfall curve. Probability levels from 10% to 90% are shown, but the 50% level (median) has been stressed by a heavier line, since it is probably the most useful statistic.

Interpretation of the curves can be illustrated by referring to the first quartile distributions in Fig. 2. The 10% curve is typical of storms in which the rainfall is concentrated in an unusually short portion of a storm. It indicates a chance of 1 in 10 that a given first quartile storm will have at least 89% of its rainfall in the first quarter of the storm period and over 95% in the first one-half of the storm. The 50% curve shows 63% and 86% of the rainfall at 25% and 50% of the storm period. The 90% curve reflects an unusually uniform distribution for first quartile storms. It may be interpreted as the distribution that will occur in 10% or less of the storms. Thus, this curve shows that in 10% of the storms, 39% or less of the rain will occur in the first quarter of the storm and 57% in the first one-half of the storm.

The curves at the various probability levels reveal characteristics of certain storm types. For example, the 10% probability curve of first quartile storms discussed above is most frequently associated with relatively short-duration storms, such as the passage of an intense, prefrontal squall line in which light rain falls from the middle cloud deck system for substantial periods following the major rain bursts. Similarly, the distribution at the 90% level is most likely to be associated with longer-duration storms, in which the rain is more evenly distributed during the storm period, and is often dominated by a series of rainshowers or a combination of showers and steady rain.

In the fourth quartile storms, the distribution at the 10% level is common to the passage of a large-scale weather system with warm-frontal rainfall at the start of the storm and more intense cold-frontal rainfall near the end. The 90% distribution may be associated with the approach and passage of a low

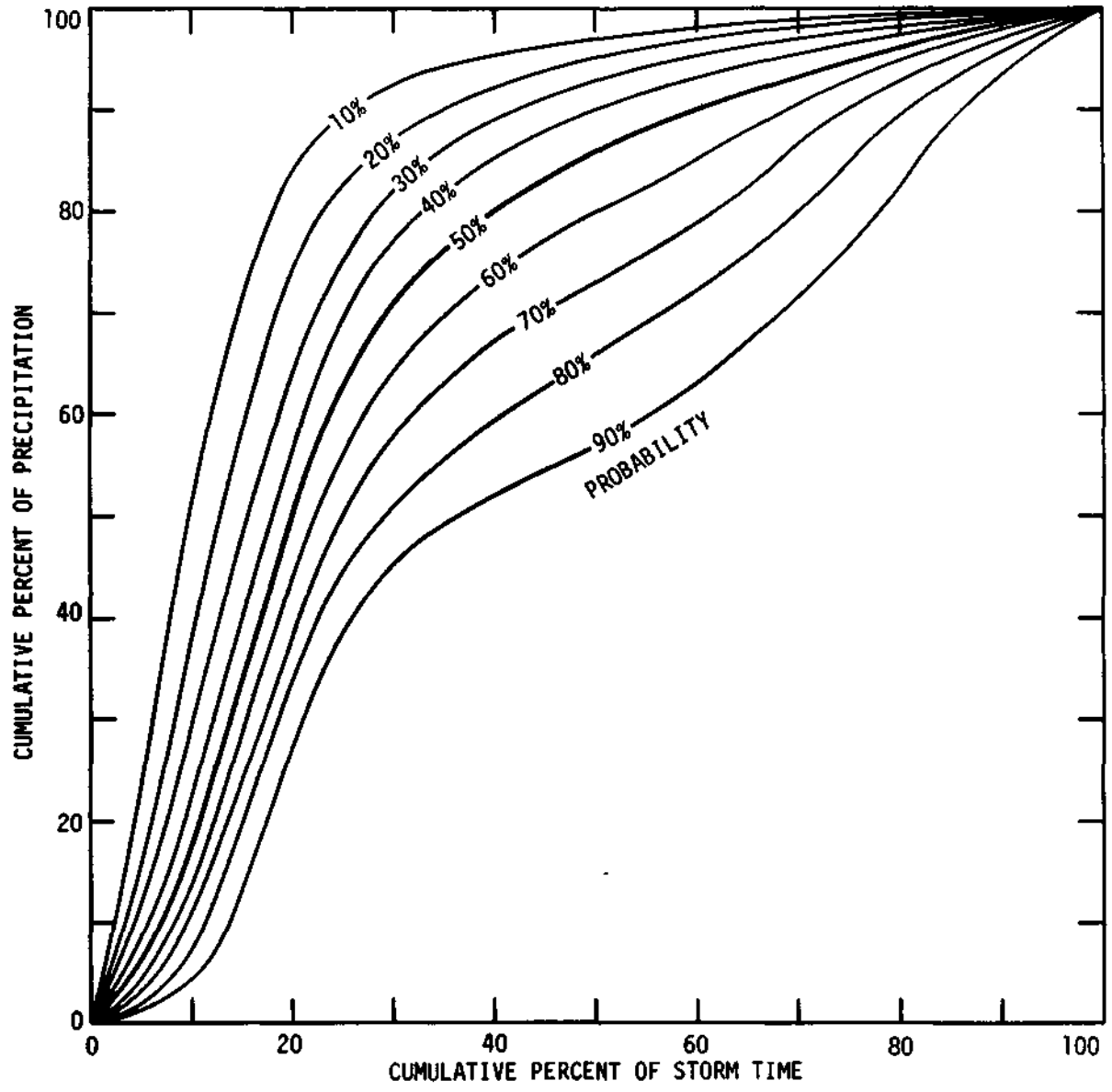

Figure 2. Time distribution of first quartile storms

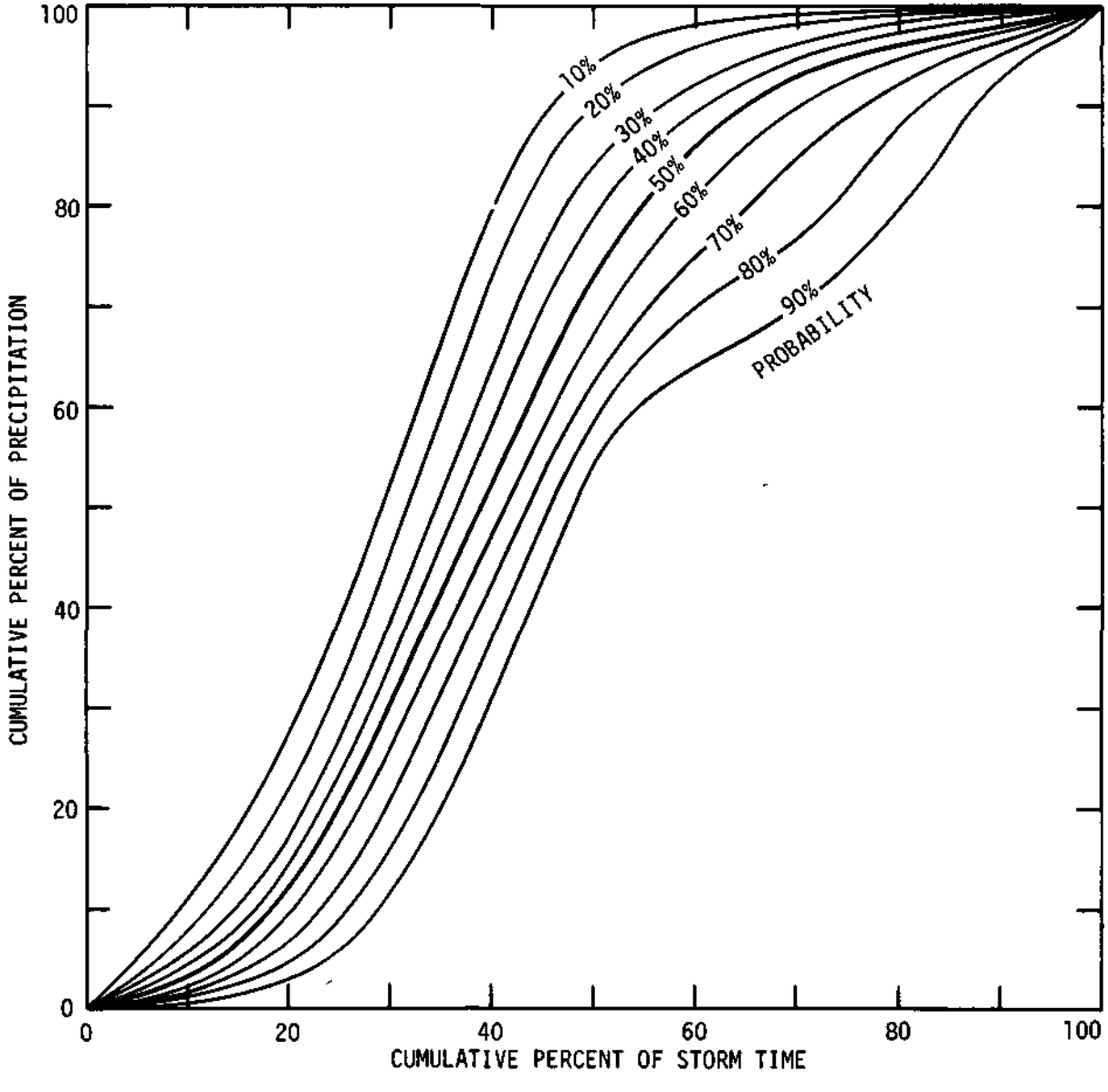

Figure 3. Time distribution of second quartite storms

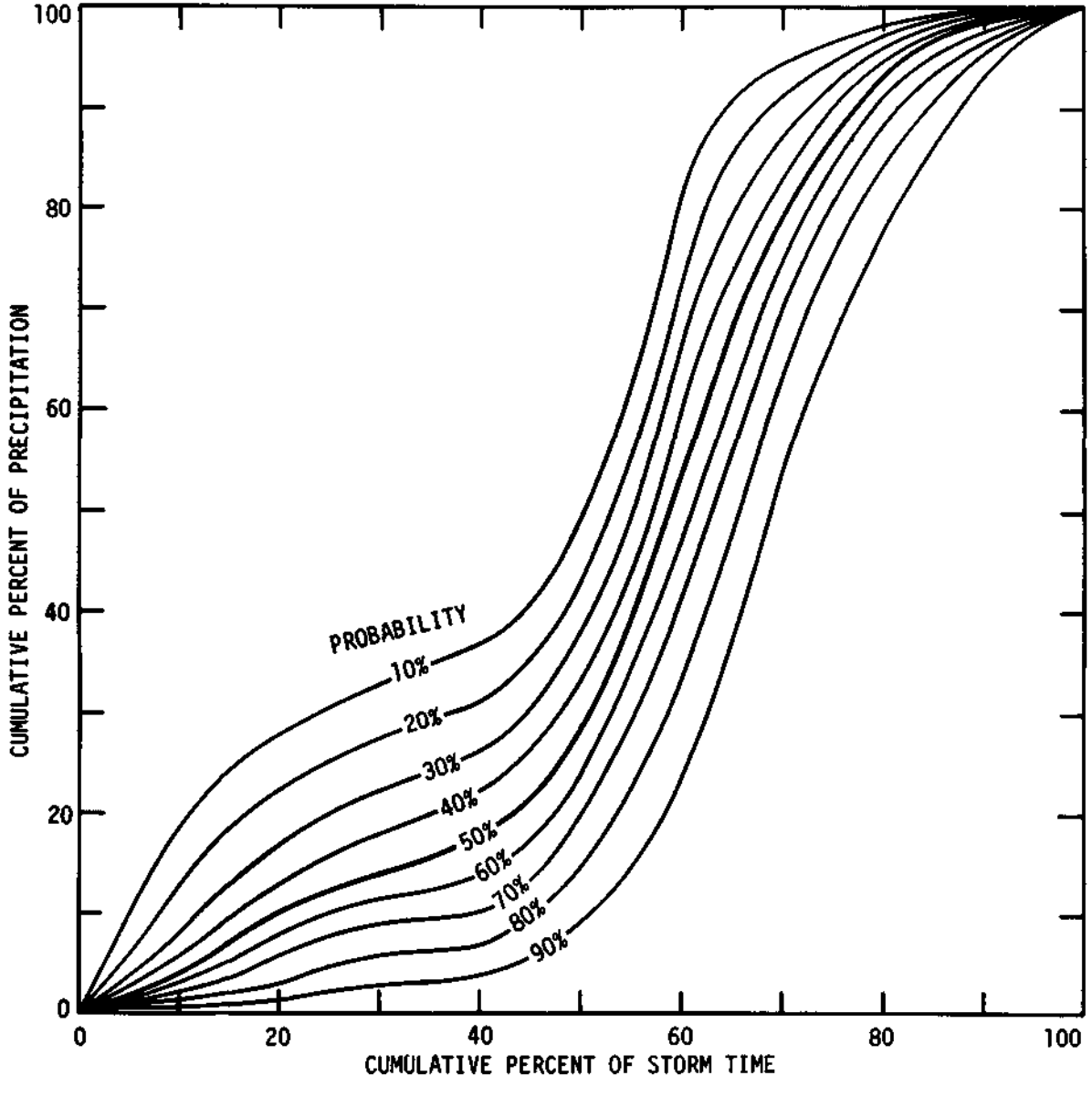

Figure 4. Time distribution of third quartile storms

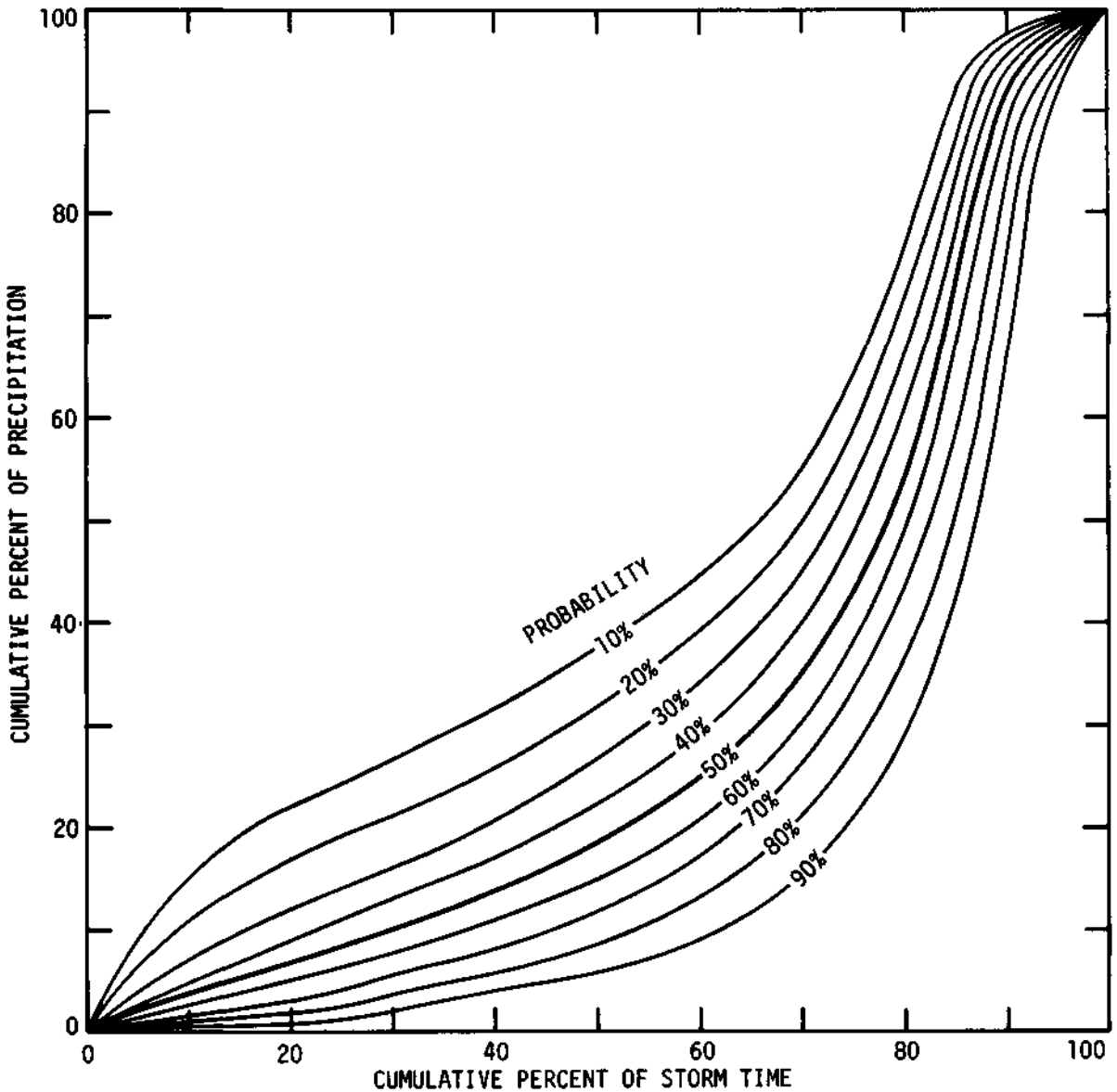

Figure 5. Time distribution of fourth quartile storms

pressure center through or near the sampling region, when light rainfall may precede the center passage for several hours and the rainfall intensity maximizes as the center passes.

In concluding the discussion of time distribution characteristics, it is emphasized that the relations presented here are empirically derived. They are not submitted as exact mathematical relationships, but rather as first approximations of a hydrometeorological parameter for which quantitative knowledge is sparse.

Figs. 6 and 7 provide additional information on the time characteristics of storm rainfall. Fig. 6 shows median quartile curves for point rainfall and Fig. 7 shows how the first quartile point curve differs from that for the largest area studied (400 mi^2). The point curve indicates larger percentages of the total rainfall at the start of storms. This tendency appears logical for rain on smaller areas. If one assumes a storm of given intensity and areal extent moving across two areas of appreciably different size, the smaller area will receive a larger percentage of its areal mean rainfall in the early part of the rain period, particularly if the storm is smaller than the network in areal extent. Table 5 illustrates the differences between the average curve for 50 to 400 mi^2 and specific areas in first quartile storms.

Table 5. Differences between average curve and specific areas for 50% probability level in first-quartile storms.

Area (mi^2)	Difference (%) for given cumulative percent of storm duration								
	10	20	30	40	50	60	70	80	90
Point	-9	-1	+5	+6	+6	+6	+5	+4	+3
50	-2	+3	+3	+2	+2	+2	+1	0	0
100	-2	-3	0	0	0	0	0	0	0
200	-2	-3	-2	-1	-1	0	0	0	0
400	+6	+4	-1	-2	-2	-1	-1	0	0

Conclusions

The time distribution characteristics of storm rainfall in midwestern warm season storms have been defined quantitatively in considerable detail by the statistical models presented in this study. Application of these models

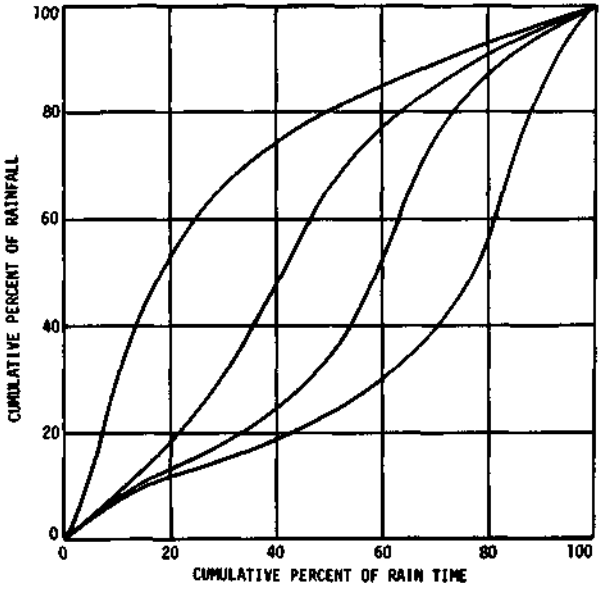

Figure 6. Median quartile curves of point rainfall

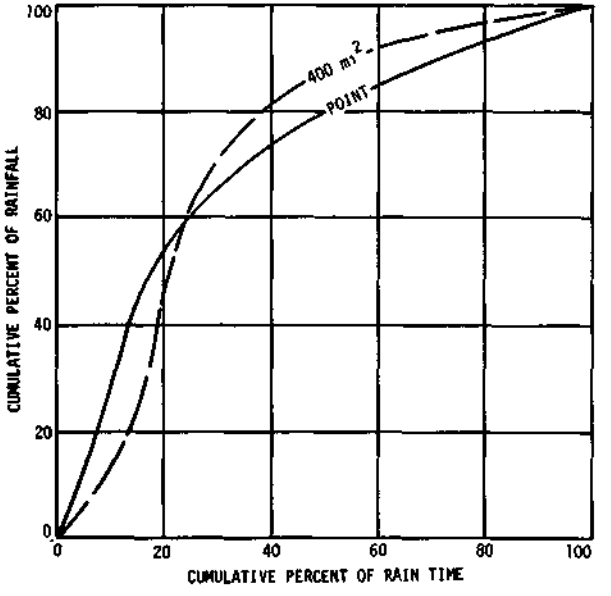

Figure 7. Differences between point and 400 mi^2 curves

as a verification tool in weather modification experiments does not appear promising at this time because of the large variability in storm time distributions that results from multiple causes. That is, the interference level of natural variability is too great for the detection of modest changes resulting from cloud seeding within a reasonable period of experimentation.

SEQUENTIAL VARIABILITY

Approach to Problem

The time rate of change in storm rainfall intensity was investigated through calculation of the sequential variability (Conrad and Pollak, 1950) at a point and on areas of 25, 50, and 100 mi^2. As employed in the Illinois study, the sequential variability $(\overline{D})$ was obtained by dividing the summation of consecutive 1-minute differences in rainfall rate by N-l, where N is the number of minutes of rainfall in the storm. The sequential variability takes account of both magnitude and sequence of rainfall rates in characterizing the time distribution of rainfall intensity. Therefore, it was considered preferable to the standard deviation of rainfall intensity, a more commonly used measure of the time variability which evaluates only magnitude of the items in a time series. Knowledge of the time rate of change of rainfall intensity provides useful background information for weather modification experiments, especially those intended to change the natural time distribution properties.

The standard deviation (S_d) of the 1-minute differences about $\overline{D}$ was then calculated. Dividing S_d by $\overline{D}$ and multiplying by 100 provides a measure of the time relative variability (V_d) which is useful for comparing the sequential variability between storms of similar types. Another definition of the time relative variability (V_{dr}) was obtained by dividing S_d by $\overline{R}$, the average 1-minute rainfall rate for the storm, and again multiplying by 100 to obtain a percentage expression. This expression provides a measure of the effect of overall storm intensity on the sequential variability of rainfall rate. It is a desirable means of defining time relative variability, since $\overline{D}$ and $\overline{R}$ are strongly related, as indicated in Table 6 by their correlation coefficients of 0.97, 0.93, and 0.98 on sampling areas of 25, 50-60, and 100 mi^2, respectively.

Table 6. Correlation of basic time variability parameters.

	Correlation coefficient for given area (mi^2)		
	25	50-60	100
$\bar{R} - \bar{D}$	0.97	0.93	0.98
$\bar{R} - S_r$	0.95	0.88	0.97
$\bar{R} - S_d$	0.90	0.85	0.89
$\bar{D} - S_d$	0.96	0.94	0.93
$S_d - S_r$	0.95	0.96	0.96

For comparison purposes, a third measure of the time relative variability (V_r) was obtained through calculation of the coefficient of variation $(S_r/\bar{R})$ of the 1-minute rates in each storm. Recapitulating, V_d is dependent upon the sequential differences in rainfall rate, V_r is determined strictly by the nonsequential magnitude of the fluctuations in 1-minute rates, whereas V_{dr}, incorporates both the effects of sequential differences and storm intensity on time relative variability.

Results of Analyses

The storm samples for 1951-1953 indicated that $\bar{D}$, V_d, and V_{dr}, the major measures of time variability used in the study, closely approach log normal distributions. This is illustrated in Fig. 8 in which data plots for the 50-storm sample on the combined areas of 50 and 60 mi^2 are shown. An excellent fit is shown for the log normal distribution of V,. Although there is more scatter about the curve of V, , the points appear to form a log normal distribution. There is some tendency for the points to depart from the log normal curve of $\bar{D}$ at the upper end; otherwise the fit is quite satisfactory, expecially considering the relatively small number of storms which may result in considerable sampling error. $\bar{R}$, S_d, and S_r also appeared to be closely approximated by a log normal distribution.

Based on the 50-storm sample, the sequential variability $(\bar{D})$ ranges from 0.13 inch/hour at the 5% level through a median value of 0.026 inch/hour

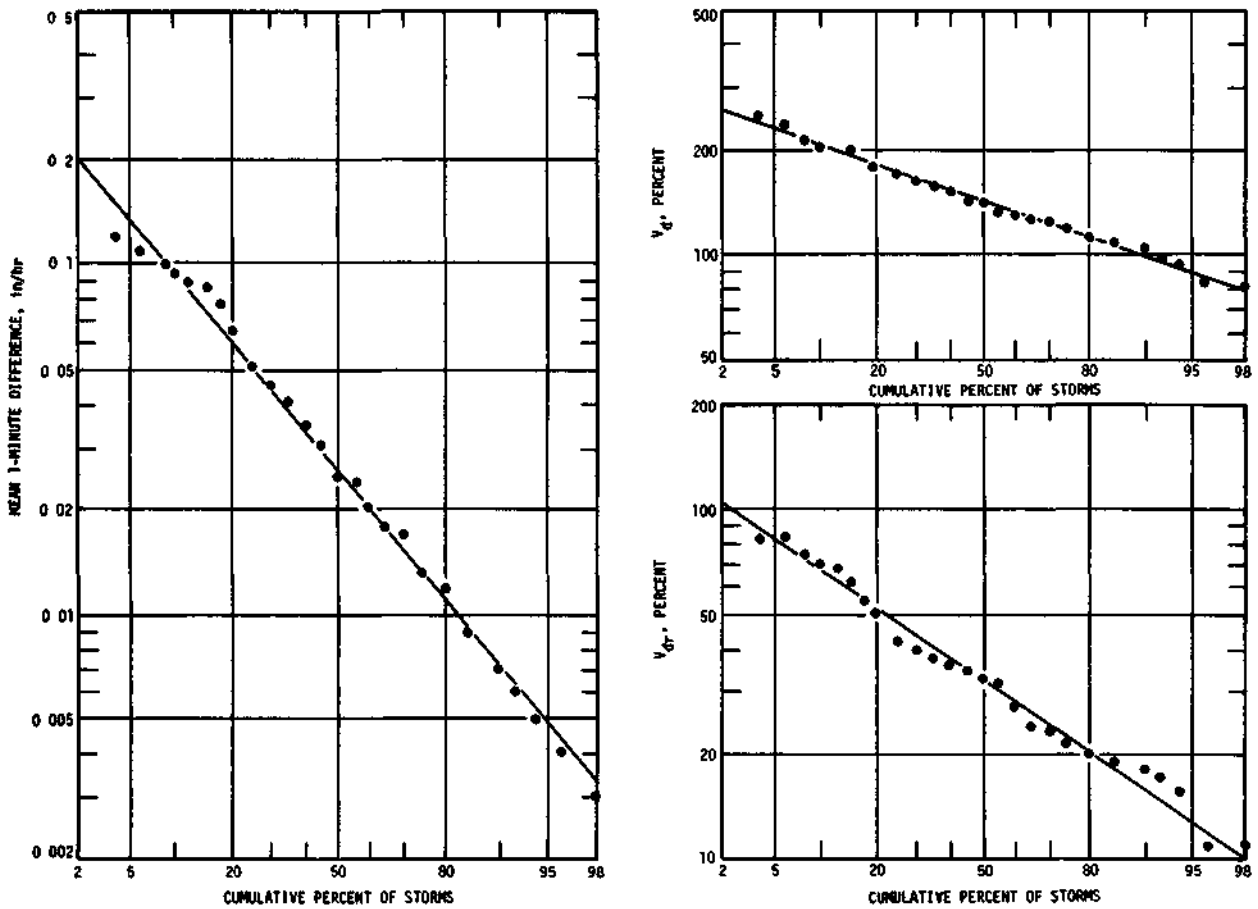

Figure 8. Log normal distributions of $\overline{D}$, V_d, *and* V_{dr}

to 0.005 inch/hour at the 95% probability (Fig. 8). This is a fivefold difference between the median and the 5% probability values.

The distribution of V_d also illustrates well the time variability in rainfall rates in warm season storms. Fig. 8 indicates a median time relative variability of 145%, however, the curve indicates that this percentage may reach as high as 235% or as low as 90% in 5% of the warm season storms.

V_{dr} in Fig. 8 illustrates further how the time variability may change radically between warm season storms. Here, we find a median of 33% which increases to 83% in 5% of the storms and lowers to 13% at the 95% level.

$\bar{D}$, S_d, S_r, V_r, V_d, and V_{dr} were found to vary exponentially with the 1-minute mean rainfall rate in storms. Fig. 9 is a scattergram illustrating the relation between $\bar{R}$ and S_d in 50 storms on the 50 and 60 mi^2 areas during the 1951-1953 sampling period. The trend is quite apparent, but considerable scatter exists about the regression curve. The dashed lines enclose 95% of the values and show a sixfold range between these limits. However, a correlation coefficient of 0.85, explaining 72% of the variance, was obtained between $\bar{R}$ and S_d (Table 6).

Regression curves relating various parameters to $\bar{R}$ on the 50 and 60 mi^2 areas are shown in Figs. 10 and 11 to illustrate the magnitude of the change in time variability with increasing rainfall intensity in warm season storms. Thus, for example, Fig. 11 shows V_{dr}, decreasing from 61% at an areal mean rainfall rate of 0.01 inch/hour to 34% at 0.10 inch/hour and 19% at 1.0 inch/hour.

The preceding discussion has been concerned with the time variability on combined areas of 50 and 60 mi^2 during 1951-1953. Available data from 29 storms for point and areal mean rainfall on areas of 25, 50, and 100 mi^2 during 1952-1953 were analyzed to determine the general effect of size of sampling area on time variability. A strong trend was found for the variability to increase with decreasing area. For example, V_{dr} on 50 mi^2 exceeded the 100 mi^2 value in 28 of the 29 storms, and the 25 mi^2 values also exceeded those on 50 mi^2 in 28 cases.

Interstorm differences in time variability and further definition of the areal effect are shown in Fig. 12. Frequency distributions of $\bar{D}$, V_d, and V_{dr} are shown for point rainfall and each of the three sampling areas used in the study. Also, an average frequency distribution of $\bar{R}$ is shown in Fig. 12,

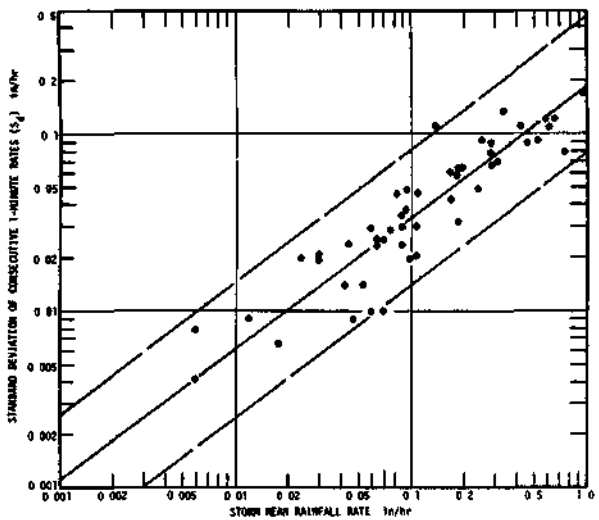

Figure 9. Relation between $\overline{R}$ and S_d in 5O storms

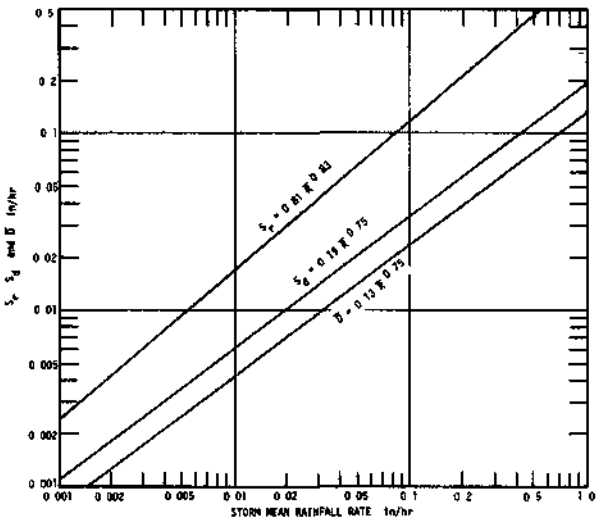

Figure 10. Relations between $\overline{R}$ and $\overline{D}$, S_d, S_r

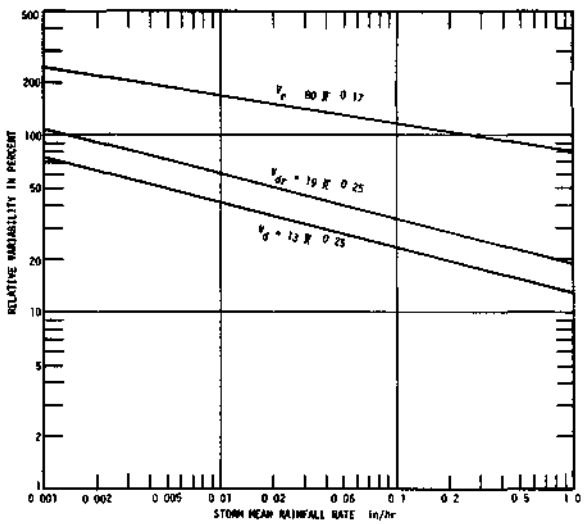

Figure 11. Relations between $\overline{R}$ and V_r, V_d, V_{dr}

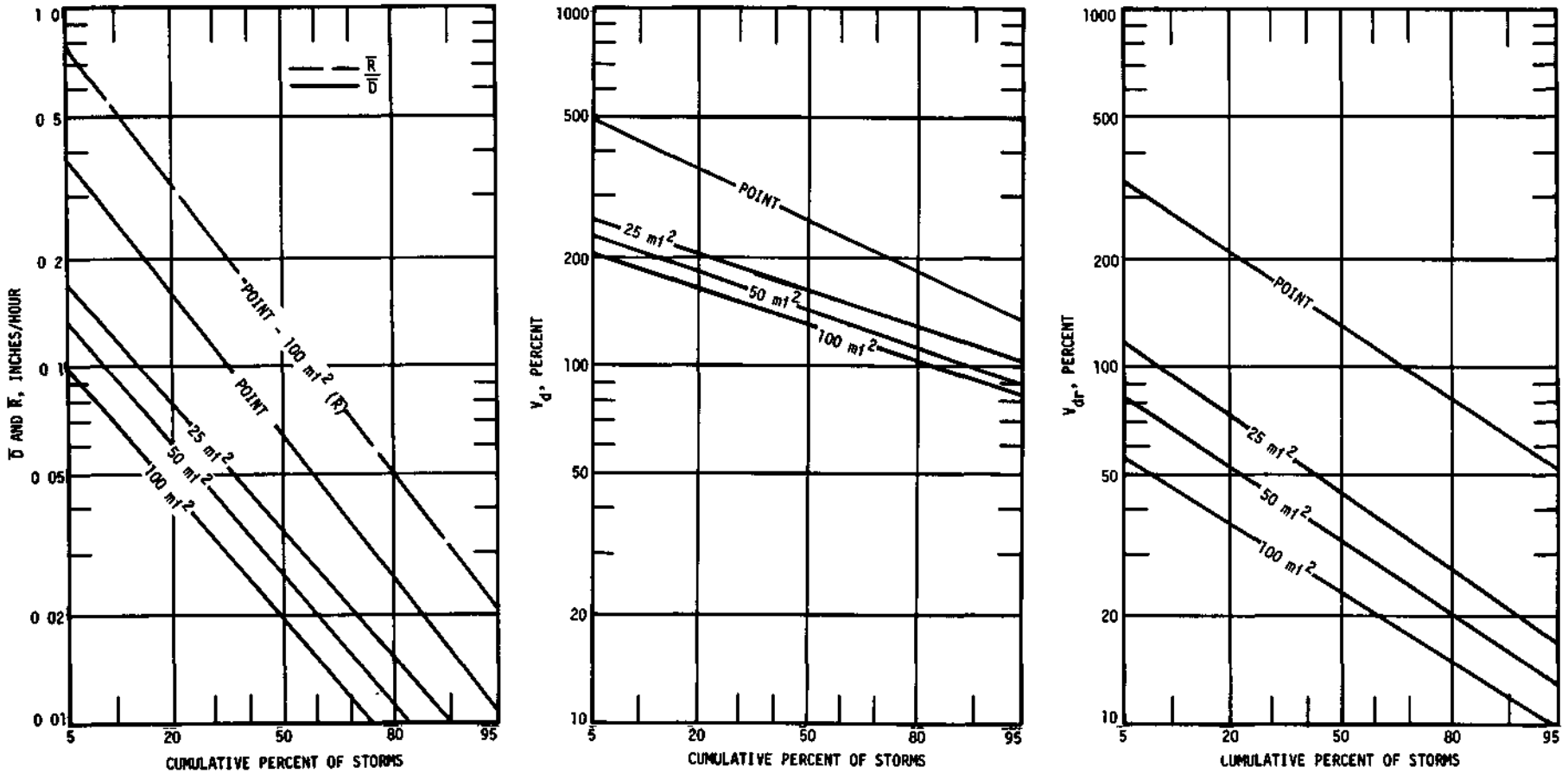

Figure 12. Frequency distributions of $\overline{D}$, V_d, V_{dr}, and $\overline{R}$ in 1952-1953 storms

since only very small differences existed between the distributions at the central point and over the three small areas. Again, it is emphasized that these frequency distributions should be considered only first approximations of the various relationships because of the sample size from which they were derived. Nevertheless, they do provide quantitative information on a subject of sparse knowledge, and, consequently, should be useful in meteorological and engineering applications involving rainfall rate.

Fig. 12 shows D for a point 3 to 4 times greater than the 100 mi^2 values. Similarly, the 25 and 50 mi^2 values are approximately 1.7 and 1.3 times greater than those for 100 mi^2. On the V_d, curves (Fig. 12), median ratios of 2.0, 1.3, and 1.1, respectively, are indicated between 100 mi^2 and the point, 25, and 50 mi^2 values. Equivalent ratios on the V_{dr}, curves (Fig. 12) are 5.6, 1.9, and 1.4. Thus, the foregoing curves provide quantitative estimates of the change in absolute variability ($\bar{D}$) and relative variability (V_d, V_{dr}) as the sampling areas increases progressively from a point to 100 mi^2 in warm season storms.

As mentioned earlier, Fig. 12 provides quantitative estimates of the range in absolute and relative variability that is likely to be encountered between storms in warm season precipitation on areas up to 100 mi^2. For example, $\bar{D}$ at the 5% level for point rainfall is 6 times the median value, whereas the 95% value is less than 20% of the median $\bar{D}$. These differences are slightly lower with areal mean rainfall on 25 to 100 mi^2.

Similarly, Fig. 12 shows V_{dr} approximately 2.5 times greater at the 5% level than at the median (50%) value, whereas the 95% relative variability is about 40% of the median value. Fig. 12 shows V_d ranging from nearly 500% at the 5% level to 135% at the 95% level with point rainfall. Similar values for 100 mi^2 are 210% and 84%. All the foregoing statistics illustrate further the large differences in time variability occurring between storms whether it is evaluated in absolute or relative terms.

Effects of Rain and Storm Type

The 50-storm sample for 50-60 mi^2 was subgrouped according to the rain and synoptic storm types described previously, to search for obvious changes in the time variability characteristics associated with such data stratifications. Steady rain was too infrequent in the warm season sample to evaluate its time

variability characteristics. Rainshowers and thundershowers were found to have nearly identical time variability characteristics, both conforming very closely to the average warm season relations. This similarity is not surprising since both are unstable types of rainfall.

Examination of the synoptic weather types showed no significant differences in time variability characteristics among the several types. Although squall lines did indicate a tendency for slightly lower than average time variability, the small sample of five storms makes this observation inconclusive. S, for these five storms had an average departure of 12% from the mean storm curve of Fig. 10. On the basis of the existing storm sample, one must conclude that there is little difference in time variability properties among synoptic weather types during warm season storms. Therefore, such data stratification is undesirable since it lowers analytical sample sizes.

Summary and Conclusions

The magnitude of both the absolute and relative time variability shows a wide range among convective storms. The variability parameters were found to fit closely a log normal distribution. Consequently, it was possible to construct first approximation probability distributions of these parameters which should aid in evaluating their utility in weather modification applications.

A strong trend was found for the time variability to increase with decreasing area. With respect to average storm rainfall intensity, the time relative variability (percentage distribution) decreases with increasing intensity, whereas the absolute variability increases as the mean intensity increases; however, there is a large amount of variance in the relations between storms. Large differences in time variability properties were not found between rain and synoptic storm types.

Because of the large interstorm variability, it is concluded that time variability relations would be useful as a verification tool only in those weather modification experiments aimed at substantially changing the time distribution properties of natural rainfall. The natural time variability is much too great to detect reliably any small changes resulting from seeding. Because time variability decreases with increasing sampling area, the optimum use of this rainfall property would be with experiments on relatively large target areas.

LAG CORRELATION ANALYSES

Lag correlation analyses were performed on the 29 storms in the 1952-1953 sample. This was done to define further the time distribution characteristics and to ascertain whether the rainfall rate structure shows cyclic or oscillatory properties within storms.

Lag correlations were made for successive lags of 1 to 60 minutes, or to the end of the storm if the duration was less than 60 minutes. Since the number of observations producing the lag correlation coefficients decreased with increasing lag, the results must be interpreted with caution. This is true particularly for lags exceeding 30 minutes. Approximately 25% of the storms had durations less than 60 minutes. However, only three storms had durations less than 45 minutes.

Analytical Results

Analyses were performed on both the 1-minute mean rainfall rate for the 100 mi^2 network and for three selected points within the network. Fig. 13 shows the average lag correlation pattern in-the 29-storm sample for the areal mean rainfall rate and for a point observation near the center of the network. Both the point and areal curves show the same general properties. There is a relatively rapid decrease in correlation as the time lag increases. In both cases, the correlation coefficient, on the average, reaches zero with a time lag of approximately 15 minutes. The largest negative correlations then occur at lags of 25 to 30 minutes.

The crossover from positive to negative correlation coefficients at a lag of 15 minutes indicates the average extent of persistence in point and areal mean rainfall rates. Examination of the 29-storm sample, however, showed a large degree of variability in the crossover. For example, with 100 mi^2 mean rates, the range extended from 5 to 50 minutes and had an average deviation of 7 minutes. The crossover of the point rainfall correlation ranged from 9 to 43 minutes with an average deviation of 6 minutes.

Another measure of the persistence factor that may be more meaningful was obtained by determining the distribution of times at which the lag correlation

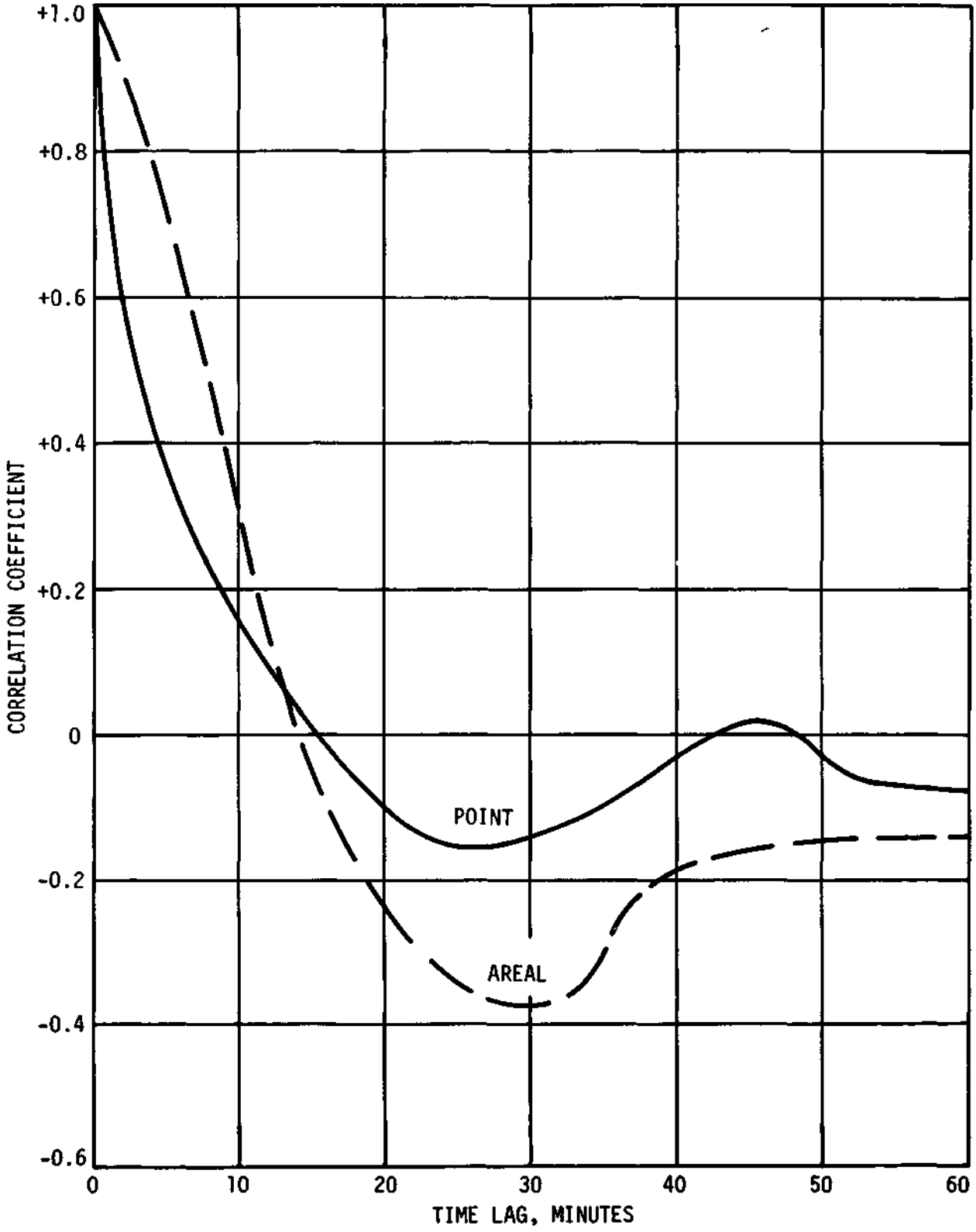

Figure 13. Average lag correlation patterns in 29 storms

first decreased below 0.71 (50% of variance explained). For the 100 mi^2 mean rate, the average was 5 minutes with an average deviation of 2 minutes, compared with an average of 1.8 minutes and an average deviation of 0.7 minute for the point rainfall sample. Thus, the persistence was considerably less at a point than on the 100 mi^2 for short lags, but was not completely eliminated any sooner. The areal correlations provide a measure of the average rate persistence in storm systems, such as the passage of a squall line or a thunderstorm complex across the network, whereas the point persistence is determined by the cellular characteristics within a storm passing the station.

When the lag correlation becomes negative, it indicates that the rainfall rates being compared are out of phase; that is, one set is increasing while the other is decreasing. In the 29-storm sample, the mean rate for 100 mi^2 showed the best negative correlation at an average lag of 30 minutes. However, there was, again, high variability in this statistic which showed a range from 13 to 60 minutes with an average deviation of 11 minutes. In 19 of the 29 storms, the negative correlation coefficient exceeded -0.5 (25% variance explained). In 12 storms it exceeded -0.7 and in 5 storms was greater than -0.9 at its best negative value. Thus, relatively strong inverse relationships occurred frequently, but not with a pronounced regularity in lag time.

After becoming negative, the lag correlations reversed and became positive again in several storms. This reversal was associated with the arrival of new storms on the network or redevelopment of storms within the network. If consecutive storms are similar in their rainfall rate time distributions, the correlations between them may reach relatively high positive values. A reversal to positive correlations was observed in 7 of the 29 storms. In 5 of these the lag correlation of mean rate on the 100 mi 2 network exceeded +0.5 and was greater than +0.7 in 3 storms. The average lag of secondary positive correlation peaks was 50 minutes, with a range from 32 to 60 minutes. These secondary maxima, of course, were based upon fewer observations than the other statistics. Both the strong negative and positive lag correlations were associated most frequently with well-defined storm systems with durations less than 90 minutes on the network.

Fig. 14 illustrates typical examples of individual storm correlations of mean rainfall rate on the 100 mi^2. Fig. 14a is a rainshower associated with a stationary front that produced a network mean rainfall of 0.45 inch over a 2-hour

period on August 3, 1952. Fig. 14b shows two thunderstorms associated with a cold front that produced an average rainfall of 0.14 inch on the network in an October 1952 storm. Fig. 14c shows the lag correlation pattern for the storm of July 5, 1953. This was a squall-line storm that deposited an average of 0.83 inch during 54 minutes.

The lag correlation data were grouped according to synoptic weather types and rain types to investigate differences that might exist between such groups. Results are summarized in Table 7, in which median correlation coefficients for each group have been tabulated at selected lag intervals. Since there were only three low center and two steady rainstorms, they have not been included. As shown in the table, the 29-storm sample was biased strongly toward the occurrence of frontal storms and thunderstorms, so that the comparisons can serve only as a first approximation of the group characteristics.

Table 7. Comparison of mean rainfall rate lag correlations between synoptic storm and rain types on 100 mi^2 network.

	Median correlation coefficient for given group				
Time lag (minutes)	Fronts	Air mass	Squall lines	TRW	RW
1	0.96	0.94	0.98	0.97	0.97
2	0.92	0.90	0.95	0.94	0.93
5	0.71	0.75	0.79	0.77	0.77
10	0.28	0.35	0.43	0.33	0.39
15	0.01	0.05	0.09	0.03	0.10
20	-0.29	-0.04	-0.33	-0.33	-0.18
25	-0.42	-0.16	-0.37	-0.39	-0.35
30	-0.45	-0.15	-0.59	-0.40	-0.46
35	-0.49	-0.07	-0.58	-0.23	-0.51
40	-0.36	0.24	-0.57	-0.27	-0.44
45	-0.30	0.23	-0.65	-0.25	-0.40
50	-0.22	-0.23	-0.36	-0.50	-0.10
55	-0.19	-0.07	-0.39	-0.30	0.11
60	-0.26	-0.28	-0.35	-0.28	-0.14
Number of storms	15	6	5	19	8

Within the limits of sampling variation expected in samples of the size used here, Table 7 does not indicate marked differences between storm and rain types. In all types, the lag correlation of areal mean rainfall rate decreased

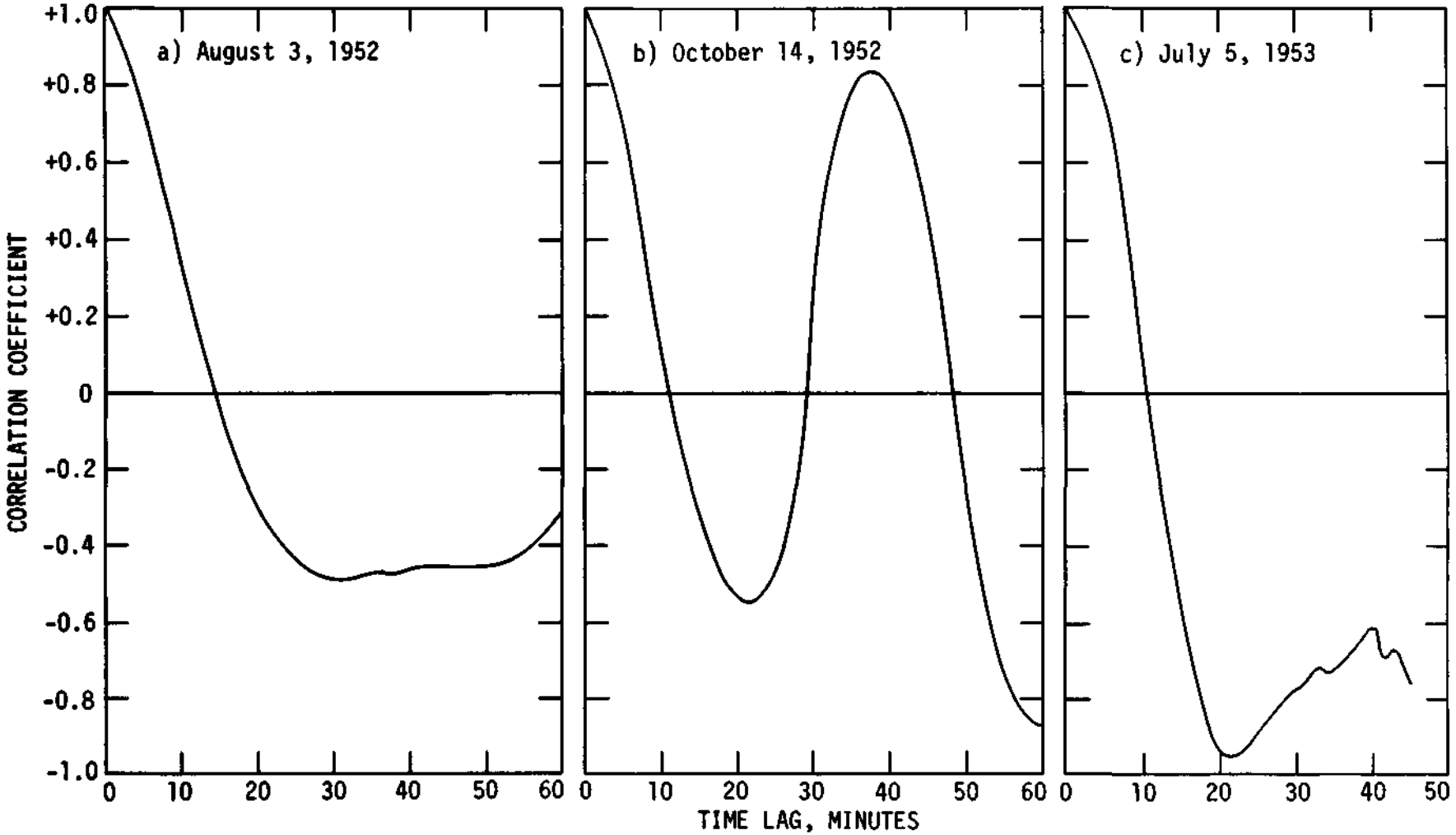

Figure 14. Log correlation patterns in selected storms

rapidly in the first 5 minutes, and the variance explained was only 50% at a lag of 5 to 6 minutes. Furthermore, in every group a crossover from positive to negative correlations took place at median lags of 15 to 18 minutes.

Conclusions

From lag correlation analyses of the 29-storm sample, no evidence was found of regular oscillations in the rainfall rate time distribution of convective storms at a point or over small areas. Consequently, it is concluded that rainfall rate time distributions could serve as one of several verification tools in weather modification experiments, especially those utilizing periodic seeding of relatively large-scale storm systems as an investigative technique. If effective, the periodic rainfall intensification should be discernible when sufficient experiments are made to overcome spurious cycles or oscillations that may be created in a small sample of storms due to random natural variability.

The lag correlation analyses also provide another measure of the large variability of the rainfall rate distribution within very small intervals of time in shower-type precipitation. As shown in Fig. 13, the average lag correlation between consecutive 1-minute rainfall rates at a point was only 0.72, and 100 mi^2 average rates showed a similar decrease in correlation in consecutive 5-minute intervals.

STORM RAINFALL DISTRIBUTION RELATIONS

An understanding of the relationship between total storm rainfall and rainfall rate distributions within storms is pertinent to the eventual use of rainfall rate data as a verification tool in weather modification experiments. Therefore, as part of the rainfall rate research, an investigation was made of this relationship in warm season storms for point rainfall and for mean rainfall on areas of 25, 50, and 100 mi2.

Relation between Mean Rainfall Rate and Total Storm Rainfall

Tabulations of 1-minute storm data were used to determine the frequency distributions of rainfall rate in the various storm samples. A family of curves developed for the 100 mi^2 network is shown in Fig. 15. These curves show the cumulative percentage of total storm rainfall occurring at various

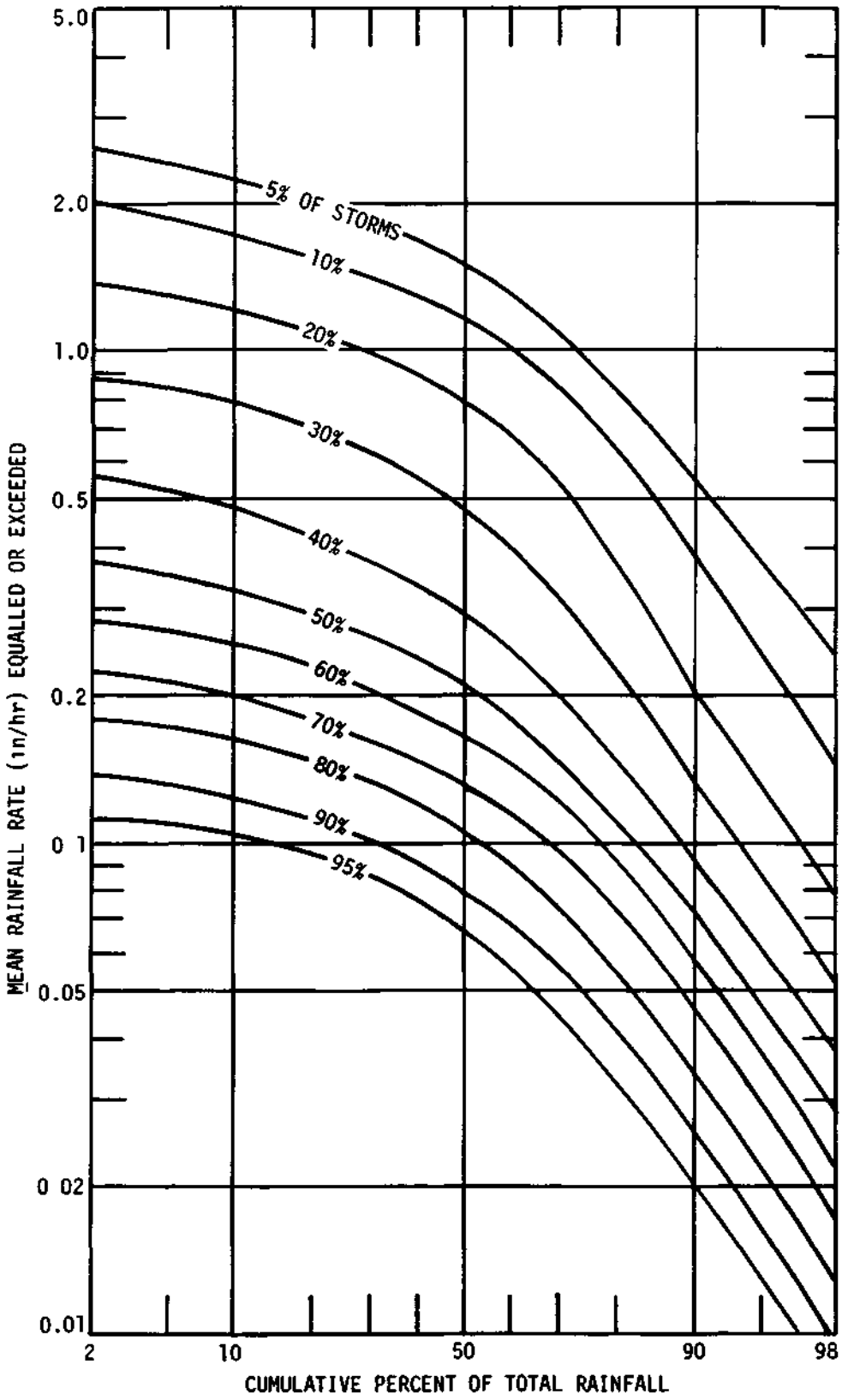

Figicre 15. Relation between rainfall rate percent of total storm rainfall, and percent of storms

rainfall rates in various percentages of the storms. For example, in 50% of the storms, 10% of the total rainfall occurred at rates of 0.33 inch/hour or greater, 50% at 0.21 inch/hour or more, and 90% at 0.09 inch/hour or greater.

For comparisons between areas, a normalization procedure was used in which the rainfall rate along each curve was expressed as a ratio to the median rainfall for that curve. Thus, in the above example for the 50% curve of Fig. 15, the ratio at 10% of the total rainfall is 0.33/0.21 or 1.57. When this was done, it was noted that these rainfall rate ratios remained essentially constant for the numerous curves making up the family. Furthermore, within the small range of areas investigated (25-100 mi^2), there was little change with increasing area, so all data were combined for the purposes of a first approximation of the distribution characteristics of rainfall rate in warm season storms. However, area should have some effect upon the distribution of storm rainfall as shown by Huff (1967). Therefore, if the range of sampling areas increases much beyond those investigated here, it would be necessary to derive relations that include the area parameter.

The average ratio curve for areas of 25 to 100 mi^2 is shown in Fig. 16, along with a similar curve derived from point rainfall data. The expected greater range in relative variability of point rainfall is indicated by the point ratio range of 3.6 to less than 0.1 between 2% and 98% of storm rainfall compared with a range of 1.8 to 0.15 for areal mean rainfall.

Assuming the curves of Fig. 16 are reasonably representative of the regional climatic average, they can be used to construct average rainfall rate distributions for various median rates of rainfall in warm season storms. This has been done for areal mean rainfall of selected rates in Fig. 17. These curves then provide typical rate distributions within convective storms and another measure of the variability of storm rainfall rates. Actually, Figs. 16 and 17 merely provide a generalization and smoothing of the various areal relations derived from the raw data, such as those shown in Fig. 15 for 100 mi^2.

Percentage Distribution of Storm Rainfall

Another method of describing the time distribution of storm rainfall is shown in Fig. 18. Here, curves have been drawn relating cumulative percentage of total rainfall to cumulative percentage of rain time for point rainfall and

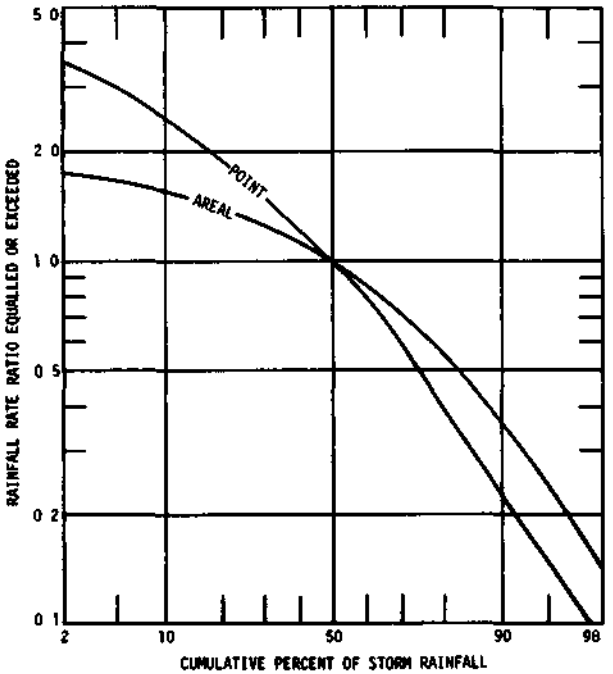

Figure 16. General relation between rainfall rate and percent of storm rainfall

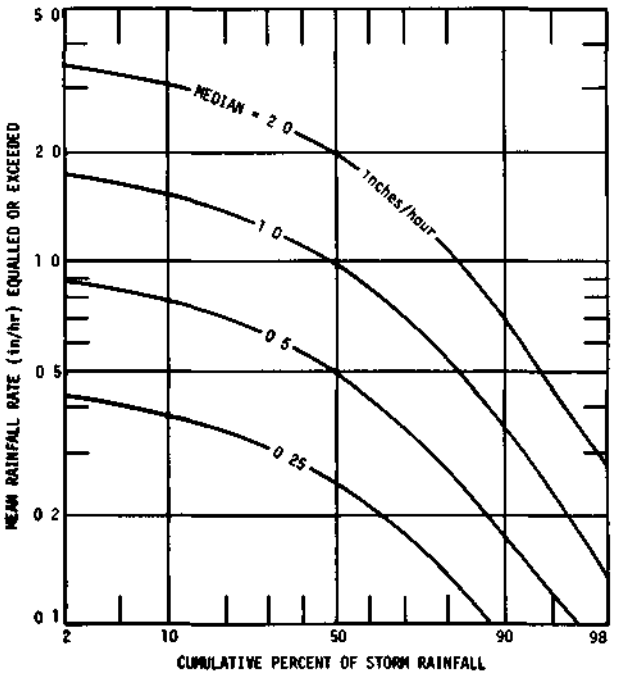

Figure 17. Generalized curves of rainfall rate and percent of storm rainfall

for areal mean rainfall on 25, 50, and 100 mi^2. These are average curves based upon 29 storms during the warm seasons of 1952 and 1953. The curves were derived from ranking of the 1-minute rainfall amounts in each storm from high to low, and, therefore, are not "real" time distributions. They were made to show what percentage of the rainfall is accounted for by a given percentage of the minutes with rain in an average storm.

Fig. 18 shows that, on the average, 10% of the storm point rainfall occurs in less than 2% of the minutes it is raining, 50% of the total rain occurs during 11% of the time rain is falling, and 90% of the total rain occurs in 37% of the time that it is raining. Thus, it is apparent that warm season rainfall tends to occur in strong bursts; that is, most of the rain occurs in a small portion of the storm.

Fig. 18 shows that as area increases it takes longer to obtain a given percentage of the total storm rainfall. Thus, as the area increases from a point to 100 mi^2, the percentage of rain time accounting for 50% of the total rain increases from 11% at a point to 13% at 25 mi^2, 15% at 50 mi^2, and 18% at 100 mi2.

Since Fig. 18 is based upon only 29 storms, it can only be used as a first approximation of the climatological relationship in warm season storms. However, as stated earlier in this report, the storm sample does not depart greatly from long-term averages with respect to the percentage distribution of point and mean rainfall amounts.

An examination was made of the 29 storms grouped by rain type and synoptic storm type. Although only two storms were classified as steady rain, the expected trend was found for thunderstorm rainfall to rank first in time concentration of total storm rainfall, followed by rainshowers and steady rain. Thus, on the 100 mi , 50% of the thunderstorm rainfall was found to occur in 16% of the rainfall minutes, whereas 18% of the rainshower minutes and 26% of the steady rain minutes accounted for 50% of the rainfall in their groups.

Only small differences were found in the distributions for fronts, squall lines, and air mass storms. Low centers, which were associated with only three storms, had a less concentrated time distribution, as expected. For example, on the 100 mi^2, 50% of the total rainfall occurred in 24% of the minutes in low center storms compared with 16% to 18% of the minutes in the other synoptic storm types.

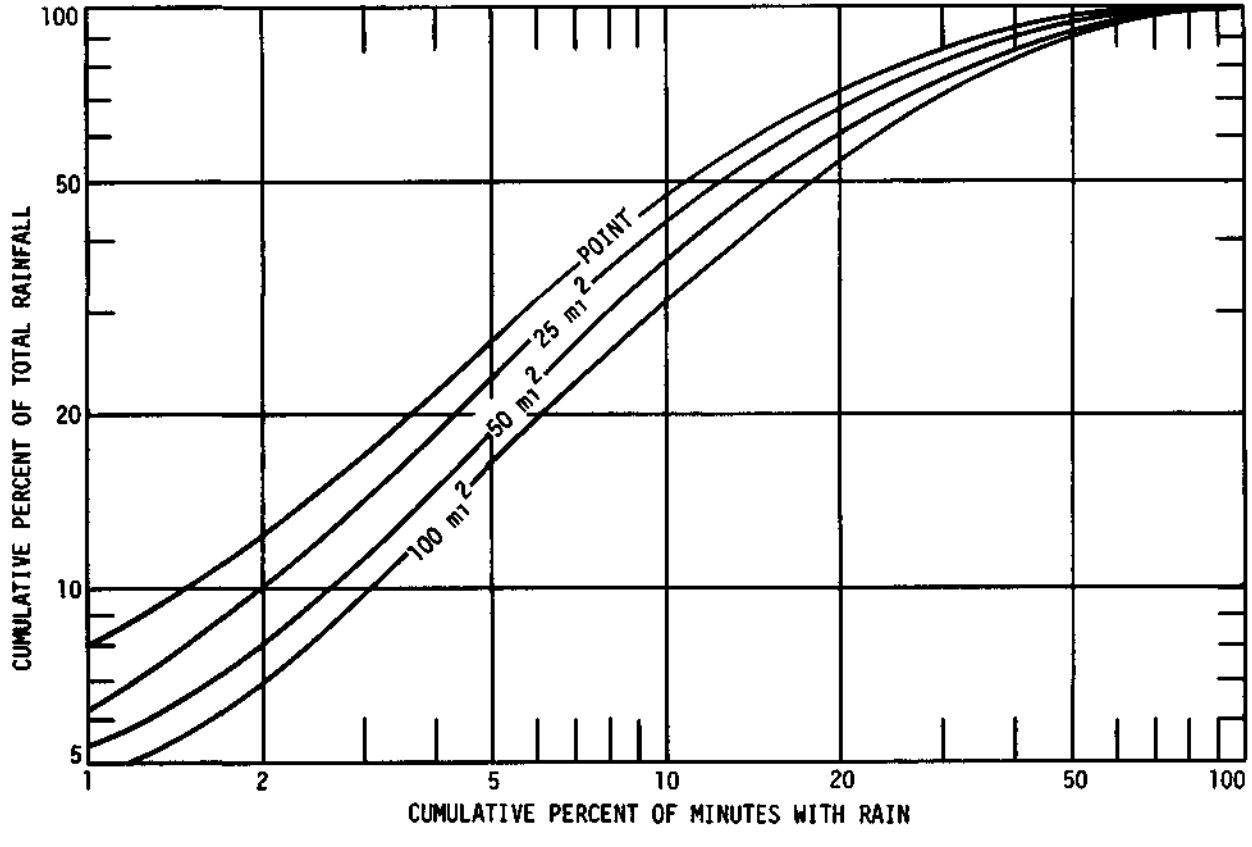

Figure 18. Percentage distribution of storm rainfall

Fig. 18 has certain implications in weather modification. From the natural distributions, one must conclude that substantial surface increases in rainfall from cloud seeding would occur if the treatment modestly intensified the rainfall intensity during the major rain-producing period of convective storms. However, the desirability of further intensification is doubtful in naturally intense storms (provided it could be achieved). If this is not accomplished, however, cloud seeding success must depend upon (1) greatly increasing the rainfall intensity during the relatively large percentage of the storm time with light rates, or (2) substantially extending the duration of the heavy intensity period within storms. The latter possibility would appear to be more likely to be accomplished.

Comparison of Point and Areal Storm Durations

Table 8 shows the relation between cumulative percentage of storms and the ratio of point to areal rainfall duration in the 29 storms on the 100 mi^2 network during 1952-1953. It provides an estimate of the probability of any point in the area experiencing rainfall in any given minute during which rain is occurring somewhere within the 100 mi^2. Thus, the median ratio is 0.34, indicating that in 50% of the storms rain will be falling at a selected point approximately one-third of the time or less when rain is being recorded within the 100 mi^2. Similarly, in 5% of the storms, the average point duration is 12% or less of the total areal rain time, and in 25% of the storms the point duration is 22% or less of the areal duration. This analysis illustrates the small areal extent of many warm season storms. Furthermore, it emphasizes the necessity of a dense raingage network or radar for the detection and location of summer showers, particularly if accurate space and time information on all storms in a sampling area is required.

Table 8. Comparison of point and areal storm durations on 100 mi^2.

Cumulative percent of storms	Ratio of point to areal rain duration
5	0.12
10	0.15
25	0.22
50	0.34
75	0.52
95	0.95

PART II

SPACE DISTRIBUTION STUDIES

ONE MINUTE RAINFALL RATE SPATIAL CORRELATIONS

The spatial correlation of rainfall rate and the sampling requirements resulting from various degrees of correlation are of primary importance in the establishment of raingage networks used for weather modification experiments. In this study, data from the 3142 minutes of rainfall in 29 warm-season storms during 1952-1953 were used to obtain initial estimates of the spatial correlation relations in storm rainfall.

Analytical Procedures

Initially, the effect of several data transformations to normalize the rainfall rate data, and hence, improve the correlation patterns was investigated. Transformations included the square root, fourth root, and logarithm of the rainfall rates. The effect of the transformations was inconsistent among the several data stratifications used in the analyses, and no marked superiority was obtained. Overall, a slight trend was noted for the correlation coefficient to decrease more slowly with distance when actual rainfall rates were used. Consequently, further analyses and all material presented in this report were restricted to untransformed data.

In the 100 mi^2 network, rows of gages along the western and northern borders were used to obtain correlation coefficients in W-E and N-S directions. Also, coefficients were calculated about the central gage in the network, in a NW-SE direction from the NW corner of the network, and in a SW-NE direction from the SW corner. These combinations were then used to determine directional effects upon spatial correlation which could result from topographical or climatic factors. For each directional analysis and each data stratification, isocorrelation maps were drawn. From these maps, variation of correlation coefficient (r) with distance was obtained through interpolation.

Analytical Results

Fig. 19 shows the average correlation pattern for the 29 storms about a gage near the central part of the network. Within less than 2 miles in all directions, the average correlation decreased to 0.8, or an explained

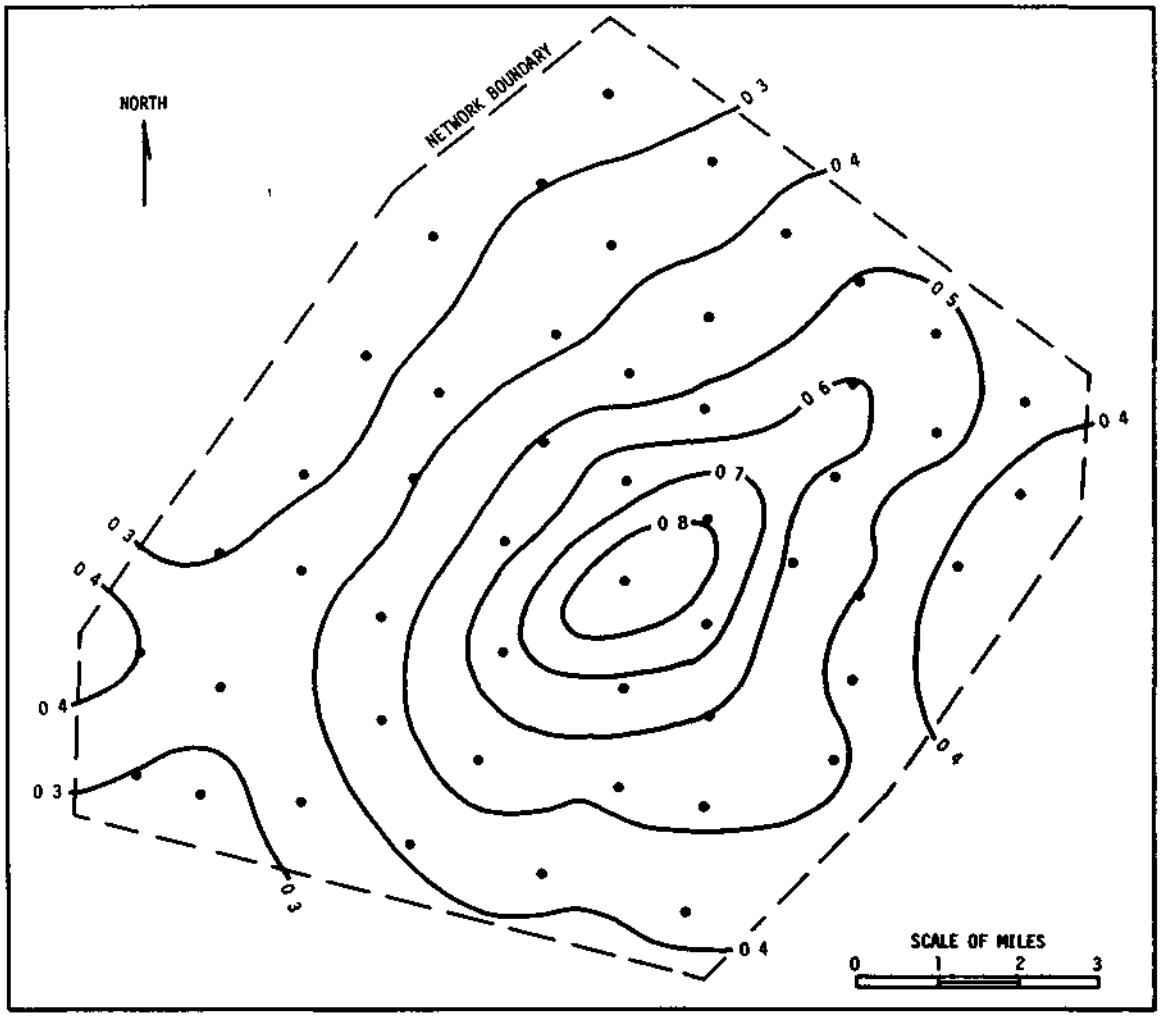

Figure 19. Average correlation pattern of rainfall rate in 29 storms

variance (r^2) of 64%. The orientation of the correlation pattern reflects the climatological trend for storm cells to move most frequently from a southwesterly direction.

Table 9 shows the average decay of correlation with distance from the point of correlation, based upon directional grouping of the data. Correlation relations are shown for all 3142 minutes of data in (1) W-E and N-S directions in which the differences were greatest, and (2) for all directions combined. Also shown is the average decay using only those minutes in which all gages in the 100 mi^2 recorded measurable rainfall. These 137 minutes provide a measure of the correlation decay in warm-season storms of large areal extent, whereas the 3142-minute sample reflects average conditions during convective storms which usually do not completely envelop the 100 mi^2 network in any given minute.

Table 9. Average correlation decay with distance of 1-minute mean rainfall rates grouped by direction.

	Correlation coefficient for given condition			
			All directions combined	
Distance (miles)	North-South	West-East	All minutes	Rain at all gages
1	0.76	0.63	0.71	0.76
2	0.64	0.48	0.58	0.65
3	0.57	0.37	0.50	0.58
4	0.50	0.28	0.41	0.51
5	0.45	0.20	0.34	0.45
6	0.40	0.13	0.28	0.39
8	0.30	0.02	0.16	0.27
10	0.20	----	----	----
Number of minutes	3142	3142	3142	137

Comparison of the W-E and N-S directions shows differences in r^2 of 16 to 18% at distances of 1 to 5 miles. This reflects the tendency for storm cells to move more frequently from a southerly direction; with the entire network seldom enveloped by rainfall at a given time, the average correlation is better along the N-S lines. Comparison of all storm minutes with the 137 having

rainfall over the entire network shows an average of 8 to 9% more for r^2 in the large-scale storms. Thus, the improvement in variance in the large-scale storms appears to be relatively small.

Table 9 provides an opportunity to obtain some first approximations of gage density requirements for the measurement of rainfall rate patterns in convective storms. For example, assume one wished to combine all data and keep the average value of r^2 between observation points at a minimum of 50% ($r = 0.71$). Table 9 shows a gage spacing of 1 mile would be required. If interest was only in those minutes with rainfall at all gages in the sampling area, the 50% minimum could be maintained with a gage spacing of 1.5 miles. In either case, a very dense network would be needed. If the accuracy requirements were increased still more to obtain a high degree of precision in the establishment of spatial patterns, the gage requirements for most research projects would become intolerable operationally. This is based upon the assumption that sampling areas would extend over hundreds of square miles in most weather modification experiments.

In Table 10, the data were stratified according to rainfall and synoptic storm types, and correlation patterns of average decay with distance were determined. There were too few steady rain cases to construct a reliable correlation curve. As expected, thunderstorms (TRW), which tend to extend over greater areas than rainshowers (RW), had a slower rate of correlation decay with distance. On the average, the rainshower correlation approached zero at a distance of 6 miles. Table 10 also shows average correlation decay with distance for the two synoptic weather types that exhibited the greatest differences in warm-season storms. Frontal storms which tend to have greater areal extent than air mass storms show a slightly slower decay rate. Low center passages were too few to include in the analysis, and squall line properties were nearly identical with the frontal relationship.

In Table 11, an evaluation has been made of the effect of storm magnitude (areal mean rainfall) on the correlation pattern. As clearly indicated, the heavier, more intense storms showed a slower rate of decay with distance than the light storms which frequently extend over only a small portion of the 100 mi^2 network at a given minute. For example, at a distance of 2 miles, the average correlation coefficient ranges from 0.61 in the heaviest storm class to 0.34 in storms with means of 0.10 inch or less.

Table 10. Average correlation decay with distance of 1-minute mean rainfall rates grouped by rain and storm type.

Distance (miles)	Correlation coefficient for given type: Rain type: TRW	Rain type: RW	Storm type: Fronts	Storm type: Air mass storms
1	0.72	0.63	0.70	0.64
2	0.59	0.48	0.57	0.51
3	0.51	0.36	0.47	0.42
4	0.44	0.26	0.40	0.34
5	0.38	0.14	0.33	0.26
6	0.31	0.03	0.26	0.18
8	0.17	----	0.13	0.02
10	0.04	----	----	----
Number of minutes	1957	1008	1665	859

Table 11. Average correlation decay with distance of 1-mmute mean rainfall rates grouped by storm mean rainfall.

Distance (miles)	Correlation coefficient for given mean rainfall (in): ≤0.10	0.11-0.25	0.26-0.50	0.51-1.00
1	0.54	0.63	0.68	0.74
2	0.34	0.45	0.53	0.61
3	0.19	0.31	0.43	0.53
4	0.07	0.20	0.35	0.46
5	0.01	0.10	0.26	0.39
6	----	0.03	0.18	0.32
8	----	----	0.02	0.18
10	----	----	----	0.05
Number of minutes	883	783	805	671

Table 12 shows correlation decay patterns in storms in which the network was under the influence of 1 to 4 cells or storm centers. These centers could be either closed centers within the 100 mi^2 or open centers at the border of the network with the central intensity somewhere off the network. Here, the outstanding characteristic is the higher correlation as the number of centers increases. Under these circumstances, the network is more likely to be encompassed completely by rainfall, and more likely to have heavier storm totals. The similarity between the 4-center relations of Table 12 and those for mean rainfall of 0.50 to 1.00 inch of Table 11 lends support to the foregoing statement.

Table 12. Average correlation decay with distance of 1-minute mean rainfall rates grouped by number of rain centers on network.

Distance (miles)	Correlation coefficient for given number of centers		
	1	2-3	4
1	0.64	0.69	0.77
2	0.50	0.55	0.65
3	0.39	0.45	0.57
4	0.28	0.34	0.51
5	0.18	0.25	0.46
6	0.11	0.18	0.42
8	0.03	0.10	0.33
10	----	0.06	0.24
Number of minutes	939	1845	275

In Table 13, the effect of storm orientation was investigated. The storm orientation refers to the azimuth of the major axis of the total storm pattern. Thus, SW refers to a major axis oriented from SW to NE. As indicated, no significant differences were found in the correlation patterns for storm orientations from SW through W. Correlation decay was somewhat less with NW oriented storms, but whether this is a true characteristic of these storm types or merely a sampling vagary has been undetermined at this time.

Table 13. Average correlation decay with distance of 1-minute mean rainfall rates grouped by storm orientation.

Distance (miles)	Correlation coefficient for given orientation NW	SW, WSW, W
1	0.77	0.69
2	0.65	0.56
3	0.57	0.46
4	0.50	0.38
5	0.45	0.32
6	0.40	0.25
8	0.30	0.14
10	0.20	0.03
Number of minutes	762	2059

Table 14 shows comparisons between the spatial correlations of 1-minute, 5-minute, and 10-mmute average rates for all minutes and all directions combined. The 5-minute and 10-minute rates were obtained by calculating running averages throughout each storm. That is, the 5-mmute means were obtained from averages of minutes 1 through 5, 2 through 6, etc., until the last minute of the storm was included. The 5-minute and 10-minute mean rates were calculated to determine if the spatial variability was decreased significantly by the averaging procedure.

Table 14 indicates slight improvement in the spatial correlation at short distances with 10-minute averages, but the increase in r^2 is only 8% at 1 mile and decreases to zero at 4 miles, after which the 1-minute r^2 is slightly greater. The 5-mmute rates showed an even faster correlation decay with distance than the 1-mmute rates. The reason for this behavior is not known. From the 29-storm sample, one must conclude that the spatial correlations of rainfall rate are not changed significantly by averaging over intervals of 5 to 10 minutes instead of using the nearly instantaneous rates provided by the 1-minute rainfall amounts.

Table 14. Comparxsons of spatial correlation of 1-minute, 5-minute, and 10-minute mean rainfall rates.

Distance (miles)	Correlation coefficient for given time period		
	1-min	5-min	10-min
1	0.71	0.72	0.77
2	0.58	0.51	0.61
3	0.50	0.37	0.51
4	0.41	0.29	0.41
5	0.34	0.24	0.32
6	0.28	0.20	0.25
8	0.16	0.13	0.15

At this point, it is interesting to bring out the great differences in correlation decay between 1-minute rainfall rate and total storm rainfall. As part of an earlier Illinois study, correlation patterns of total storm rainfall were constructed for approximately 300 storms on the East Central Illinois Network (ECIN) of 49 gages in 400 mi^2. A comparison of the rainfall rate curve based on all 1952-1953 data with a similar curve for the May-September storms on ECIN is shown in Fig. 20. Based on these two curves and an assumed requirement for an r^2 of 50%, on the average, a gage spacing of approximately 1 mile would be needed for rainfall rate pattern definition compared with a spacing of more than 10 miles for total storm rainfall. If an r^2 of 75% between observation points was required, then a spacing of about 0.3 mile for 1-minute rainfall rate would be needed compared with approximately 7,5 miles with total storm rainfall.

Conclusions

In general, the correlation analyses indicated better spatial correlation of rainfall rate (1) in south-north directions than in west-east directions, (2) in thunderstorms than in rainshowers, (3) in frontal storms than in air mass storms, (4) in heavy storm rainfalls than in light storms, and (5) in multicellular storms than in single-cell storms. No significant improvement was obtained when 5-minute and 10-minute average rates were used in place of

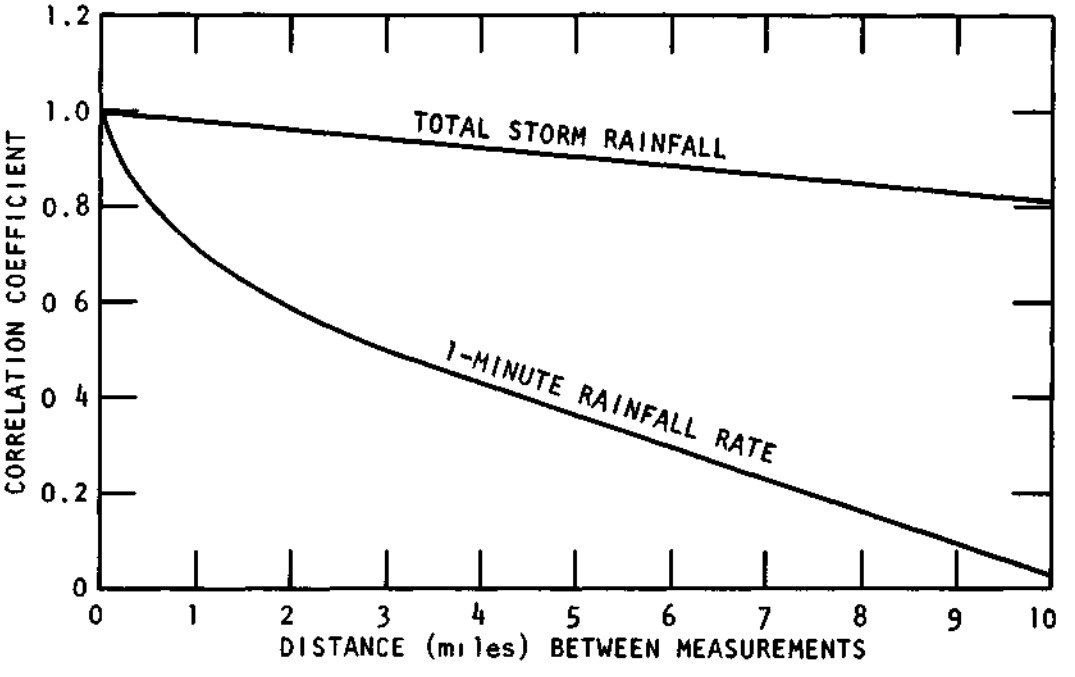

Figure 20. Comparison between correlation decay with distance of 1-minute mean rainfall rate and total storm rainfall

1-minute rates. In all data groupings the correlation decay with distance was rapid. Therefore, raingage networks with sampling densities adequate to define accurately instantaneous rainfall rate patterns at the surface for use in weather modification experiments may be beyond operational and/or economic feasibility. If interest is only in mean rainfall rate over an area, then the sampling requirements will decrease significantly, a subject treated in another section of this report.

AREA-DEPTH RELATIONS

A convenient method of describing the spatial distribution of storm rainfall rates is through the computation of area-depth relations. Consequently, area-depth curves of average and enveloping rainfall rates, a basic tool used in hydrologic design problems, have been studied to aid in the definition of the spatial characteristics and to detect properties potentially useful in precipitation modification experiments. For a given sampling area, these two types of area-depth curves provide a measure of the rainfall gradient, maximum point rainfall, volumetric distribution, and information relative to the skewness in the rainfall distribution (Huff, 1968).

Area-Depth Envelope Relations

Considerable use has been made of area-depth envelope curves in the spatial studies. From these curves the rainfall rate equalled or exceeded over any fractional part of the sampling area can be determined. In a uniformly distributed network of raingages, the curve is constructed from a ranking of raingage values from high to low. Otherwise, the curve is determined from planimetering of network isohyetal maps.

In this study, primary emphasis has been placed upon analyses of area-depth envelope relations obtained from the 29-storm, 3142-minute sample on the 50-gage network of 100 mi^2 operated in 1952-1953. Area-depth curves were calculated for each 1-minute rainfall in each storm.

First, a frequency distribution of area-depth envelope relations on the 100 mi^2 was determined from the 3142-minute sample. Results are summarized in

Fig. 21 in which the rainfall rate equalled or exceeded is related to cumulative percentage of the sampling area for various percentages of the minutes making up the sample. Thus, the 5% curve shows the rainfall rate equalled or exceeded in the 5% of the minutes with the heaviest rainfall rates for any fractional part of the area enveloped in the range from 2% to 98% of the area. It should be understood that the fractional areas in Fig. 21 are not fixed. That is, the 2% of the area with heaviest rates may change in location from minute-to-minute within storms as well as between storms. It specifies the heaviest rates experienced any place on the network in a given minute.

Interpretation of Fig. 21 is illustrated by referring to the 2% of the area with heaviest 1-minute rates in the 29 storms. There, it is seen that 5% of the 3142 minutes had rates equalling or exceeding 4.6 inches/hour. This decreased gradually to 0.36 inch/hour in the 50% of the minutes with heaviest rates, and to 0.04 when 95% of all minutes were included. Similarly, over 50% of the area, 5% of the minutes had a rate of 0.5 inch/hour or greater, and this decreased to 0.03 inch/hour for the upper 50% of the minutes, and to less than 0.01 inch/hour when 95% of the 3142 minutes were included.

Fig. 21 does not include a sufficient number of storms to accept it as a true frequency distribution of rainfall rates. However, as indicated in other analyses, it does serve as a first approximation of the frequency distribution in warm season storms. Also, it provides quantitative information on the spatial variability of rates within a fixed area of 100 mi^2 and the degree of time variance of rates. For example, the 5% curve shows a spatial range from 4.6 to 0.07 inches/hour as the area for which the enveloping rainfall rate is determined increases from 2 to 98 mi^2. Similarly, for the 2% of area with the heaviest rates in the 3142 minutes, the rate ranges from 4.6 inches/hour to 0.04 inch/hour between 5% and 95% of the total minutes.

The 3142-minute sample from 29 storms was used in making other analyses to define further the spatial distribution characteristics of rainfall rate, with particular emphasis on the time variability in the spatial distribution. One result of these analyses is summarized in Fig. 22a (left figure). This figure shows a family of median area-depth envelope curves on the 100 mi^2 for selected percentages of the storms. The family was derived in the following manner. For each storm, area-depth envelope curves of rainfall rate were

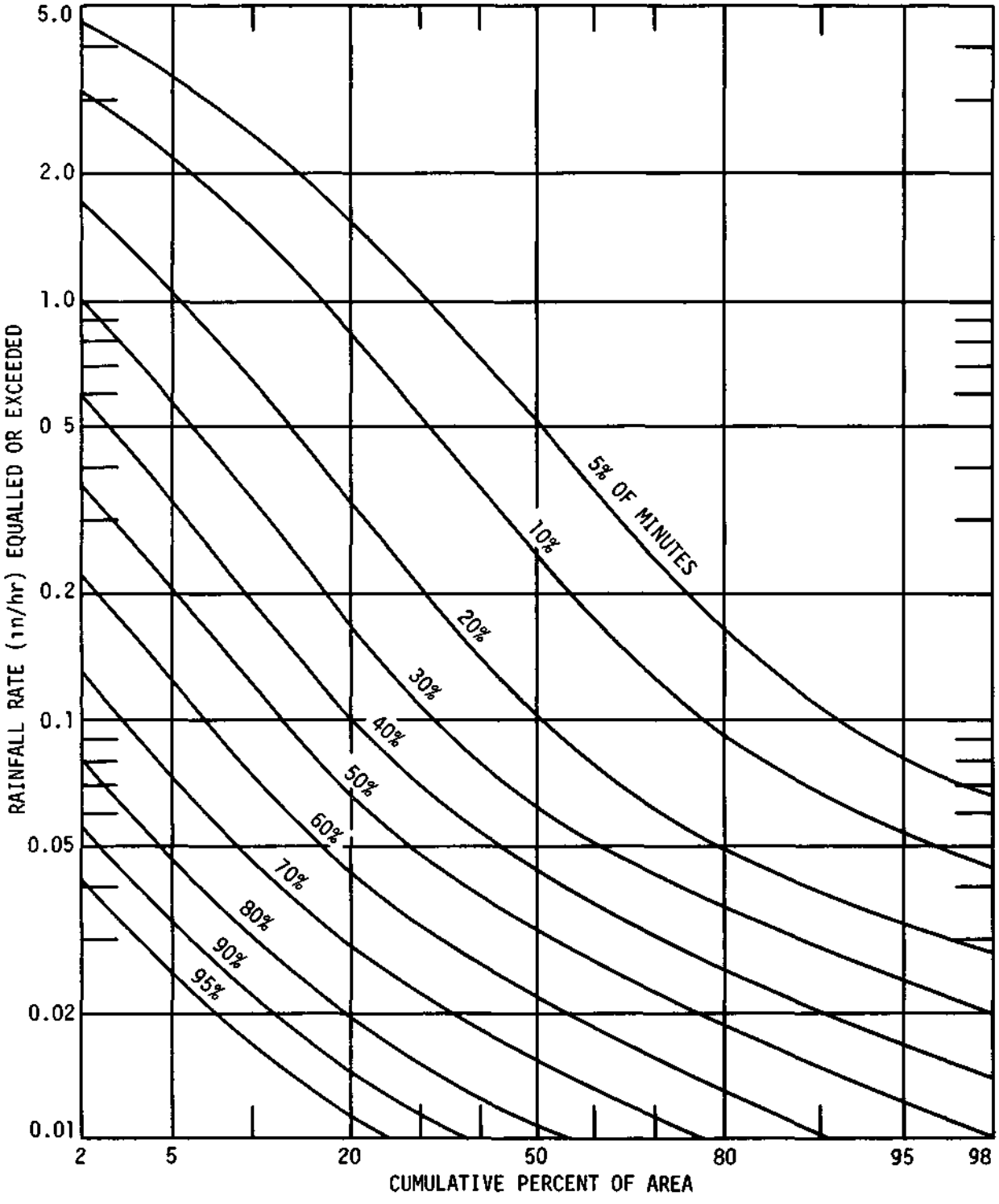

Figure 21. Frequency distribution of area-depth envelope values

calculated for each minute during the storm. At selected fractions of the 100 mi^2 area, the 1-mmute rainfall rates for the storm were ranked from high to low. The median values from each storm were then used to construct the family of curves in Fig. 22a. These curves were found to fit closely an equation of the form.

$$\text{Log } R_e = a + b\, A^{0.5} \qquad (1)$$

where R_e is the enveloping rainfall rate, A is area enclosed, and a and b are regression constants.

Fig. 22a provides a statistical model of typical area-depth curves of 1-mmute rainfall rate in warm season storms of various intensity. Thus, the median rainfall rate distribution in the most intense storms in the 29-storm sample is portrayed by the curve for 5% of the storms. This curve shows the enveloping rainfall rate ranging from 3.8 inches/hour over the 2 mi^2 of heaviest intensity to 0.03 inch/hour over the entire 100 mi^2. Similarly, the 50% curve shows a range from 0.43 inch/hour to less than 0.01 inch/hour. These individual percentage curves provide a quantitative measure of the spatial variability in storms of varying intensity.

For some purposes, one may be more interested in extreme rates rather than median or average rainfall rates to be expected in storms. The ranked 1-minute data for each storm can be used also to obtain a measure of the distribution of heavy rates, and this has been done in Fig. 22b (center figure). Here, the area-depth envelope curves for the 10% of the minutes with heaviest rainfall in each storm were used to derive the family of curves. Interpretation of this family is the same as for Fig. 22a. Thus, in 10% of the storms sampled the area-depth envelope curve for the 10% of the storms with heaviest intensities had enveloping rainfall rates decreasing from 5.8 inches/hour at 2 mi^2 to 0.3 inch/hour over the entire 1-0 mi^2. All storms (100%) had rates of 0.42 inch/hour or more on 2 mi^2 during the heaviest part of the storm but less than 0.01 inch/hour when the entire 100 mi^2 is included. Together, Figs. 22a and 22b provide quantitative estimates of median and extreme rates likely to occur in typical warm season storms.

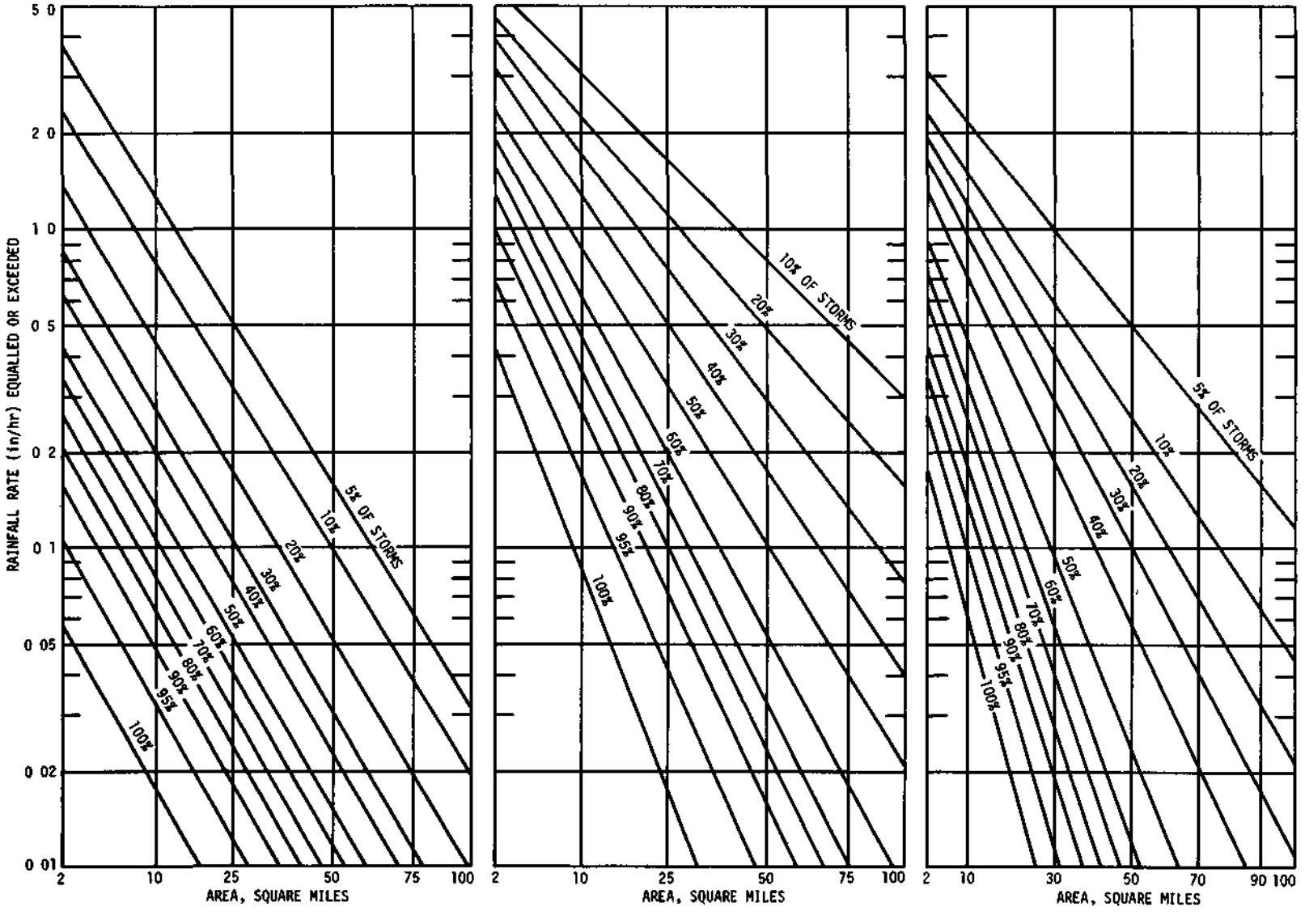

Figure 22. Area-depth envelope distributions derived from median, extreme, and average values

Fig. 22c (right figure) shows a family of curves similar to those in Fig. 22a. Method of determination was the same, except average rates rather than median rates were employed in development of Fig. 22c, since some users may be more interested in this statistic. In this case, the family of curves were found to fit an equation of the form

$$\text{Log } R_e = a + b\, A^{0.8} \qquad (2)$$

Because of the extreme skewness in the distribution of 1-minute rainfall rates in the 29 storms, substantial differences exist between the average and median sets of curves. In most cases, the average curves show substantially higher rainfall rates for a given area and given percentage of storms.

Fig. 23a (left figure) shows a median space-time distribution of storm rainfall rates derived from the 29-storm sample. It was obtained in the following manner. For each storm an area-depth envelope curve of rainfall rate was obtained for each minute. Thus, a family of curves similar to Fig. 22a was obtained for each storm. Then, the median curve for each 10% of the minutes from the 29 storms was used to construct Fig. 23a. Based on the 29-storm sample, Fig. 23a can be interpreted as a typical space-time frequency distribution in warm season storms. Fig. 23b (right figure) provides the same type of information, but is based upon averages rather than medians.

An effort was made to evaluate the effects of rain type and synoptic storm type on area-depth envelope relations. Grouping of the data resulted in most types having too few samples to define quantitatively relations for each type with a satisfactory degree of accuracy. With only two steady rainstorms, little can be said about the general characteristics of their spatial distribution. However, it did appear, as one might expect, that the steady rains had less spatial variability, and, therefore, smaller rainfall gradients than the TRW and RW types. Similarly, air mass storms tended to have more intense rainfall gradients than frontal storms, but less areal extent.

The storms were also grouped according to quartile in which the heaviest rainfall occurred and mean area-depth curves developed for each of the four quartiles. The heaviest intensities were found to occur with the first and second quartile storms, whereas the fourth quartile storms had the lightest rates, in general.

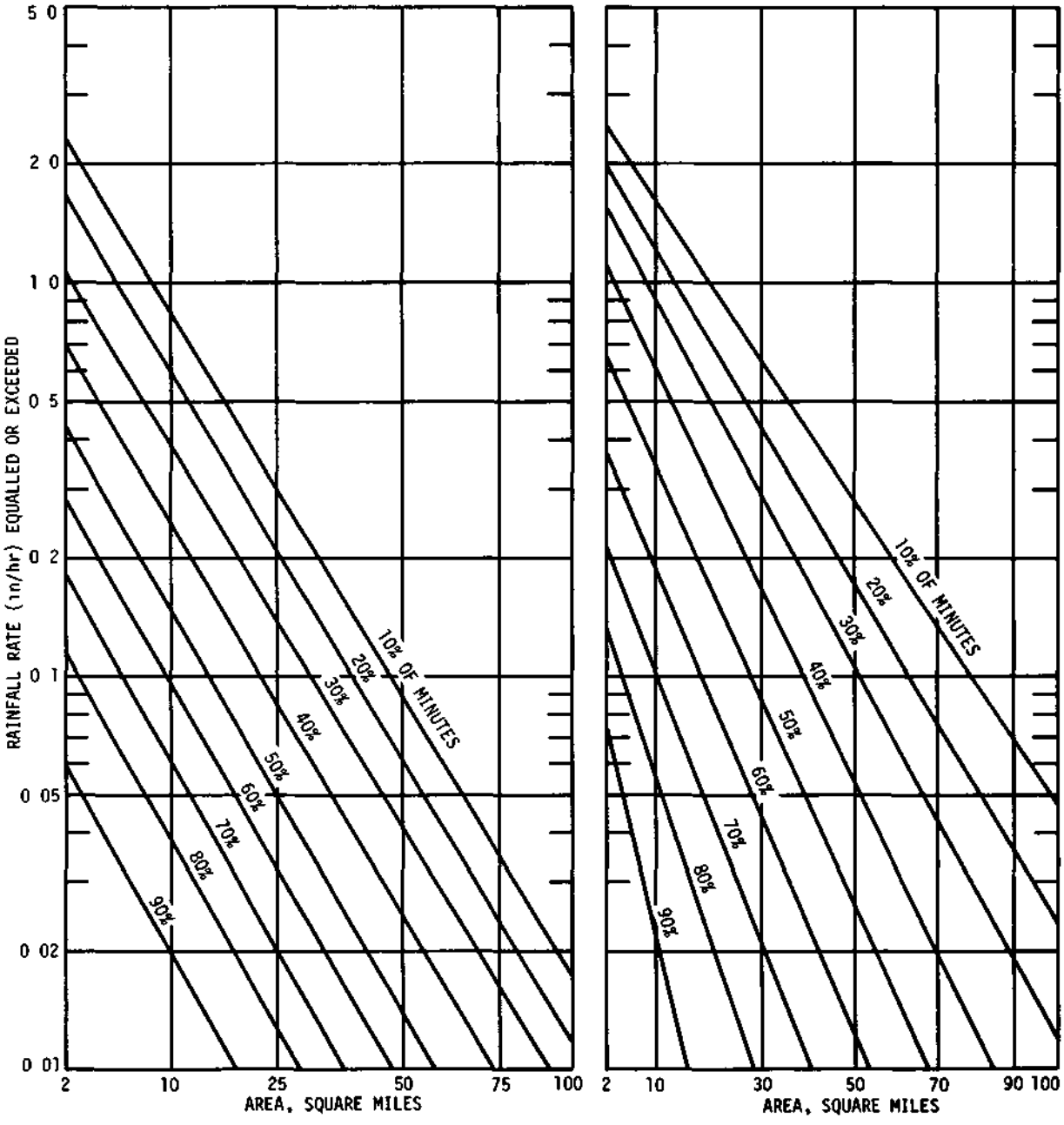

Figure 23. Area-depth envelope storm models based on median and average values

Area-depth envelope relations were developed also for 25- and 50-mi^2 areas within the 100-mi^2 network. Characteristics of the envelope curves were similar to those for 100 mi^2. Consequently, they have not been included in this report, particularly since such small areas are seldom (if ever) employed as targets in weather modification experiments.

Average Area-Depth Relations

Average area-depth relations of 1-minute rainfall rates were investigated also. This is the standard hydrologic area-depth presentation in which the basin rainfall is ranked from high to low and averaged from the area of heaviest intensity to the area of lightest rainfall. The intercept of the resulting curve represents the maximum point rainfall, the end-point of the curve is the areal mean rainfall, and the curve slope is an integrated measure of the rainfall gradient.

Storm models derived from the 29-storm sample are shown in Figs. 24a and 24b for areas of 25 and 100 mi^2. These families of area-depth frequency curves were based upon median values from the storms, and were derived in the same manner as the envelope frequency curves of Fig. 23. In both figures, the slope of the curves is smallest with the heaviest areal mean rainfalls. That is, the spatial relative variability tends to minimize with the heaviest mean rates on a given sampling area.

The wide range of rainfall rates normally experienced in convective storms is illustrated by Fig. 24. For example, on the 100 mi^2, the network mean ranges from 0.05 inch to 1.25 inches between the 5% and 95% limits of the typical storm curve. Thus, the heavier 100 mi^2 mean rates are approximately 25 times greater than the relatively light rates in the typical warm season storm derived in this study. Over the 10 mi^2 of heaviest rainfall rates on the 100 mi^2, the range is from 0.22 inch to 4.10 inches, a ratio of 18 to 1. Similarly, on the 25 mi^2 the network mean rate ranges from 0.04 inch to 1.32 inches between the 5% and 95% limits of the typical storm curve.

Figs. 24a and 24b provide considerable information on the typical variation of rainfall rates with both time and area within warm season storms. Of course, relatively great interstorm variability existed, so that in individual storms large differences from the typical storms of Figs. 24a and 24b, based upon median

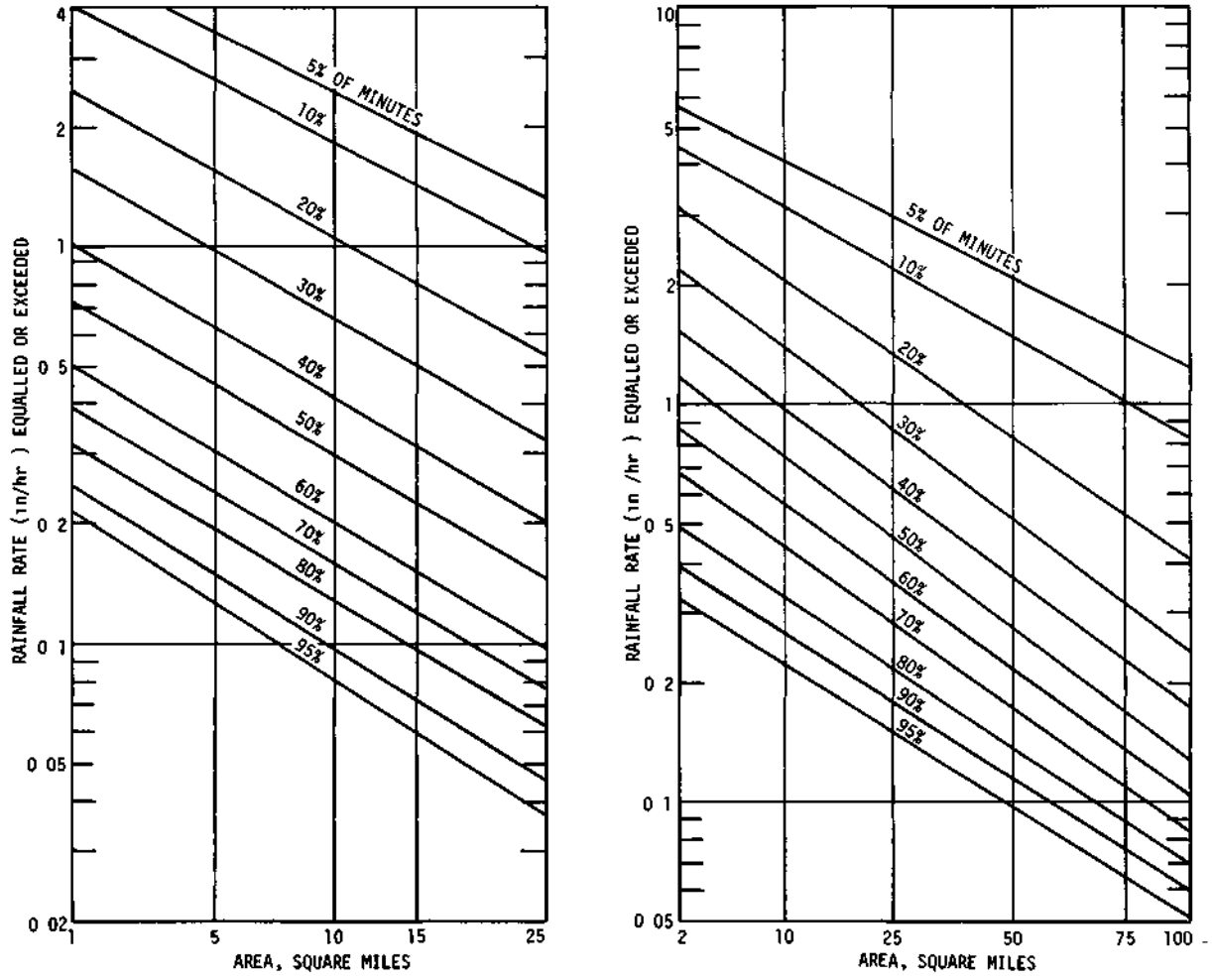

Figure 24. Average area-depth storm models for 25 and 100 m² derived from 29 storms

median values of 29 storms, may occur. For example, the 100 mi^2 mean rate for the 5% of the minutes with heaviest rates in individual storms ranged from 0.07 to 1.54 inches/hour. Moving up the 5% curve to 10 mi^2 where the typical curve shows a rate of 4.10 inches/hour, the 29-storm range in rates was 0.18 to 5.70 inches/hour.

Summary and Conclusions

Area-depth curves of average and enveloping rainfall rates were derived to aid in the definition of the space-time characteristics of 1-minute rates. These curves provide measures (directly or indirectly) of the rainfall gradient, maximum point rainfall, areal mean rainfall, and skewness of the distribution. In weather modification experiments, it is important not only to determine average precipitation in the target and control areas, but also to ascertain other characteristics of the spatial distribution that may be affected by seeding. The area-depth curves provide one means of acquiring additional information. When calculated for specific intervals of time throughout a storm, a convenient time-space distribution measure is provided by a single family of curves, and this distribution can be expressed mathematically if desired.

This study was devoted primarily to determining the natural rainfall properties of area-depth relations in warm season storms of the Midwest. Definition of the relations in natural rainfall must be made before they can be applied effectively in weather modification.

A frequency distribution of area-depth envelope relations was determined from the 29-storm sample. This provides a first approximation of the frequency distribution of area-depth envelope values in convective-type storms. Also, this distribution provides quantitative information on the spatial variability of rates within a fixed area of 100 mi^2 and the degree of time variance in these rates. Typical area-depth curves were derived from the data to provide quantitative estimates of median, average, and extreme rates likely to occur in warm season storms with respect to their space and time distribution characteristics between and within storms. As expected, substantial variability was found in the area-depth relations from minute to minute within storms and between storms of similar type.

With respect to application in weather modification, the area-depth curve is one of several useful tools that may be employed in the verification of seeding experiments. Because of the great space-time variability in natural rainfall, it is extremely doubtful that any single precipitation parameter or measurement will uniquely define seeding effects. Since it provides information on several areal precipitation properties, the area-depth curve should be utilized. As pointed out by Huff (1968), it can help answer questions (1) regarding changes that seeding may be producing in the time distribution of rainout from the associated cloud system (2) concerning tendencies for seeding to intensify or decrease the average rainfall gradient in treated storms, and (3) regarding changes in the skewness of the distribution resulting from seeding.

RELATIVE VARIABILITY OF RAINFALL RATES

Another measurement of the spatial distribution of rainfall rates can be obtained through calculations of the relative variability. This was done for 1-minute rates in the 29 storms of 1952-1953 on the 100 mi^2 network. The spatial relative variability was obtained by the simple method presented by Conrad and Pollak (1950), in which it is defined as

$$V = 100(S/M) \qquad (3)$$

where V is the relative variability in percent, M is the mean of the sample, and S the average deviation from the mean.

First, the variability was calculated for only those minutes during which rain fell at every network gage. This provides a measure of the rainfall rate dispersion during the passage of relatively large-scale precipitation systems. There were only 137 minutes, 4.4% of the total 3142 minutes, which met the above requirement. These minutes occurred in 11 of the 29 storms.

Next, the rate dispersion within rain areas in all types of storms was investigated by calculating V after eliminating all network gages with no measurable rainfall (1-minute rate less than 0.06 inch/hour). A third variability

calculation was made through use of all raingage values (including zeroes) during rainfall on the network. This provides a measure of spatial relative variability over a fixed sampling area of 100 mi .

The average relative variability for the 137 minutes with rain over the entire network was 52% with a standard deviation of 16%. Table 15 summarizes results for the larger samples involving all gages and only those gages with measurable rainfall. Results are presented in the form of frequency distributions of relative variability.

Table 15. Frequency distribution of relative variability of 1-minute rainfall rates on 100 mi^2 network.

	V (%) for given cumulative percent of minutes										
	5	10	20	30	40	50	60	70	80	90	95
All gages	196	193	188	176	164	144	125	103	80	61	51
Gages with measurable rainfall	95	88	78	71	64	57	50	43	36	31	27

Thus, when only gages with measurable rainfall were used in the calculations, the relative variability ranged from 95% for the highest 5% of the minutes to a median value of 57%, and then decreased to 27% for the lowest 5% of the cases. As expected, the relative variability increases greatly when it is calculated for the fixed area of 100 mi^2 through use of all 50 gages, since frequently a considerable portion of the network will have no measurable rainfall in a given minute in small-scale convective storms. Thus, the fixed area median is 144% compared with 57% for the rain-enveloped areas. As mentioned earlier, only 4% of the minutes in the 29-storm sample had rainfall at all gages.

Stratification of the data according to mean rainfall rate was not done since the relationship was very weak. For example, correlation analyses indicated that the variance explained by mean rainfall rates was approximately 5% for the 137 minutes in which the entire network had rain. On the basis of all network gages on the fixed area of 100 mi^2, the variance in V explained by mean rate was only 3%. When only gages with measurable rainfall were used, the variance explained increased to 20%. Overall, a weak trend for the relative variability to decrease with increasing mean rate was observed.

RAINFALL RATE PROFILES

Another method of evaluating space and time distribution characteristics of rainfall rates is through the analyses of storm profiles. A profile portrays the rainfall rate distribution along a line of sight through a storm. Profile analyses were performed on the 29-storm sample of 1952-1953 on the 100 mi^2 network. The profile for any minute provides a measure of the spatial variability. The change along a given profile from minute-to-minute aids in definition of the time variability.

Frequency Distribution of Profile Rates

First, analyses were performed to determine whether the frequency distribution of rainfall rates differed substantially along profiles in different directions. Investigations were made of four profiles across the network. These were oriented S-N, SW-NE, W-E, and NW-SE. A frequency distribution of mean rainfall rates along each profile was made at 1.5-mile intervals for the 3142 minutes of rainfall in the 29 storms. That is, the distribution was determined for the first 1.5 miles from the starting point, then for the first 3.0 miles, continuing in like manner across the network. Results indicated only small differences in profile values for the four directions for any given distance along them. Consequently, all four directions were combined to obtain an overall frequency distribution of rates along profiles through warm season storms.

Examination of the profiles for each distance indicated the average profile rate decreasing with increasing distance for a given percentage of the rain occurrences. For example, the average 3-mile rate for 10% of the rain minutes tended to be greater than the 6-mile or 9-mile rates. This trend is illustrated in Table 16 which shows the frequency distribution of profile rates for selected occurrence intervals.

In the lower part of Table 16, a normalization procedure has been used in which the rate for any given percentage of minutes and distance is expressed as a ratio to the median rate for the given distance. These ratios show a trend to decrease slightly with increasing distance. They provide another quantitative measure of space-time variations in rainfall rates.

Table 16. Frequency distribution of profile mean rainfall rates in 29 storms.

Percent of minutes	Rainfall rate (inch/hour) equalled or exceeded for given distance (mile)					
	1.5	3.0	4.5	6.0	7.5	9.0
2	3.08	2.64	2.44	2.35	2.20	2.09
5	1.90	1.78	1.63	1.50	1.39	1.28
10	1.26	1.14	0.96	0.88	0.82	0.78
20	0.60	0.50	0.44	0.40	0.40	0.37
30	0.30	0.27	0.22	0.21	0.20	0.20
50	0.12	0.11	0.10	0.10	0.10	0.10
75	0.09	0.06	0.05	0.04	0.03	0.03
95	0.06	0.03	0.02	0.01	0.01	0.01

	Ratio to median rainfall rate					
	1.5	3.0	4.5	6.0	7.5	9.0
2	25.7	24.0	24.4	23.5	22.0	20.9
5	15.8	16.2	16.3	15.0	13.9	12.8
10	10.5	10.4	9.6	8.8	8.2	7.8
20	5.0	4.5	4.4	4.0	4.0	3.7
30	2.5	2.5	2.2	2.1	2.0	2.0
50	1.0	1.0	1.0	1.0	1.0	1.0
75	0.8	0.5	0.5	0.4	0.3	0.3
95	0.5	0.3	0.2	0.1	0.1	0.1

In Table 17, the median relative variability along the SW-NE profile on the network is shown for all storms combined and for the data grouped according to the major rain types and synoptic storm types experienced in the 29 storms. This profile represents the most frequent direction of storm movement on the network. The relative variability used in this table was obtained by dividing the standard deviation by the mean and multiplying by 100. It is based upon data from six gages located along the SW-NE profile. The large degree of skewness in the data does not permit interpretation of the standard deviation and relative variability strictly in accordance with statistical theory. However, the relative variability as calculated from these skewed distributions does provide an index of the profile variability of rainfall rate through warm season storms.

Among synoptic storm types and rain types, the relative variability was greatest with air mass storms and smallest with squall lines. Little difference was indicated between thunderstorms and rainshowers, the major rain types in the warm season.

Table 17. Median relative variability along SW-NE profile based on 3142 rain minutes in 29 storms.

Group	Number of minutes	Relative variability (%)
All storms	3142	122
Air mass	859	155
Squall lines	389	91
Fronts	1665	128
Thunderstorms	1957	117
Rainshowers	1008	122

Individual Storm Profiles

Profile analyses along the SW-NE line were made for each storm in the 1952-1953 sample. Distance intervals were the same as in the frequency distribution analyses described previously. Average storm rates were calculated for each of five distance intervals. The average deviation, a measure of the time variability from minute-to-minute, was then determined. The relative time variability in percentage was calculated also by dividing the average deviation by the average storm rate and multiplying by 100.

Results are summarized in Table 18 which shows the three statistics (average rate, average deviation, and relative variability) in each storm for point rainfall near the SW corner of the network and for mean rate over distances of 5 and 10 miles. In each storm, only those minutes in which rainfall occurred at the given point or distance were used. That is, if in a 60-minute storm the 5-mile path was enveloped completely by rainfall in only 30 minutes, then the statistics would be based on the 30 rain minutes only. Three storms in which the number of minutes with rain along the SW-NE profile were too few

Table 18. Time variability of 1-minute rates in 1952-1953 storms for SW-NE profile.

Storm date	Point rainfall			5-mile profile			10-mile profile		
	Avg. rate (in/hr)	Avg. dev. (in/hr)	Rel. var. (%)	Avg. rate (in/hr)	Avg. dev. (in/hr)	Rel. var. (%)	Avg. rate (in/hr)	Avg. dev. (in/hr)	Rel. var. (%)
7/ 2/52	0.42	0.48	114	0.42	0.48	114	0.24	0.24	100
7/ 3/52	0.12	0.06	50	0.12	0.06	50	0.06	0.02	33
7/ 7/52	0.66	0.84	127	0.24	0.24	100	0.12	0.18	150
7/ 8/52	0.18	0.12	67	0.18	0.18	100	0.18	0.24	133
7/16/52	0.18	0.12	67	0.18	0.24	133	0.06	0.04	67
8/ 3/52	0.48	0.36	75	0.54	0.54	100	0.60	0.90	150
8/20/52	0.24	0.24	100	0.18	0.24	133	0.24	0.18	75
9/ 1/52	0.12	0.03	25	0.18	0.18	100	--	--	--
9/14/52	0.54	0.30	56	0.90	0.54	60	--	--	--
9/18/52	0.48	0.36	75	0.84	0.72	86	1.02	0.84	80
10/14/52	0.18	0.12	67	0.18	0.12	67	0.24	0.18	75
4/ 9/53	0.12	0.06	50	0.24	0.12	50	--	--	--
4/24/53	0.12	0.02	17	0.06	0.06	100	--	--	--
5/ 6/53	0.12	0.06	50	0.18	0.12	67	0.12	0.06	50
6/ 5/53	0.54	0.48	89	0.72	0.54	75	0.96	0.60	63
6/ 8/53	0.54	0.48	89	0.72	0.36	50	0.90	0.54	60
6/25/53	1.14	0.84	74	1.98	1.26	64	1.26	0.84	67
7/ 2/53	0.36	0.42	117	0.42	0.42	100	0.36	0.36	100
7/ 5/53	1.08	1.02	94	1.56	0.90	58	1.86	1.20	65
7/16/53	0.66	0.78	118	0.60	0.54	90	0.24	0.36	150
7/17/53	0.36	0.30	83	0.36	0.24	67	0.06	0.24	400
8/ 7/53	0.66	0.72	109	0.66	0.60	90	0.90	0.60	67
8/ 8/53	0.48	0.30	63	--	--	--	--	--	--
9/ 6/53	0.18	0.12	67	0.12	0.12	100	0.12	0.06	50
9/18/53	0.18	0.12	67	0.12	0.12	100	--	--	--
11/20/53	0.06	0.02	33	0.18	0.18	100	--	--	--

to determine the three statistics satisfactorily have been omitted from Table 18. Several of the 10-mile calculations have been omitted in the table also because of insufficient samples. The frequent repetition of certain rates in the table results from the round-off of 1-minute amounts to three decimal places, this results in rates being expressed to the nearest 0.06 inch/hour.

Table 18 provides quantitative estimates of the time variability in rainfall rates along a given path in a typical group of warm season storms. It also illustrates the large interstorm differences in the profile properties.

Fig. 25 is a typical example of the time variability in rainfall rate along a storm profile. In this illustration from the storm of July 5, 1953, the variation in point rainfall rate from minute-to-minute is shown for a gage near the SW corner of'the network. Above this is shown the time variability in average rainfall rate for the first 5 miles starting at the SW corner. The top graph is for a 10-mile profile beginning at the SW edge of the network. The time variability becomes less pronounced as the distance used in the calculations increases. However, successive minute differences exceeding 0.5 inch/hour occur during several periods when the rate is averaged over the 10-mile profile.

Summary and Conclusions

Analyses were made of both the frequency distribution of rainfall rates along storm profiles and the properties of individual storm profiles to obtain quantitative estimates of the time-space characteristics of rainfall rate distribution along lines of sight through warm season storms. The frequency distribution of profile rates was found to vary insignificantly with profile direction in the 29-storm sample. However, significant differences were found in the frequency distribution properties with increasing length of storm profile. As expected, minute-to-minute variability of average rates within individual storms was relatively large in many cases, as was the range in rates along the profile in a specific minute. Large interstorm variability in the profile properties was observed.

Again, storm profiles are only one of several rainfall measurement tools that may be useful in weather modification application under certain circumstances.

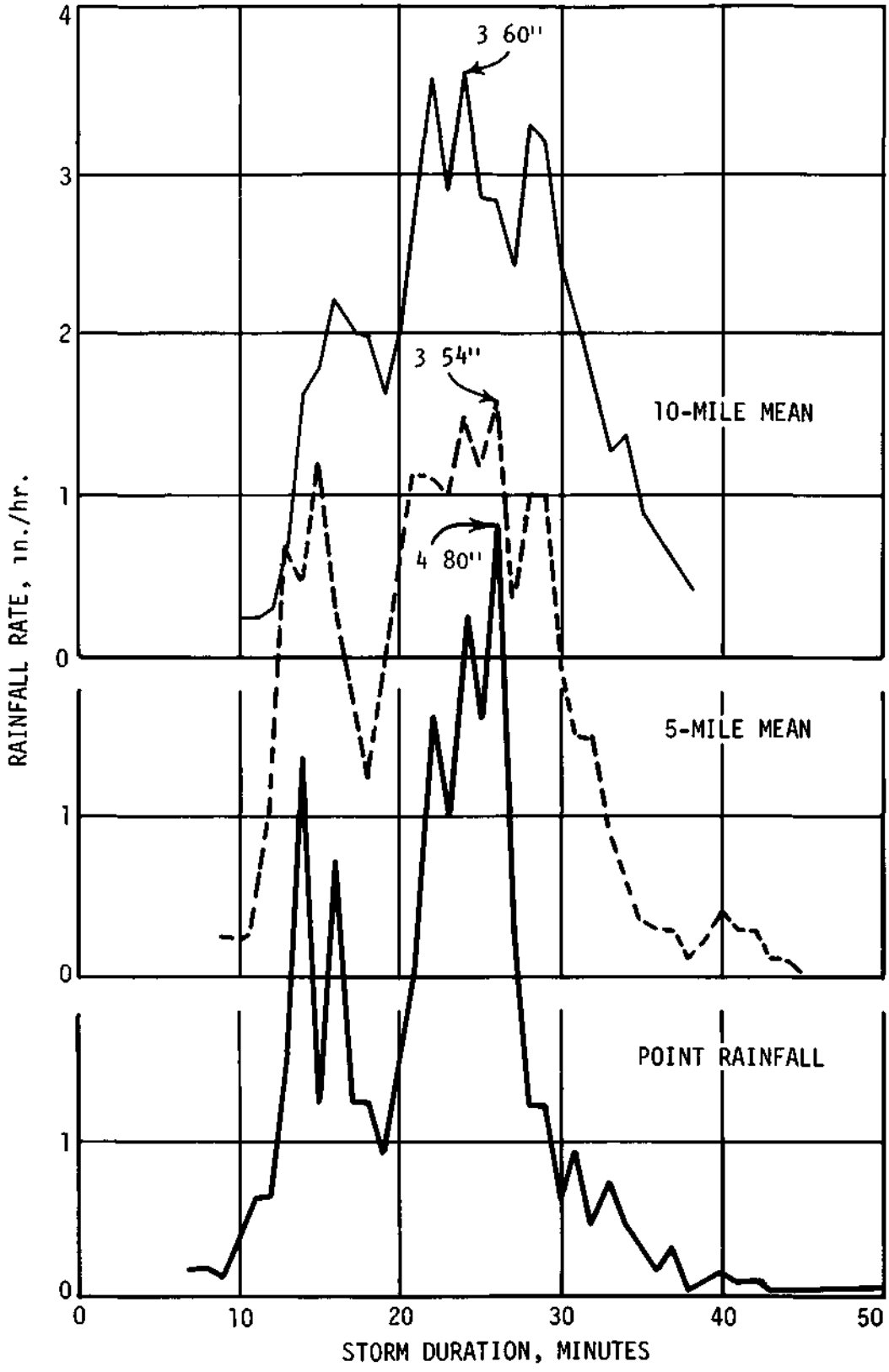

Figure 25. Time distribution of rates for SW-NE profile on 7/5/53

The time-space variability in profiles creates a strong background interference level that would make it difficult to separate induced from natural effects. Major changes in the space-time characteristics of rainfall rate would have to be induced by cloud seeding to be discerned readily by profile analyses.

VARIATION OF RAINFALL RATE WITH DISTANCE

As another measure of the spatial variability of rainfall rate, an investigation was made of the variation of 1-minute rates with distance between observation points. Data from the 29 storms on the 100 mi 2 network in 1952-1953 were used in this study of rainfall rate gradients in warm-season storms.

The most central gage (No. 29) was used as the comparison gage. Average differences in 1-minute rainfall amounts between the central gage and the gages within 1-mile intervals were made. Thus, there was an average difference for each minute in each storm for various range intervals starting with 1 mile. There were no gages in the 0-1 mile range. Minutes with no rainfall at the central gage were not used in the calculation of the differences. This restriction resulted in a sample of 2000 minutes in the 29 storms.

On the basis of plotting and testing of the data and previous experience with similar problems, it was decided to fit the 1-minute data to an equation of the form.

$$\text{Log } D = a + b \text{ Log } R + c \text{ Log } M \qquad (4)$$

where D is the average difference (inch/minute) at a given point at distance M (mile) from the comparison gage, R, with its rainfall rate expressed in inches per minute. Combining all data from the 29 storms, the following equation was obtained.

$$\text{Log } D = -0.460 + 0.90 \text{ Log } R + 0.15 \text{ Log } M \qquad (5)$$

A multiple correlation coefficient of 0.81, explaining 66% of the variance, was obtained for this equation.

Table 19, obtained from the above equation, shows the average variation of 1-minute point rainfall rates with increasing distance from a given reference point for various rate intensities and distances. Differences have been converted to percentages and rates to inches per hour to facilitate interpretation and maintain consistency with other analyses performed under this research program.

Table 19. Average variation of point rainfall rates with distance.

Starting point rate (in Air)	Average difference (%) for given distance (mile)					
	1	2	4	6	8	10
0.1	64	74	81	87	90	93
0.2	61	69	78	82	85	87
0.5	56	63	71	75	77	79
1.0	52	58	65	69	72	74
2.0	49	54	60	64	67	69
5.0	45	49	55	58	60	62

Table 19 shows the expected average trend for the rainfall rate percentage differences to increase with distance and decrease with increasing rainfall intensity. However, the primary importance of Equation (5) and Table 19 is that they provide some quantitative estimates of these differences as distance and rainfall intensity vary in warm-season storms. Furthermore, they provide information on the average gradients of rainfall intensity in convective cells, and this knowledge should be of interest to cloud physicists concerned with the mechanisms of precipitation development in clouds.

The relatively large percentage differences at 1 mile in Table 19 indicate that an extremely dense raingage network would be required if a highly accurate measurement of the areal rainfall rate pattern is required in weather modification experiments or in other applied research problems. In the author's opinion, detailed measurements of rate patterns could be achieved best with a

combination of raingages and 10-cm radar. The operation, data collection, and data reduction with raingages alone would be extremely difficult with the required density of gages (in the order of one per mi^2) extending over several hundred square miles.

SAMPLING ERRORS IN MEASUREMENTS OF STORM MEAN RAINFALL RATES

One factor governing the use of rainfall rate in the verification of weather modification experiments is the raingage sampling density needed to measure reliably the average rate over a given target area at any specified time. Therefore, data from the 29-storm sample on 100 mi^2 were used to obtain quantitative estimates of sampling errors associated with various sampling densities. The results obtained provide a partial answer to the problem outlined above.

In the approach used here, average sampling error was related to 1-minute mean rainfall rate and raingage density by an equation of the form:

$$\text{Log } E = a + b \text{ Log } R + c \text{ Log } G \qquad (6)$$

where E is the average sampling error in inches, R is 1-minute rate in inches/minute, G is gage density in mi^2/gage, and a, b, and c are regression constants. The form of the equation was determined by (1) graphical plots of the raw data, (2) evaluation of the effects of various data transformations in achieving normalization of the rainfall data, and (3) application of knowledge gained in previous rainfall studies, such as those of Huff and Neill (1957).

A separate equation was determined for each storm through use of all minutes in which rainfall occurred on the network. The various equations were then grouped by rain type, storm type, total storm rainfall, storm duration, and storm mean intensity to investigate further the relative effects of these factors upon the magnitude of the sampling error for a given gage density and 1-minute mean rate on the 100 mi^2. None of these factors showed

strong trends to indicate major importance in defining the sampling error, although all undoubtedly exert some influence. The 29-storm sample is too small to ascertain these influences with a high degree of accuracy and only general effects can be determined.

Among storm types, slightly lower percentage errors were obtained with squall-line and low center storms than with frontal and air mass storms. No trend could be discerned among the rain types; however, the number of steady rains was too small to establish real effects. Storm duration showed a weak trend for the percentage sampling errors to decrease with increasing duration. Erratic trends were obtained with the groupings by total storm precipitation and average storm intensity, with some evidence of a slight decrease in percentage sampling errors with increasing values of the two parameters.

Other factors also affect the sampling error with a given gage density, area, and frequency distribution of 1-minute rainfall rates in a storm. Among these are the location of the storm center with respect to the center of the sampling area, the direction of movement and orientation of the major axis of the storm, and the number and distribution of individual storm cells at any given time in the sampling area. Consequently, unless huge samples are available to permit groupings according to all of the various factors influencing the rainfall pattern characteristics, the sampling error with a given gage density may vary considerably between storms which are similar in many respects.

This sampling error variability between storms is illustrated in Fig. 26 which was constructed from the 29 individual storm equations. For easier interpretation, the sampling error has been expressed in percent and 1-minute rainfall rate in inches/hour. In this illustration, the frequency distribution of the average percentage sampling error (E) has been shown for selected gage densities (G) and a 1-minute mean rate (R) of 0.20 inch/hour on the 100 mi^2 network. Fig. 26 also provides a measure of the rate of increase of E with decreasing G.

With a gage density of 50 mi^2/gage, over four times the average climatic network density in Illinois, E ranges from over 100% in 5% of the storms to 17% or greater when 95% of the storms are included. Referring to the median (50%) value on the abscissa, E increases from 16% with G = 5 mi^2/gage to 38% with 25 mi2/gage, 53% with 50 mi^2/gage, and 76% with 100 mi2/gage.

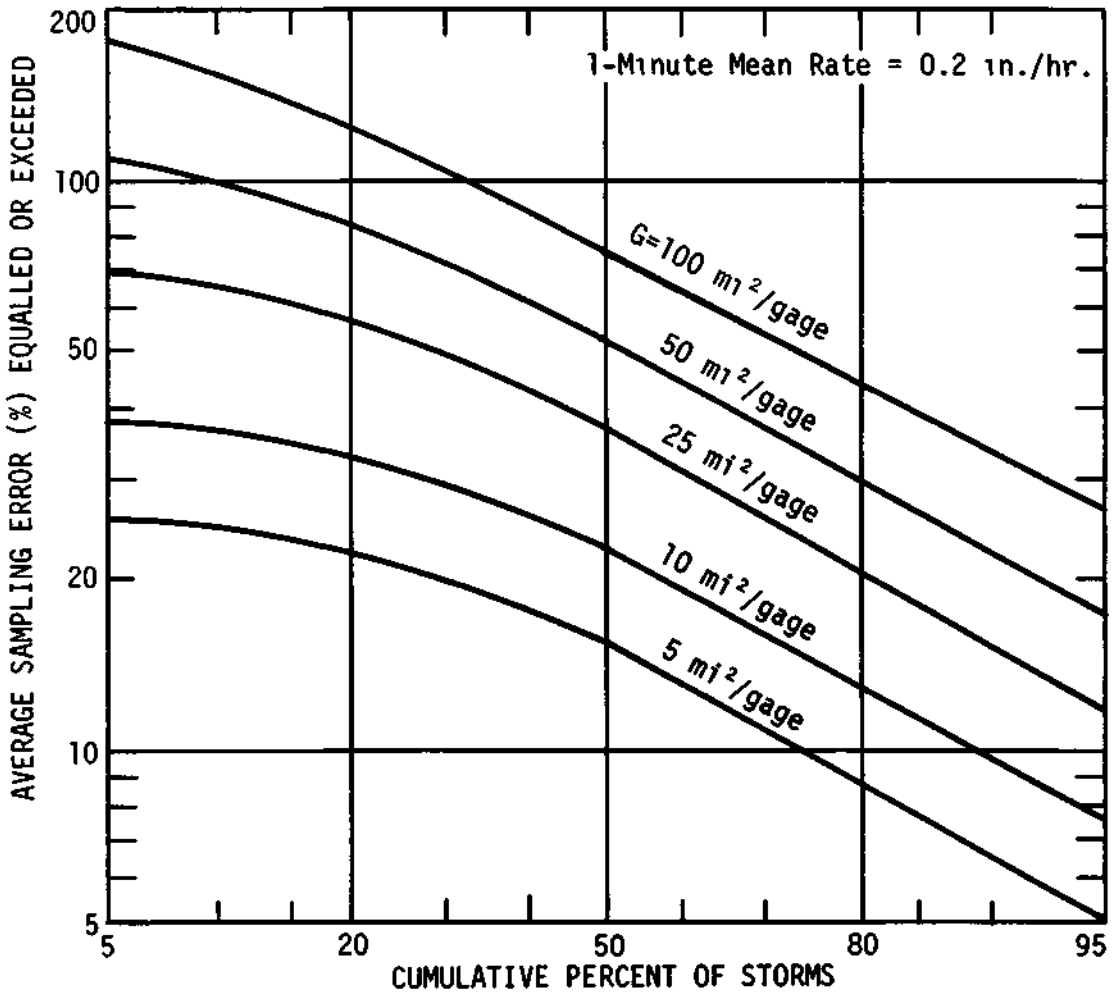

Figure 26. Effect of gage density on sampling errors of 1-minute rates on 100 ml^2 network

Table 20. Percentage sampling error of storm mean rate for G = 10 mi^2/gage.

1-minute mean rate (in/hr)	Average percentage errors from equation for given storms			
	7/2/52	9/18/52	6/8/53	7/5/53
0.05	19	33	40	22
0.1	17	28	30	19
0.2	16	23	23	16
0.5	14	18	16	13
1.0	13	15	12	11
2.0	12	12	9	9
$\bar{R}$	0.22	0.31	0.52	0.92
T	181	181	71	54
P	0.67	0.94	0.61	0.83
Storm type	Warm front	Cold front	Squall line	Squall line

Gage density requirements are illustrated further in Table 20 which shows percentage sampling errors with various 1-minute mean rates and G = 10 mi/gage in four selected thunderstorms. Storm type, storm mean intensity ($\bar{R}$), duration (T), and total storm rainfall (P) are also shown. These storms show the generally observed trend for decreasing percentage error with increasing 1-minute rainfall rate. However, in some storms the opposite trend was observed, as shown in Table 21 which contains the regression constants of each individual storm equation, as applied to Equation (6). Both Tables 20 and 21 stress the variability in sampling error with a given gage density between storms of the same general type.

From the individual storm equations, a median equation was derived:

$$\text{Log } E = -1.522 + 0.87 \text{ Log } R + 0.52 \text{ Log } G \qquad (7)$$

in which the parameters have the same interpretation as in Equation (6). This equation may be used to derive generalized estimates of the average sampling error of 1-minute mean rainfall rates on 100 mi^2. Table 22 was calculated from this equation to illustrate the magnitude of the percentage errors with this generalized equation.

Table 21. Regression constants for storm equations

Date	Log intercept	R-exponent	G-exponent
7/ 2/52	-1.889	0.86	0.76
7/ 3/52	-2.622	0.61	0.58
7/ 7/52	-0.905	1.09	0.69
7/ 8/52	-1.352	1.02	0.57
7/16/52	-0.160	1.31	0.47
8/ 3/52	-1.114	1.07	0.79
8/ 3/52	-1.534	0.92	0.68
8/20/52	-1.811	0.84	0.48
9/ 1/52	-1.516	0.85	0.51
9/14/52	-1.068	0.92	0.35
9/18/52	-1.751	0.72	0.42
10/14/52	-2.334	0.70	0.60
4/ 9/53	-0.721	1.10	0.51
4/24/53	-3.243	0.39	0.45
5/ 6/53	-2.381	0.66	0.56
6/ 5/53	-1.374	0.88	0.38
6/ 8/53	-2.180	0.59	0.52
6/25/53	-1.154	0.95	0.43
7/ 2/53	-2.013	0.82	0.63
7/ 5/53	-1.805	0.76	0.41
7/16/53	-1.529	0.97	0.57
7/17/53	-1.178	0.92	0.38
8/ 3/53	-1.182	0.95	0.62
8/ 7/53	-1.635	0.83	0.46
8/ 8/53	-1.275	1.02	0.74
9/ 6/53	-1.044	1.02	0.52
9/18/53	-1.763	1.08	0.48
11/20/53	-1.740	0.78	0.52

The median 1-minute rate from the 1952-1953 storm sample was 0.2 inch/hour. Table 22 indicates an average sampling error with this rate ranging from 16% with G = 5 mi^2/gage, increasing gradually to 38% at 25 mi^2/ gage, and to 76% at 100 mi^2/gage. This example illustrates the extremely dense network that would be needed to derive 1-minute mean rates with a high degree of accuracy for a specific minute of time within a storm. If rainfall rate is to serve as a verification tool in weather modification, it appears more logical to turn to a combination of raingages and 10-cm radar to evaluate short-period rainfall rate properties and their changes in space and time within midwestern convective storms. The initial cost and operational requirements would be prohibitive in most experiments to support the necessary raingage network density.

Table 22. Generalized estimates of percentage sampling error of 1-minute mean rate.

1-minute mean rate (in/hr)	Percent sampling error for given gage density (mi^2/gage)				
	5	10	25	50	100
0.05	20	29	46	66	94
0.1	18	26	42	59	84
0.2	16	23	38	53	76
0.5	14	20	33	46	66
1.0	13	18	29	42	60
2.0	12	17	26	38	54
5.0	10	14	23	33	46

Table 23 further defines the sampling problem. This table shows multiple correlation coefficients in each storm between E and the two independent variables, R and G, of Equation (6). The variance explained in percent is also listed for each storm, along with total storm rainfall and storm duration. The unexplained variance must then be attributed to various other factors influencing the sampling error, including the several mentioned earlier. Over 50% of the variance is unexplained in 50% of the storms shown in Table 23.

STORM OF JULY 5, 1953

The storm of July 5, 1953, has been selected to illustrate several characteristics of the 1-minute rate distributions in an individual storm. The illustrations are based primarily upon average rates for the 100 mi^2 network. This storm was associated with thunderstorms accompanying a squall line passage. It had a network duration of 54 minutes, an average total storm rainfall of 0.83 inch, and an average 1-minute rate of approximately 0.92 inch/hour.

Fig. 27 shows the distribution of areal mean rainfall rates with advancing time through the storm. Basically, it was a single-line storm.

Table 23. Correlation of sampling error with 1-minute mean rainfall rate and gage density in individual storms.

Date	Correlation coefficient	Variance explained (%)	Total rainfall (in)	Storm duration (min)
7/ 2/52	0.71	50	0.67	181
7/ 2/52	0.86	74	0.04	120
7/ 3/52	0.60	36	0.03	83
7/ 7/52	0.83	69	0.10	74
7/ 8/52	0.51	26	0.22	275
7/16/52	0.60	36	0.26	257
8/ 3/52	0.72	52	0.11	46
8/ 3/52	0.82	67	0.45	131
8/20/52	0.60	36	0.25	226
9/ 1/52	0.59	35	0.05	29
9/14/52	0.82	67	0.10	76
9/18/52	0.70	49	0.94	181
10/14/52	0.57	32	0.14	87
4/ 9/53	0.80	64	0.05	39
4/24/53	0.45	20	0.11	88
5/ 6/53	0.53	28	0.26	154
6/ 5/53	0.83	69	0.36	79
6/ 8/53	0.58	34	0.61	71
6/25/53	0.72	52	0.75	80
7/ 2/53	0.73	53	0.49	100
7/ 5/53	0.66	44	0.83	54
7/16/53	0.64	41	0.61	104
7/17/53	0.64	41	0.14	61
8/ 3/53	0.77	59	0.05	51
8/ 7/53	0.76	58	0.39	84
8/ 8/53	0.77	59	0.10	70
9/ 6/53	0.67	45	0.08	141
9/18/53	0.77	59	0.08	164
11/20/53	0.61	37	0.03	36
Median	0.70	49	0.14	84

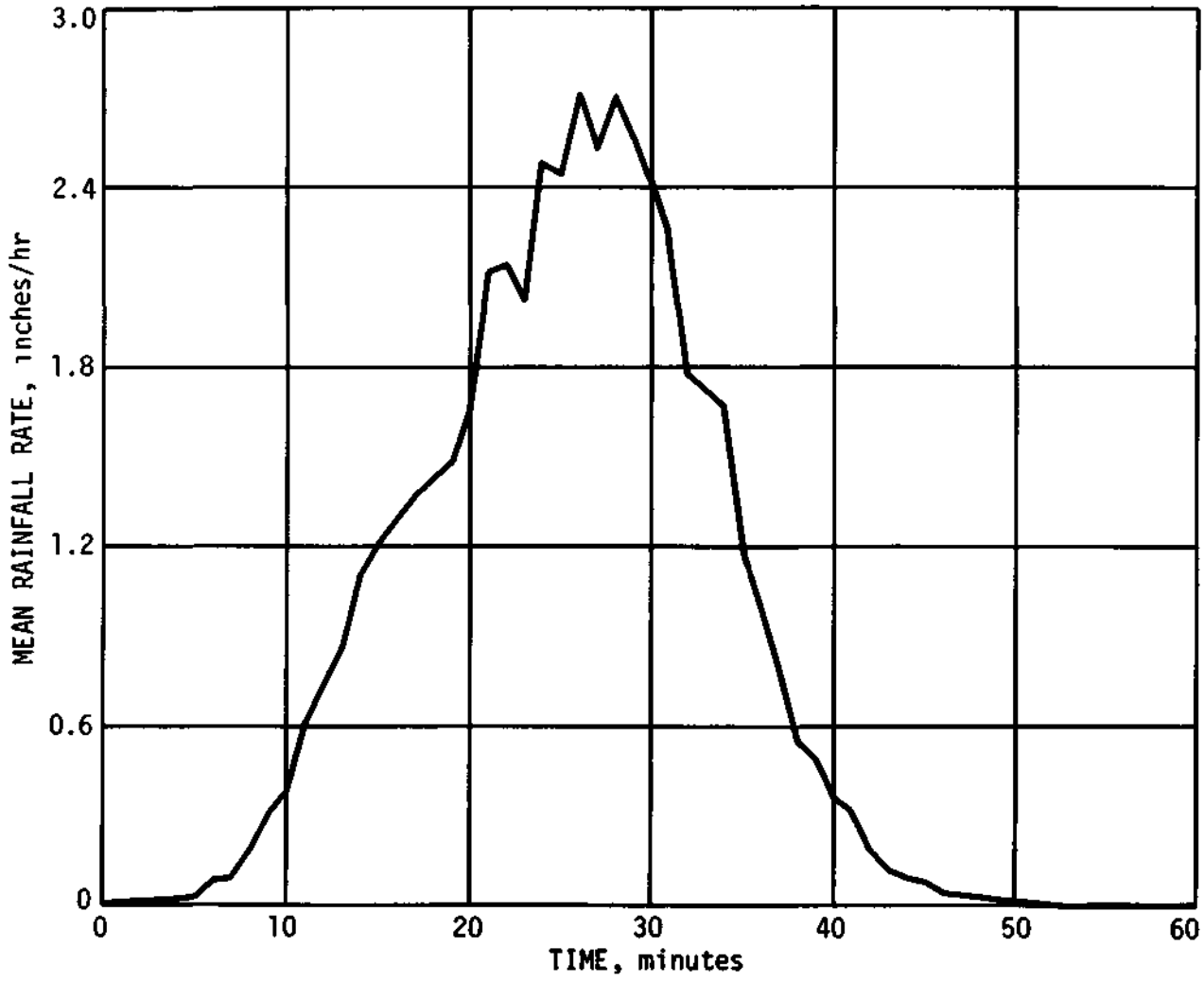

Figuve 27. Time distribution of areal mean rate on 7/5/53

Fig. 28 shows the time distribution at gage 29 near the center of the network. At this point, there are indications of the passage of two strong cells within the squall line, the first peaking in intensity about 13 minutes after the start of rainfall and the second at 22 minutes after the storm began. The peak 1-minute rate was 6.0 inches/hour at gage 29 compared with a 2.7-inch peak average over the 100 mi^2 about the same time.

Fig. 29 shows the average time rate of change in rainfall rate (sequential variability) from minute-to-minute throughout the storm on the 100 mi . The sequential variability (D) was 0.11 inch/hour in this storm. The relative variability of D was 110% in the July 5 storm. Similar statistics for gage 29 were 0.42 inch/hour for the sequential variability and 147% for the relative variability.

The spatial correlation pattern about gage 29 is illustrated in Fig. 30. Typically, the correlation coefficient decreases quite rapidly with distance, especially westerly from the correlating point. The correlation pattern for this storm is quite similar to the average pattern for the 29 storms in 1952-1953 shown in Fig. 19.

Fig. 31a was constructed from Fig. 27 to define further the time distribution characteristics of the storm and to normalize and type the time distribution for comparison and combining with other storms. This is an example of a second quartile storm, one in which the heaviest rainfall occurs in the second 25% of the storm period.

Table 24 shows average area-depth relations of 1-minute rainfall rate on the 100 mi^2 during 10 minutes of the heaviest rainfall. These data illustrate both the relatively rapid change in areal mean rainfall rate within a given area and the time variation in rate on the area from minute-to-minute. As pointed out earlier, the area-depth presentation provides a measure of both the spatial and time variability in one set of curves (or tables). Table 25 shows area-depth envelope relations for the same 10 minutes. Interpretation of this table can be illustrated by referring to minute 20. During this time, the 2 mi^2 with heaviest rainfall had rates equalling or exceeding 4.2 inches/hour. This decreased gradually to 1.8 inches/hour over the 50% of the 100 mi^2 with heaviest rates. By the time all 100 mi^2 was included, the enveloping rate was down to 0.1 inch/hour. This presentation also provides both a space and time measure of the variation in rainfall rate in a single family of curves.

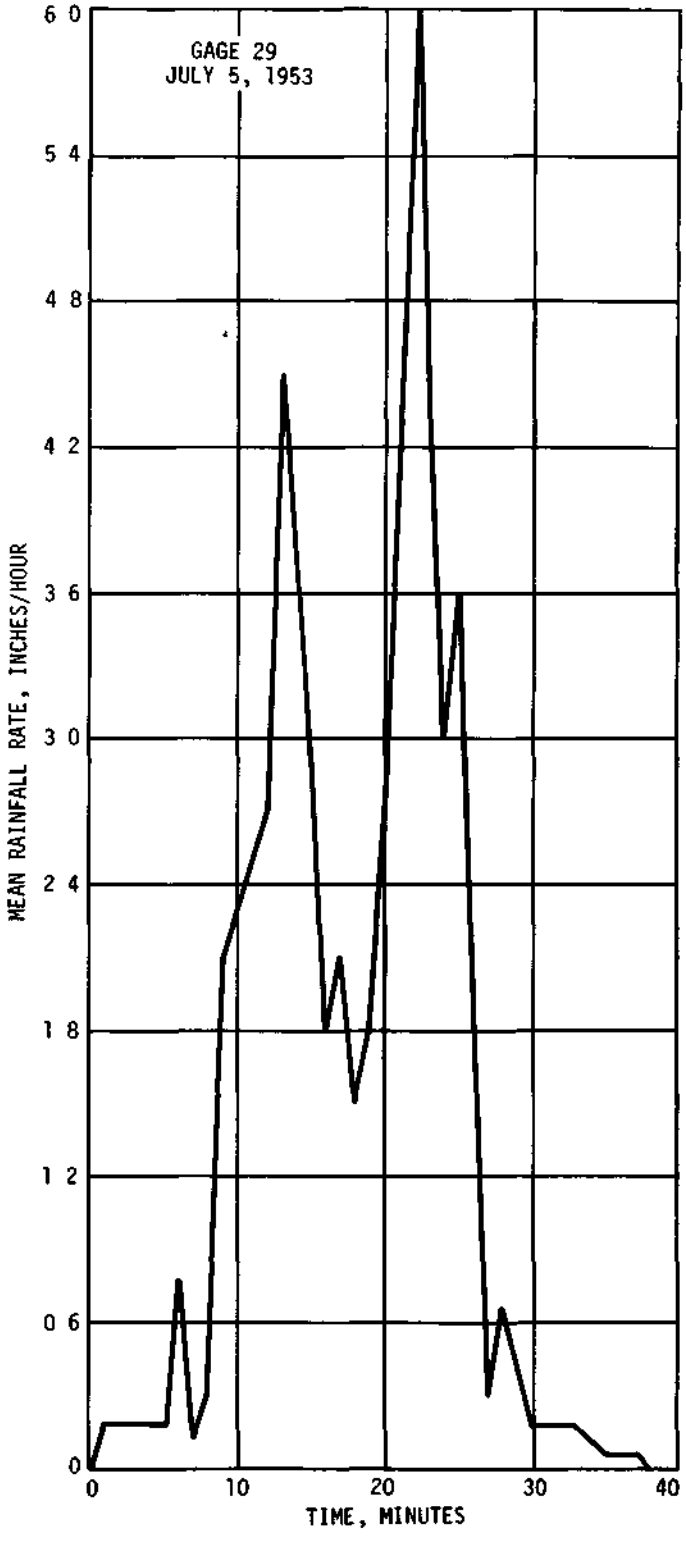

Figure 28. Time distribution of point rate on 7/5/53

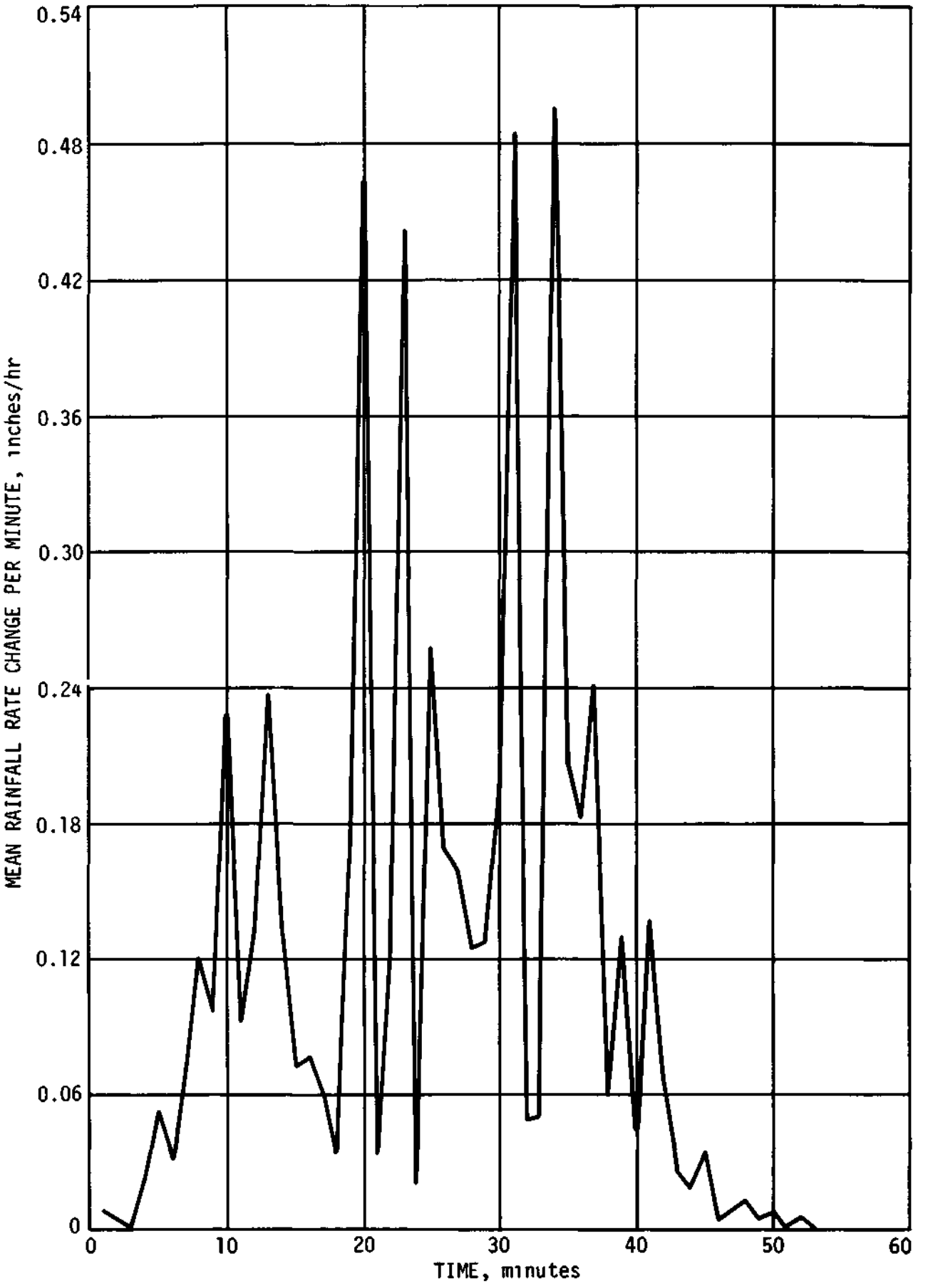

Figure 29. Sequential variability in mean rate on 7/5/53

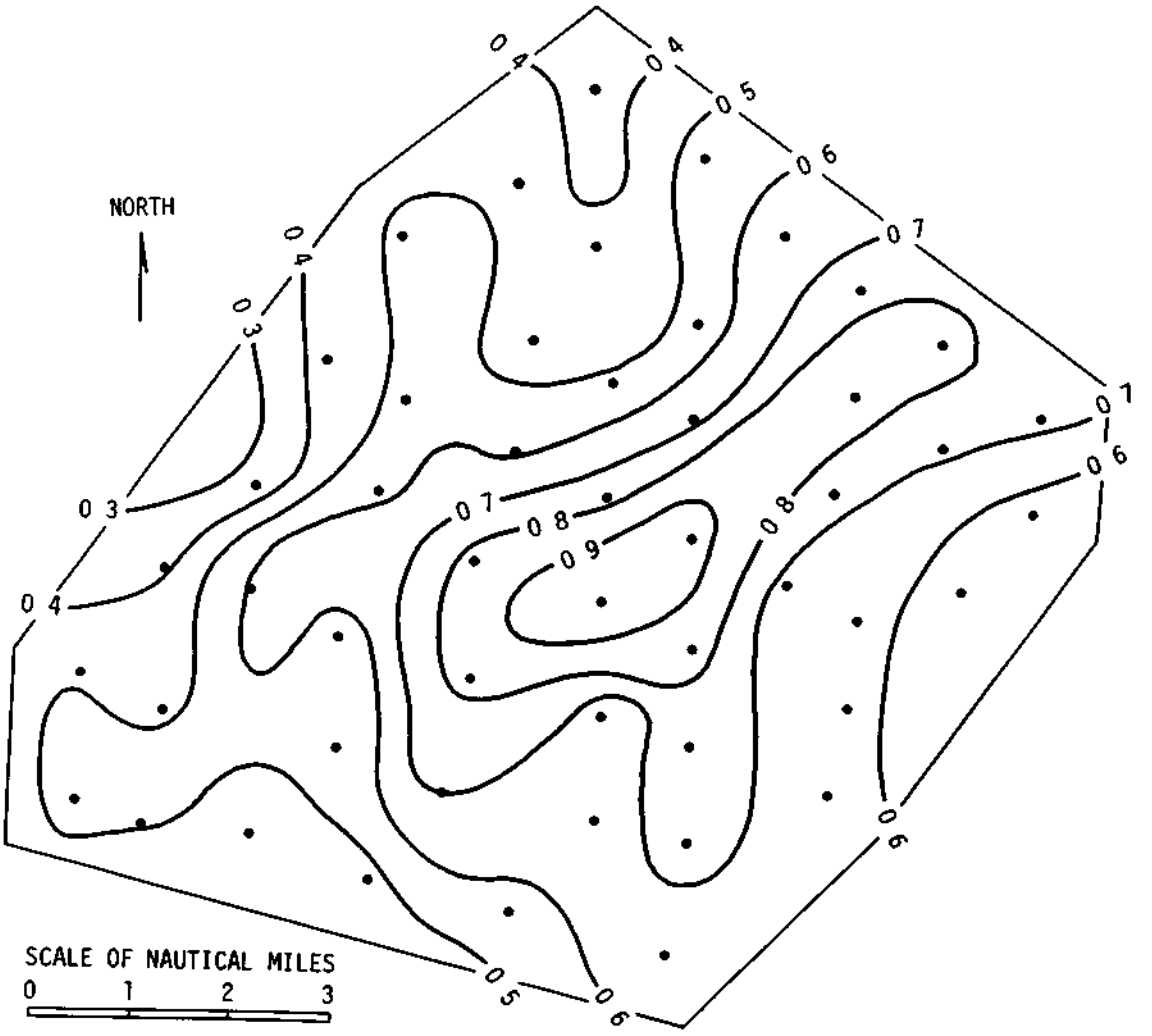

Figure 30. Spatial correlation pattern on 7/5/53

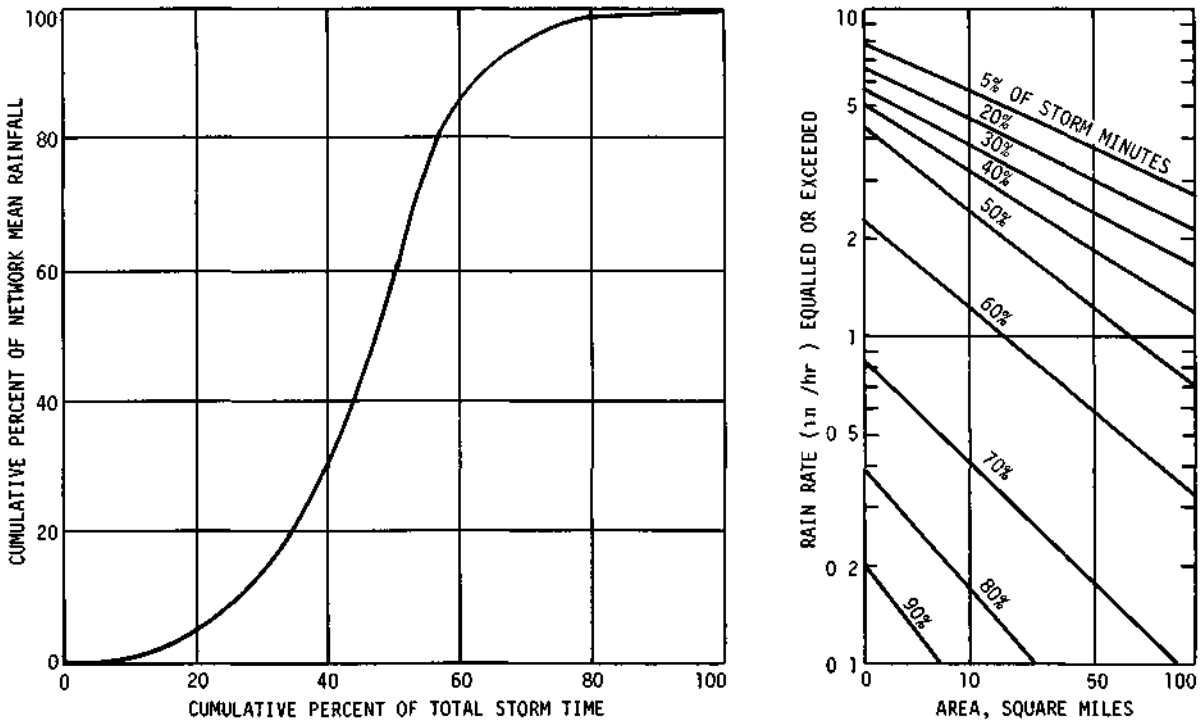

a. Normalized time distribution of storm rainfall *b. Average area-depth relations*

Figure 31. Time-space characteristics of rain distribution on 7/5/53

Table 24. Average 1-minute area-depth relations during period of heaviest rainfall on July 5, 1953.

Area (mi^2)	Average rainfall rate (in/hr) for given minute 10-min 20	21	22	23	24	25	26	27	28	29	median	10-min range
2	4.20	5.76	4.80	5.04	6.30	6.00	5.10	5.46	6.96	6.90	5.6	4.2 - 7.0
10	3.75	4.78	4.51	4.10	4.69	4.85	4.72	4.69	5.83	5.10	4.7	3.7 - 5.8
20	3.32	4.32	4.15	3.62	4.34	4.28	4.36	4.06	5.21	4.55	4.3	3.3 - 5.2
30	3.00	3.89	3.88	3.34	4.11	3.90	4.06	3.71	4.66	4.19	3.9	3.0 - 4.7
40	2.79	3.50	3.56	3.14	3.85	3.60	3.80	3.48	4.17	3.89	3.6	2.8 - 4.2
50	2.60	3.24	3.32	2.97	3.59	3.36	3.60	3.28	3.81	3.64	3.3	2.6 - 3 8
60	2.40	2.98	3.05	2.78	3.35	3.15	3.42	3.10	3.53	3.42	3.1	2.4 - 3.5
70	2.19	2.73	2.80	2.57	3.13	2.98	3.24	2.94	3.29	3.19	2.9	2.2 - 3.3
80	1.99	2.51	2.57	2.37	2.91	2.80	3.07	2.80	3.06	2.98	2.8	2.0 - 3.1
90	1.81	2.30	2.35	2.19	2.68	2.63	2.90	2.67	2.87	2.78	2.7	1.8 - 2.9
100	1.65	2.11	2.15	2.03	2.47	2.45	2.71	2.54	2.70	2.58	2.5	1.6 - 2.7
(Network mean rate)												

Table 25. One-minute area-depth envelope relations during period of heaviest rainfall on July 5, 1953.

Area (mi^2)	Rainfall rate (in/hr) equalled or exceeded for given minute										10-min median
	20	21	22	23	24	25	26	27	28	29	
2	4.2	5.8	4.8	5.0	6.3	6.0	5.1	5.5	7.0	6.9	5.6
10	3.3	4.3	4.2	3.5	4.3	4.2	4.4	3.6	5.1	4.3	4.3
20	2.7	3.6	3.6	3.0	3.9	3.5	3.8	3.1	4.2	3.8	3.6
30	2.3	2.7	3.0	2.7	3.6	3.0	3.3	2.9	3.3	3.3	3.0
40	2.1	2.3	3.4	2.4	3.0	2.6	3.0	2.7	2.5	2.7	2.6
50	1.8	2.1	2.1	2.1	2.4	2.3	2.7	2.4	2.3	2.5	2.3
60	1.2	1.4	1.5	1.7	1.9	2.1	2.4	2.1	2.1	2.0	2.0
70	0.8	1.2	1.2	1.2	1.6	1.8	2.1	1.9	1.7	1.7	1.7
80	0.5	0.8	0.7	0.9	1.1	1.5	1.8	1.8	1.5	1.4	1.3
90	0.4	0.5	0.5	0.7	0.7	1.1	1.4	1.5	1.3	1.1	0.9
100	0.1	0.3	0.1	0.4	0.5	0.5	0.6	1.2	0.9	0.3	0.5

Fig. 31b shows the frequency distribution of average area-depth relations for 1-minute intervals throughout the storm. Thus, during the minute of maximum intensities, the rate averages 2.8 inches/hour over the 100 mi^2, increasing to 6.0 inches/hour over the 10 mi^2 of heaviest rainfall within the network, and to 7.4 inches/hour in the 2 mi^2 at the intensity center of the storm. Similarly, 10% of the minutes had 100 mi^2 mean rates equalling or exceeding 2.4 inches/hour. The mean rate decreased to 0.67 inch/hour when 50% of the minutes are included, and to less than 0.01 inch/hour when 70% of the minutes are enveloped.

Fig. 32 shows an example of the effect of gage density on sampling the average rainfall rate on the 100 mi^2 during the 54-minute storm. Here, we have related sampling error in percentage to mean rainfall rate (inch/hour) for selected sampling densities of gages. The assumption was made that the 50 gages provided a very close approximation of the true mean, and, based upon previous experience with similar studies, the data were fitted to an exponential regression equation. Fig. 32 indicates that under the conditions of this storm (or storms of similar characteristics), 1 gage in the 100 mi^2 would have had an average error of nearly 30% in measuring mean rainfall rates of 1 inch/hour. This sampling error gradually decreases to 21% with 50 mi^2 per gage, 11% with 10 mi^2 per gage, and 8% with 5 mi^2 per gage.

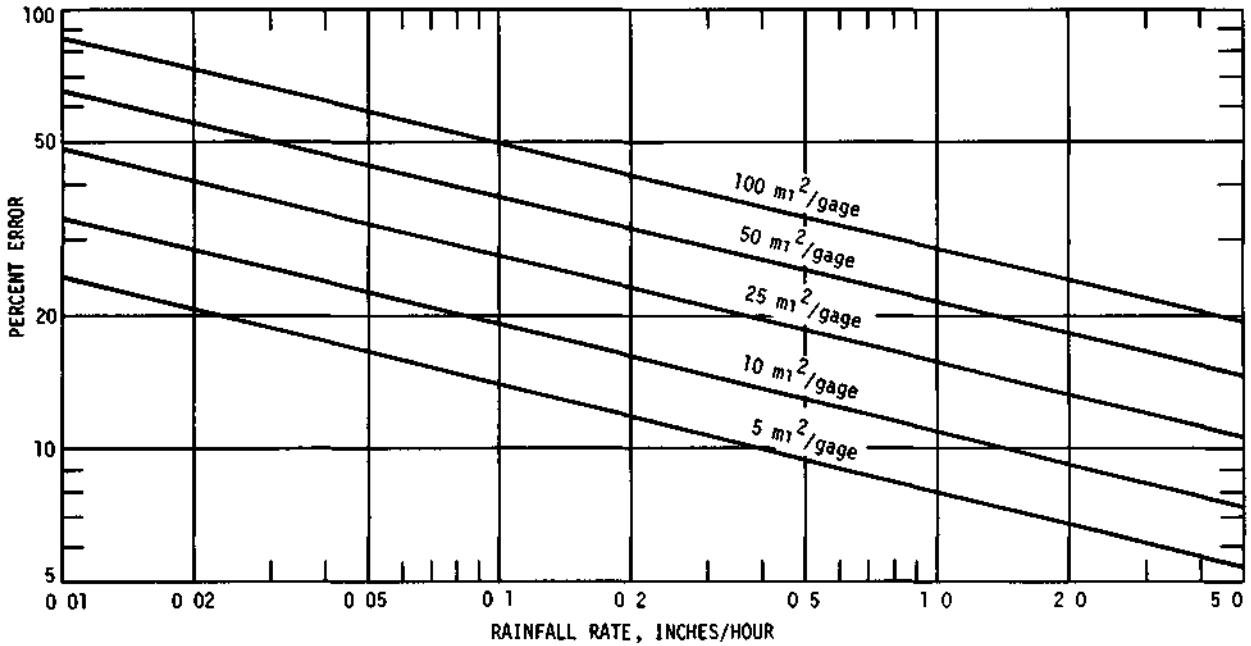

Figure 32. Rainfall rate sampling relations on 7/5/53

This storm provides an excellent example of the time and space variability in relatively intense thunderstorms during the warm season in the Midwest. Typical differences in point and areal time distributions have been shown in Figs. 27 and 28. A convenient method of typing time distributions has been illustrated in Fig. 31a. The sequential variability, shown in Fig. 29, further defines the time distribution and emphasizes its great variability from minute-to-minute. Spatial characteristics are portrayed by the correlation pattern of Fig. 30 and the area-depth relations presented in Tables 24-25 and Fig. 31b. The problem of measuring areal mean rainfall rates accurately is brought out by the gage density requirements shown in Fig. 32.

PART III

STATISTICAL TESTS

USE OF RAINFALL RATE MEASUREMENTS FOR THE EVALUATION OF WEATHER MODIFICATION EXPERIMENTS

The evaluation of a cloud seeding experiment to increase or decrease precipitation is a problem of tremendous complexity. Although many physical and biological experiments can be conducted under various controlled conditions, in the weather modification experiment, many of the important variables such as pressure, temperature, and wind cannot be controlled. Further, present day forecasting methods are not sensitive enough to predict the amount of rain that would have fallen had cloud seeding not been conducted.

To resolve the evaluation problem, experimenters have turned largely to one of two basic experimental plans with their various modifications in order to attach statistical significance to the results. The first of these is the target-control method. In this design, the rainfall in one area (the "seeded" or target area) is compared with that in another area (the "non-seeded" or control area) in which it is assumed that none of the seeding agent is present. The comparison is usually achieved through the use of an "historical" regression line. If a successful application of this method is to be made, there must be a high degree of correlation between the rainfall of the two areas. An often used variation in this method is to construct a regression line for both the seeded and non-seeded years and test to determine if the two lines coincide (Dennis and Kriege, 1966).

The second frequently used plan employs randomization of seeded and non-seeded days over a single (target) area. This plan allows for proper randomization, and several statistical tests may be employed. The Arizona experiment (Battan, 1966) and the Project Whitetop experiment (Braham, 1966) were designed along these lines. A modification of this method, called crossover, is one in which two nearby experimental areas are seeded with random choice of area (Smith et al., 1965). Practically all evaluation schemes using these methods have involved a summation of the rainfall over an increment of time (usually a day or a storm) in a particular area so that a total or average rainfall value is obtained. This average is then used as the experimental unit in the subsequent statistical analysis. Hence, there may be no effect on the average areal rainfall, but subtle changes may be occurring in the rainfall

rate which may be producing beneficial or detrimental effects on the industry and/or agriculture of the region.

It is the objective of this section to determine the feasibility of using changes in rainfall rate to evaluate the effect of seeding. In this study, three experimental designs and two statistical tests were used to define the duration of an experiment needed to detect various degrees of change in rainfall rate that might be produced by seeding efforts.

Theoretical Frequency Distributions

The 1-minute rainfall amounts for every 5 minutes from the start of each storm in the 29-storm sample for the 25, 50, and 100 mi^2 areas and gage 29 were grouped together to form frequency distributions. Thus, a "typical" warm season storm was formed in which the frequency distributions were specified for every 5 minutes. This partitioning included the zero rainfall amounts from the end of each storm in the 29-storm sample until the end of minute 130. The zero rainfall amounts during certain minutes within each storm were also included in the sample, thus providing 29 1-mmute amounts(I.e., rainfall rate) for every 5 minutes. A mixed distribution function was then estimated on the basis of two assumptions. First, there is a non-zero probability of rain on every 5 minutes from the start of the storm. Secondly, when rain does occur, the 1-minute amount of rainfall is distributed as a log-normal or gamma variable. The general form of the mixed distribution function can be written as:

$$G(x) = P(X < a) = P(X = 0) + P(X > 0) \cdot P(X < a \mid X > 0) \qquad (8)$$

where:

$P(X < a)$ = probability of receiving less than a specified 1-minute amount of rain at the end of a given 5-minute period

$P(X = 0)$ = probability of receiving no rain at the end of a given 5-minute period and is equal to the number of zero rainfall amounts divided by 29

$P(X > 0)$ = probability of receiving some rain at the end of a given 5-minute period and is equal to the number of non-zero 1-minute rainfall amounts divided by 29

$P(X < a \mid X > 0)$ = probability of receiving less than a specified 1-minute amount of rain given that rain has occurred at the end of a given 5-minute period

The term $P(X < a \mid X > 0)$ is given by:

$$P(X < a \mid X > 0) = F(x) = \int_0^a f(x)dx \qquad (9/$$

The density function, f(x), can be specified as any distribution. For this study, mixed distributions with the log-normal and gamma density functions were used. The log-normal and gamma density functions were then fitted to the area and point data, and the data from the 100 mi^2 area are shown in Fig. 33. The density function for the log-normal distribution is;

$$f(x) = \frac{1}{x\sigma_y \sqrt{2\pi}} e^{-(y-\mu_y)^2/2\sigma_y^2} \qquad x > 0, -\infty < \mu < \infty, \sigma > 0 \qquad (10)$$

where:

$y = \ln x$

μ_y = mean of the ln x

o_y = standard deviation of the ln x

The density function for the gamma distribution is:

$$f(x) = \frac{1}{\beta^\gamma \Gamma(\gamma)} x^{\gamma-1} e^{-x/\beta} \qquad x > 0, \gamma > 0, \beta > 0 \qquad (11)$$

The symbols ß and γ are location and shape factors, respectively, and are estimated by the method of maximum likelihood (Thorn, 1958). The sample estimates of the log-normal parameters are listed in Table 26 and those for the gamma parameters are shown in Table 27.

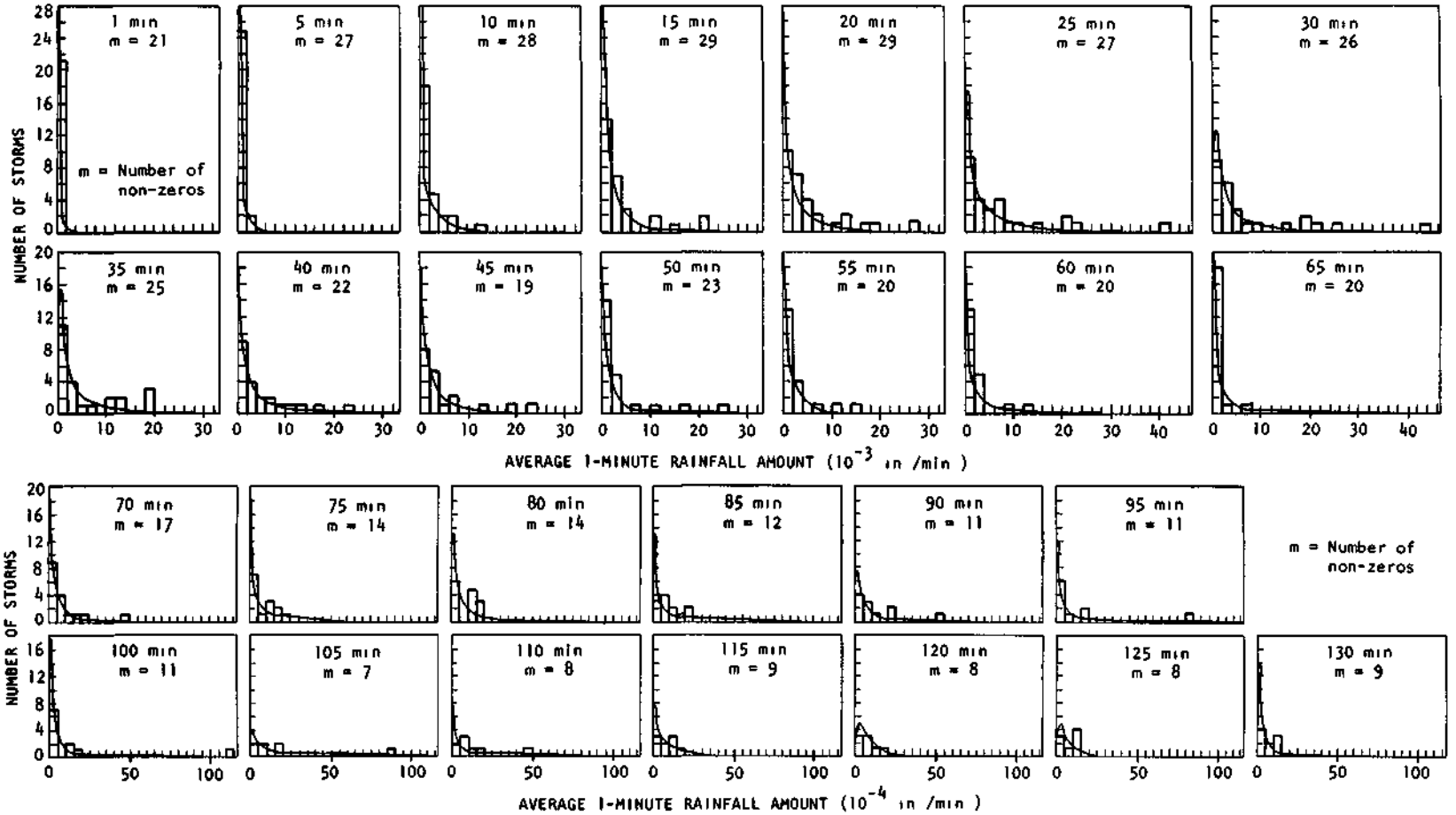

Figure 33. Frequency distributions of average 1-minute rainfall amounts for selected times during storms

Table 26. Sample estimates of the log-normal distribution for the various areas and for gage 29.

Min. from start of storm	μ_y - log mean 25 mi^2 area	50 mi^2 area	100 mi^2 area	Gage 29	σ_y - log standard deviation 25 mi^2 area	50 mi^2 area	100 mi^2 area	Gage 29
1	-8.806	-8.864	-9.416	—	.763	1.292	1.216	--
5	-7.470	-7.761	-8.270	—	1.184	1.342	1.558	--
10	-6.611	-7.316	-7.198	-4.987	1.815	1.882	1.723	1.055
15	-6.026	-6.388	-6.511	-5.254	1.554	1.648	1.663	1.148
20	-6.014	-5.998	-6.141	-5.109	1.793	1.705	1.742	1.200
25	-5.310	-5.574	-5.761	-4.794	1.513	1.476	1.623	1.152
30	-5.624	-5.542	-5.742	-4.861	1.642	1.320	1.472	1.440
35	-5.645	-5.934	-6.012	-5.202	1.636	1.607	1.558	1.168
40	-5.964	-6.0303	-6.241	-5.545	1.660	1.571	1.659	1.335
45	-6.289	-6.121	-6.263	-5.646	1.575	1.573	1.718	1.163
50	-6.581	-6.664	-7.176	-5.554	1.691	1.655	1.985	1.351
55	-6.443	-6.792	-7.107	-5.784	1.093	1.583	1.705	.967
60	-6.375	-7.179	-7.456	-6.055	1.308	1.978	2.093	.672
65	-7.244	-7.612	-7.907	-6.125	1.303	1.533	1.621	.723
70	-7.474	-7.891	-8.190	—	1.369	1.569	1.558	--
75	-7.394	-7.601	-8.287	—	1.157	1.282	1.845	--
80	-6.984	-7.614	-7.828	-6.134	1.189	1.448	1.576	.162
85	-6.974	-7.082	-7.705	-6.125	.999	1.092	1.714	1.047
90	-7.025	-7.148	-7.424	-6.426	.865	1.105	1.445	.500
95	-6.850	-7.739	-7.782	-5.459	1.120	1.633	1.717	1.100
100	-7.302	-7.966	-8.062	-6.089	1.387	1.670	1.774	.530
105	-6.486	-6.569	-7.173	—	.782	.959	1.550	--
110	-6.450	-6.564	-7.494	—	.528	.692	1.660	--
115	-7.212	-7.510	-7.657	-6.631	1.023	1.359	1.291	.555
120	-7.315	-7.715	-7.537	-6.411	.939	1.068	.880	.432
125	-7.505	-7.418	-7.519	—	1.218	.966	.937	--
130	-6.486	-7.267	-8.192	—	.495	1.022	1.593	--

From Table 26 it is seen that the maximum log mean rainfall rate occurs at minute 30 for the 50 and 100 mi^2 areas and at minute 25 for the 25 mi^2 area. For the areal data the means are very stable up to minute 120. The instability from this point on is largely due to decreasing sample size. From minute 130 on the trend becomes erratic and the sample size is too small to attach meaningful conclusions to the data. This is the reason for forming distributions only for minutes less than or equal to minute 130. For the point data, represented by gage 29, the log-normal mean tends toward greater instability

and was estimated from a smaller number of non-zero rainfall amounts. When the number of non-zero rainfall amounts were less than 5 for a given minute, the log mean is not included in the table because of the unreliability of the estimate.

For all areas, and for gage 29, the log standard deviation is very unstable and the pattern over time tends toward a random series.

Table 27. Sample estimates of the gamma distribution for the various areas and for gage 29.

	γ = gamma shape parameter				ß = gamma location parameter			
Mm. from start of storm	25 mi^2 area	50 mi^2 area	100 mi^2 area	Gage 29	25 mi^2 area	50 mi^2 area	100 mi^2 area	Gage 29
1	1.604	.724	.798	—	.0001	.0005	.0002	--
5	.999	.913	.684	—	.0010	.0009	.0010	--
10	.597	.548	.613	1.464	.0070	.0042	.0036	.0068
15	.696	.654	.642	.936	.0086	.0069	.0064	.0106
20	.651	.720	.677	.963	.0105	.0083	.0082	.0116
25	.085	.821	.765	1.012	.0123	.0098	.0098	.0146
30	.652	.795	.733	.715	.0149	.0107	.0103	.0262
35	.715	.688	.720	1.034	.0120	.0097	.0082	.0094
40	.676	.697	.675	.628	.0098	.0086	.0075	.0176
45	.676	.707	.669	.938	.0071	.0076	.0074	.0071
50	.628	.555	.479	.549	.0063	.0074	.0071	.0237
55	1.024	.618	.564	1.141	.0028	.0053	.0048	.0045
60	.744	.525	.523	2.563	.0053	.0054	.0042	.0011
65	.733	.665	.545	1.740	.0023	.0020	.0019	.0017
70	.750	.638	.630	—	.0017	.0016	.0012	--
75	1.034	.987	.397	—	.0011	.0009	.0019	--
80	1.165	.853	.815	35.330	.0013	.0012	.0010	.0006
85	1.674	1.689	.798	.981	.0008	.0007	.0012	.0041
90	1.920	1.329	.829	4.180	.0006	.0009	.0015	.0004
95	.968	.625	.558	.978	.0020	.0020	.0025	.0080
100	.677	.498	.463	3.820	.0026	.0029	.0033	.0007
105	1.602	1.105	.671	—	.0013	.0022	.0030	--
110	3.353	1.915	.745	—	.0006	.0010	.0018	--
115	1.431	1.061	1.119	2.754	.0008	.0009	.0007	.0006
120	1.280	1.169	1.839	5.668	.0008	.0006	.0004	.0003
125	1.122	1.532	1.749	—	.0082	.0006	.0004	--
130	4.143	1.593	.777	—	.0004	.0006	.0008	--

Table 27 reveals that the maximum of the gamma location parameter 8 occurs at minute 30 for all areas and for gage 29. Again, more instability occurs with smaller areas and with gage 29, and the pattern of (3 over time is very stable up to minute 70.

The behavior of the shape factor *y* is very erratic and tends toward a random series similar to the log standard deviation.

The probabilities of rain, $P(X > 0)$, for non-zero 1-minute rainfall amounts at the end of each 5-minute period of the "typical" storm were then computed as described in Equation 8. A plot of $P(X > 0)$ for each area and for gage 29 versus the time from the start of the storm is illustrated in Fig. 34. First, it is seen that the probability of rain at the end of a given 5-minute period is largest for the time period 15-20 minutes from the start of the storm. Secondly, the larger the area, the larger the probability of rain becomes. Finally, for gage 29, and for the 25 and 50 mi^2 areas, the probability of 1-minute rainfall amounts for a given time at the beginning of the storm is approximately the same as it is for the period 80 to 130 minutes after the start of the storm. Equation 8 and Table 26 or 27 can be used to obtain the probability of specific rainfall rates at the end of any 5-minute period. The term $P(X < a \mid X > 0)$ can be obtained from tables of the log-normal distribution and the incomplete gamma distribution.*

The log-normal and gamma distributions were then tested to ascertain how well they fit the prescribed data. The Kolmogorov-Smirnov "goodness of fit" test was used because it is more valid for small samples than is the chi square test. Since both parameters of each distribution are estimated from experimental data, the more common tables of D_n were not used, nor are they valid. Liffiefors (1967) has recently computed new tables which take this factor into consideration. The test statistic D_n (the maximum departure of the cumulative probabilities of the theoretical distribution from that of the actual distribution) was computed and the resulting probabilities $P(D > D_n)$ (i.e., the probability of obtaining a larger difference from random sampling) are tabulated in Table 28 for all areas and for gage 29.

* IBM 360 computer programs for computing these probabilities are available upon request from the Illinois State Water Survey.

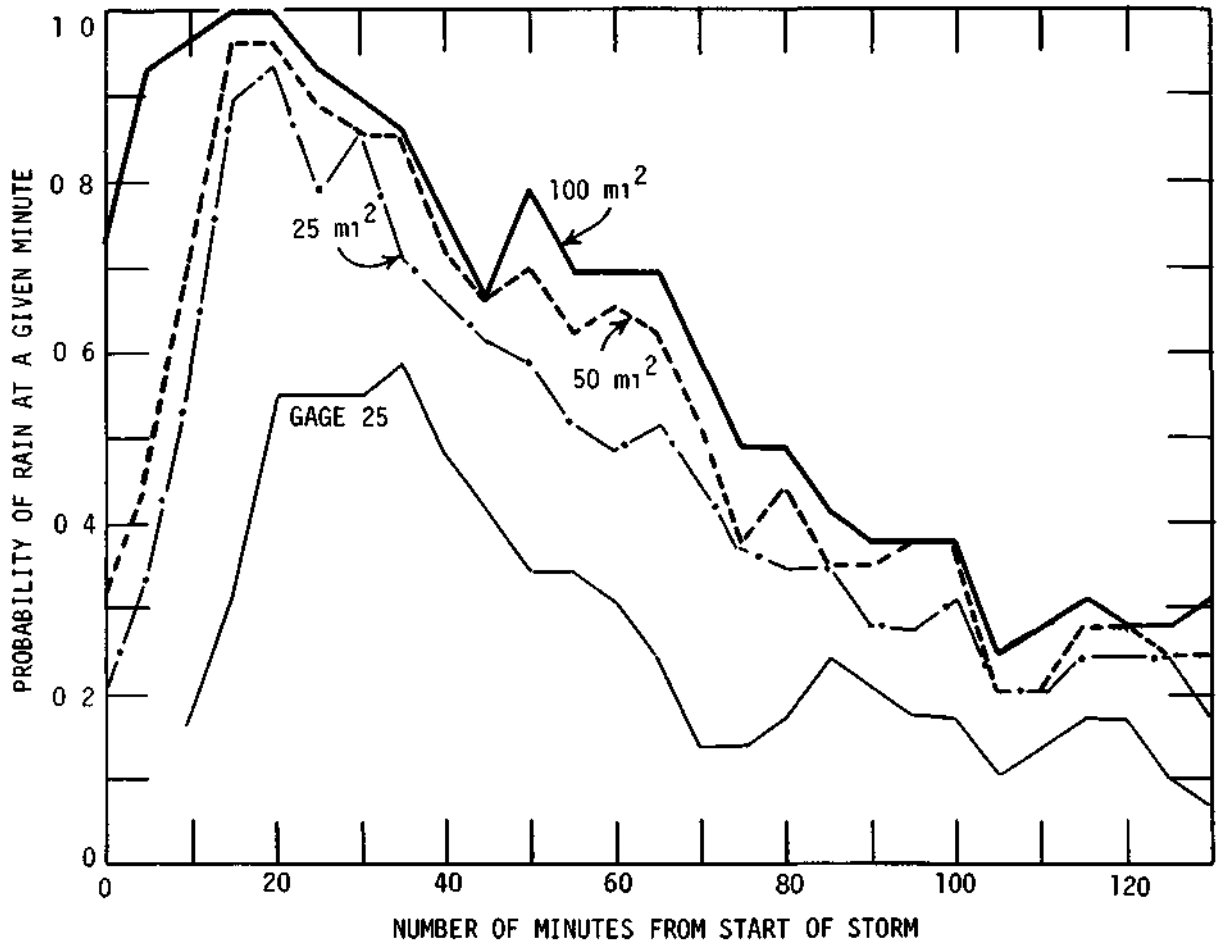

Figure 34. Probability of rain for various minutes during a storm

Table 28. "Goodness of fit" test for the log-normal and gamma distributions.

$P(D > D_n)$

Min. from start of storm	Log-normal				Gamma			
	25 mi^2 area	50 mi^2 area	100 mi^2 area	Gage 29	25 mi^2 area	50 mi^2 area	100 mi^2 area	Gage 29
1	> .20	> .20	> .20	—	> .20	.118	> .20	--
5	> .20	> .20	> .20	—	> .20	> .20	> .20	--
10	> .20	> .20	> .20	> .20	> .20	> .20	> .20	> .20
15	> .20	> .20	> .20	> .20	> .20	> .20	> .20	> .20
20	.05	> .20	> .20	> .20	> .20	> .20	> .20	> .20
25	> .20	.12	> .20	> .20	> .20	> .20	> .20	> .20
30	> .20	> .20	> .20	> .20	> .20	> .20	.124	> .20
35	> .20	> .20	> .20	> .20	> .20	> .20	> .20	> .20
40	> .20	> .20	> .20	.189	> .20	> .20	> .20	< .01
45	> .20	> .20	> .20	> .20	> .20	> .20	> .20	> .20
50	> .20	> .20	> .20	> .20	> .20	.188	> .20	.05
55	> .20	> .20	.10	> .20	> .20	.20	> .20	> .20
60	> .20	.19	.19	> .20	.07	> .20	> .20	> .20
65	> .20	> .20	> .20	> .20	> .20	> .20	> .20	> .20
70	> .20	> .20	> .20	—	> .20	> .20	> .20	--
75	> .20	> .20	> .20	—	> .20	> .20	.112	--
80	> .20	.10	< .01	> .20	> .20	.183	.029	< .01
85	> .20	.13	< .01	> .20	> .20	> .20	.144	> .20
90	> .20	> .20	> .20	> .20	> .20	> .20	> .20	> .20
95	> .20	> .20	> .20	> .20	> .20	> .20	> .20	> .20
100	> .20	> .20	> .20	> .20	> .20	.143	> .20	> .20
105	> .20	> .20	.19	—	> .20	> .20	> .20	--
110	> .20	> .20	> .20	—	> .20	> .20	> .20	--
115	> .20	.09	> .20	> .20	> .20	> .20	> .20	> .20
120	> .20	> .20	> .20	> .20	> .20	> .20	> .20	> .20
125	> .20	> .20	> .20	—	> .20	> .20	> .20	--
130	> .20	> .20	> .20	—	> .20	> .20	> .20	--

The table indicates that the rainfall rate data can be fitted extremely-well by the log-normal and gamma distributions. Since most of the probabilities are greater than 0.20, and since both distributions appear to fit the data equally well, it was decided to use the log-normal distribution in subsequent studies of sample size requirements. The only two data sets that do not fit the log-normal distribution at the often cited 0.05 significance level are the

data sets for minute 80 and 85 from the 100 mi^2 area. These two sets of data were then fitted by truncated log-normal distributions and it was discovered that truncation points of a = 0.00101 and a = 0.00061 were required to obtain a fit. Six values were truncated from the 80-minute sample and three from the 85-minute sample out of the non-truncated samples which had 14 and 12 values, respectively. The resulting probabilities, $P(D > D_n)$, were greater than 0.20 for the 80-minute sample and equal to 0.181 for the 85-minute sample. The truncated log means were -8.355 and -7.936 for the 80- and 85-mmute samples, respectively, as compared with original values of -7.828 and -7.705. The truncated log standard deviations were 1.327 and 1.596 compared with original values of 1.576 and 1.714 for the 80- and 85-minute samples. By random chance, one would expect only 19 out of 20 distributions to fit. For this reason, and for the fact that the differences between truncated and non-truncated parameters were small, the log-normal distribution was used exclusively in the computations of sample size.

Experimental Design and Tests of Hypothesis

The number of storms and years required to obtain significance was computed for three designs and two tests using the rainfall rate data. These designs included (1) randomization of storms over a single target area into seeded and non-seeded storms with the non-seeded storms being the control, (2) random choice of storms to be seeded over a single target area with the historical record being the control, and (3) continuous seeding (on all potential storm days) with the historical record being the control.

Another design considered was the target-control continuous seed regression design wherein the data from the seeded days are compared with the data from a nearby control area. A small correlation coefficient eliminates the effectiveness of a target-control approach. As noted earlier in this report, the correlation of rainfall rates decreases rapidly as the distance between observational points increases (Table 9, Fig. 19).

The final design considered was the crossover design wherein the area to be seeded on a particular day is chosen at random. However, for rainfall rates the correlation coefficient is essentially zero for distances that would be required between areas in a crossover design. Under these conditions, the sample size requirements for the crossover design are identical to design (2) above.

In the statistical analysis the classical (non-sequential) analysis was employed. The components of the particular test being used were computed for the non-seeded distributions, then, with assumed changes in the distribution parameters, the sample size was computed through algebraic relations. In this analysis the storms which formed the distributions of rainfall rate for the various minutes were treated as the experimental units.

The normal 1-sample and 2-sample tests were used with all of the experimental designs. Under the assumption that the rainfall rate data were log-normal distributed, the following formula was used to obtain the number of observations required for the 2-sample non-sequential test (Davies, 1954):

$$n = \frac{2(\mu_\alpha + \mu_\beta)^2 s^2}{D^2} \qquad (12)$$

where*

μ_a = the normal deviate for a probability level

$\mu_ß$ = the normal deviate for ß probability level

D = difference in means it is desired to detect

s^2 = the variance

Various reductions of 6 equal to 0.05, 0.10, 0.20, 0.40, 0.60, and 0.80 were assumed and applied to the non-transformed data. The corresponding scale change was made on the transformed scale by the addition of the logarithm of (1-6). The variances were assumed to be equal, since the variance of the log-normal distribution is unaffected by scale changes in the variate. Equation 12 was then applied with s^2 equal to the variance of the logarithms and D equal to the logarithm of (1-o). For the random 1-sample test, Equation 12 is used directly to compute sample size. For the 1-sample continuous design, Equation 12 is divided by 2.0. With the daily single area random design, both samples must be obtained from the same area, therefore, Equation 12 must be multiplied by 2.0.

At this point, some thought should be given to how the data would actually be collected in this type of scheme for verifying changes in rainfall rate for selected times during the storm. In most seeding experiments, the data are collected for the seeded and non-seeded samples, and then a test of significance

IS made between the parameters of the resulting seeded and non-seeded distributions. In this method, many of the more subtle changes are masked, and the end result is an attempt to verify the results by changes in the overall average of these effects. For example, once the rainfall rate data were collected in an experiment, all of the non-seeded 1-minute rainfall amounts would have formed one distribution, the seeded 1-minute rainfall amounts would have formed another distribution.

The proposal being set forward here is to form a seeded and non-seeded distribution for every 5 minutes of the "typical" storm discussed previously. For the data in our 29-storm sample, this would mean 27 seeded and 27 non-seeded distributions since there are 27 distributions of 1-minute amounts when every 5 minutes through minute 130 are considered. The data would be collected in the same manner as described above, but once the data were collected, they would then be stratified to form the distributions for the various minutes. This method eliminates the sequential analysis approach (Schickedanz, Changnon, and Lonnquist, 1969) since the entire sample would be collected before the partitioning can occur. Thus, one is limited to the classical non-sequential approach for the rainfall rate experiment.

Fig. 35 illustrates the trend of the various distributional parameters for a 100 mi^2 area during the "typical" warm season storm in Illinois. For the first seeding model (model A) it is proposed that the average rainfall rate (upper left hand figure) could be increased at the end of every 5-minute increment during the storm. An alternate to model A is to decrease the rainfall rate at the end of each 5-minute increment.

The major emphasis in this report is on seeding model A. However, it has been suggested by some experimenters that seeding produces rainfall rates that are more uniform than those that occur naturally under similar meteorological conditions. Therefore, limited computations were performed to obtain a first approximation of the sampling requirements involved in verifying this type of seeding effect. In this model (model B), the rainfall rate regime was changed to an average constant rainfall rate over the entirety of the storm. This would effectively flatten the mean rainfall rate curve in Fig. 35.

For our pilot study of model B, the sample size requirements were computed for changing the rainfall rate to a constant rate of 0.25 inch/hour. It is

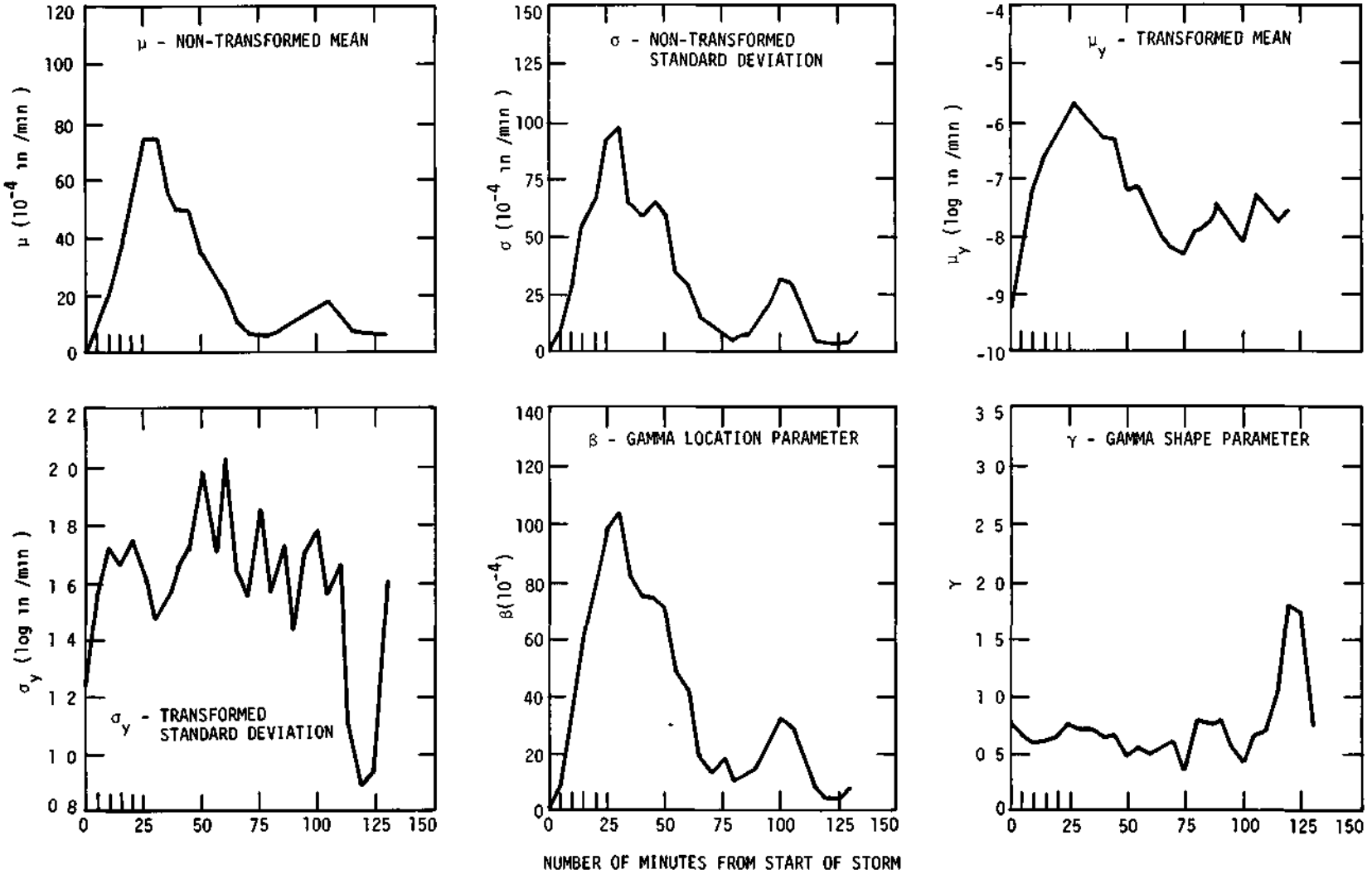

Figure 35. Relation of various distributional parameters with time from start of storm on 100 mi^1 area

realized that this is not a very realistic physical model, but computations based on this assumption do provide a first approximation of the magnitude of the sampling requirements. Time was insufficient to evaluate further other rainfall rates. The rate of 0.25 inch/hour was chosen for testing because it would provide beneficial quantities of water for agricultural and hydrologic purposes in warm season storms, and it is not an uncommon rate in such storms.

At a given minute in time, the sample size as computed by Equation 12 for a given a and ß level, and for a given increase or decrease, is independent of the magnitude of μ_y (the log mean). Thus, for seeding model A, the sample size is directly proportional to the log standard deviation. In model B, the magnitude is important because this determines the size of increase or decrease that is required to obtain a specified rainfall rate. For either model, the prediction of o_y (the log standard deviation) from μ (the non-transformed mean) and u_y is of interest, and can be estimated by the following relation (Schickedanz, 1967).

$$\sigma_y = \sqrt{\frac{2\,(\ln \mu - \mu_y)}{(1 - \lambda)^2}} \qquad (13)$$

where λ is equal to 1/n, n being the sample size. Equation 13 was used to compute σ_y for each of the log-normal distributions in the various areas and for gage 29. Table 29 contains a listing of the actual and computed values of σ_y along with the percentage differences for the 100 mi^2 area. It is seen that the minimum departure is 0.09% and the maximum departure is 20.94%. The average departure is 10.33%. The average departures for the 50 and 25 mi^2 areas and gage 29 are 11.07%, 11.60%, and 17.26%, respectively. This indicates that one can estimate σ_y in first approximation from p and u. This becomes important since the sample size is then directly proportional to σ_y .

In the computation of sample size for the rainfall rate experiment, all values must be adjusted to obtain the "effective" sample size. For example, if minute 1 requires 60 storms with non-zero amounts to obtain significance, and minute 25 requires 50 storms with non-zero amounts to obtain significance, how many storms are required for each minute to insure that both minutes will

have sufficient sample size? The number would not be 60 or 50 since the probabilities of obtaining a non-zero rainfall amounts for the 100 mi^2 area is 0.724 for minute 1 and 0.931 for minute 25. The effective sample size (ESS) can be computed by the following relation:

$$ESS = NZS/[P(X > 0)] \quad (14)$$

where:

NZS = is the non-zero sample size for a specific minute

P(X > 0) = is the probability of rain for a specific minute

Thus, for the above example, 42.2 would be the effective sample size for minute 1 and 53.7 for minute 25. Hence, 54 storms would be required to insure that both minutes would have sufficient sample sizes to obtain significance. The probabilities of rain for each minute of all three areas and for gage 29 are tabulated in Table 30.

Results

The number of years required to obtain significance was computed for all tests and designs. Fig. 36 is a comparison of the number of storms required to obtain significance for various decreases and for the type I error (a) of 0.05 and type II error (ß) Of 0.50. The upper scales represent the number of years to obtain significance for all three designs. If one is interested in detecting a 40% increase in the log mean, and σ_y is increased from 1.0 to 2.0, the sample required for detection is increased by 5 years for the 2-sample random test, 2.5 years for the 1-sample random test, and 1.3 years for the 1-sample continuous test. In order to detect a 20% increase, the corresponding numbers are 16, 8, and 2, respectively. The 5% curve required such exorbitant sample sizes that it was not included on the figure. If one knows the profile of X and σ through the storm, σ_y can be estimated from Equation 13 and then the sample size can be determined from Fig. 36. The other alternative is to compute σ_y (the standard deviation of the logarithms) directly. Once the sample size is computed from this figure or from Equation 12, the ESS (the effective sample size) must be computed using Equation 14 and Table 30.

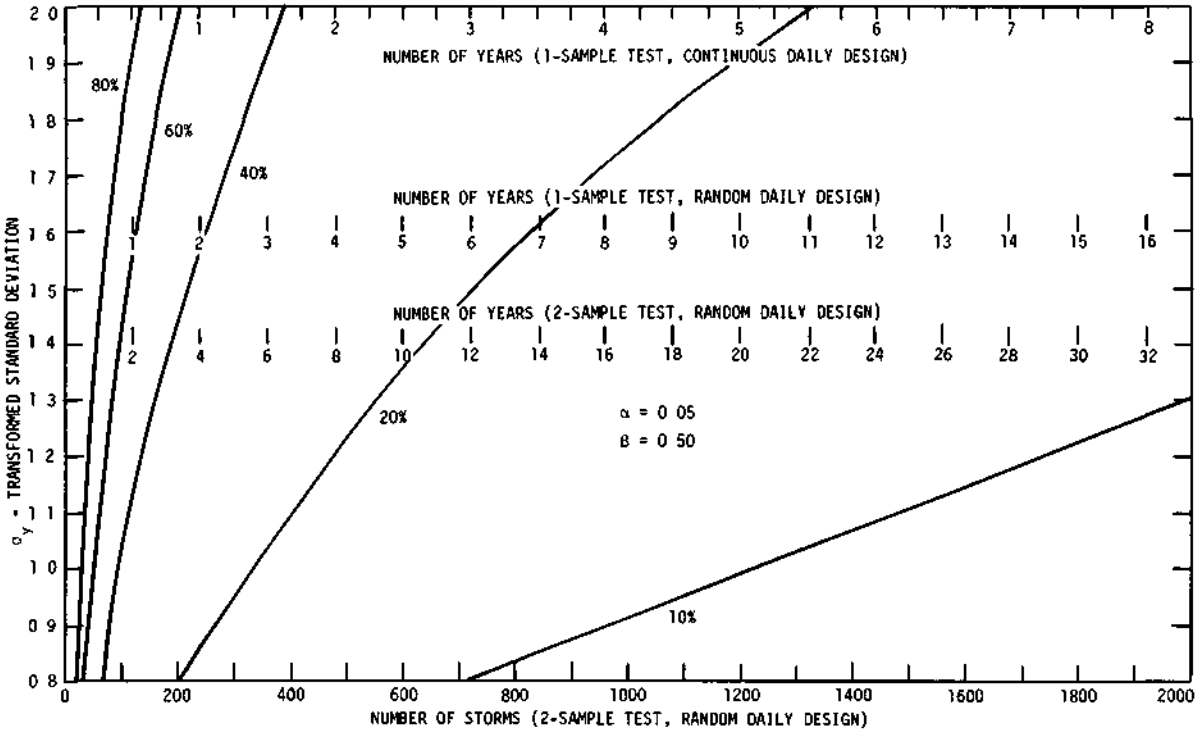

Figure 36. Comparison between the transformed standard deviation and the number of years to obtain significance for various increases vn average rainfall rate on 100 mi^2

Table 29. Comparison of the computed and actual log standard deviations for the 100 mi_2 area.

Min. from start of storm	σ_y (actual)	σ_y (computed)	σ_y (computed) - σ_y (actual)	Percentage difference
1	1.216	1.305	.089	7.28
5	1.558	1.1+19	- .139	8.91
10	1.723	1.521	- .202	11.73
15	1.663	1.474	- .190	11.41
20	1.742	1.424	- .317	18.21
25	1.623	1.373	- .250	15.41
30	1.472	1.361	- .111	7.53
35	1.558	1.379	- .179	11.51
40	1.659	1.444	- .215	12.97
45	1.718	1.463	- .255	14.84
50	1.985	1.809	- .177	8.89
55	1.905	1.629	- .277	14.53
60	2.093	1.714	- .379	18.08
65	1.621	1.509	- .111	6.88
70	1.558	1.530	- .028	1.79
75	1.845	1.583	- .262	14.20
80	1.576	1.321	- .255	16.17
85	1.714	1.355	- .359	20.94
90	1.445	1.335	- .110	7.60
95	1.717	1.714	- .003	.20
100	1.774	1.949	.175	9.86
105	1.550	1.614	.064	4.14
110	1.660	1.494	- .165	9.97
115	1.291	1.144	- .147	11.38
120	.880	.881	.008	.09
125	.937	.905	- .032	3.40
130	1.593	1.419	- .174	10.93

Table 31 lists the number of non-zero amounts required for each minute, as well as ESS for the 100 mi2 area and for a = 0.05, ß = 0.50. The ESS have been divided by 60 (the average number of storms for the warm season, May-September, per year) to obtain the ESS in terms of years rather than storms. From this table it is seen that the number of years required is quite large for increases of 20% or less. For a 20% increase, the minimum ESS is 5.5 years. The maximum ESS for the 20% increase is 26.9 years which represents the number of years required to insure that significance would be obtained for all minutes.

The minimum sample size for the 40%, 60%, and 80% is 1.6, 0.8, and 0.5, respectively. The maximum number for these increases (also the number of years required to insure sufficient sample size for all minutes) is 7.9, 4.0, and 2.6 years, respectively.

Table 30. Probabilities of rain for a specific minute for the various areas and gage 29.

Min. from start of storm	P(X > 0) - Probability of rain for given minute			
	Gage 29	25 mi^2 area	50 mi^2 area	100 mi^2 area
1	—	.207	.310	.724
5	—	.345	.448	.931
10	.172	.586	.724	.966
15	.310	.897	.966	1.000
20	.552	.931	.966	1.000
25	.552	.793	.897	.931
30	.586	.862	.862	.897
35	.483	.724	.862	.862
40	.414	.655	.724	.759
45	.345	.621	.655	.655
50	.345	.586	.690	.793
55	.310	.517	.621	.690
60	.241	.483	.655	.690
65	.138	.517	.621	.690
70	.138	.448	.517	.586
75	.172	.379	.379	.483
80	.241	.345	.448	.483
85	.207	.348	.345	.414
90	.172	.276	.345	.379
95	.172	.276	.379	.379
100	.103	.310	.379	.379
105	.138	.207	.207	.241
110	.172	.207	.207	.276
115	.172	.241	.276	.310
120	.103	.241	.276	.276
125	.069	.241	.241	.276
130	—	.172	.241	.310

Table 31. Sample size required to obtain significance for all increases and for a 1-sample normal test.

100 mi^2 area random design, a = .05, ß = .50

Min. from start of storm	Number of years					
	5%	10%	20%	40%	60%	80%
1	76.9	20.2	5.5	1.6	.8	.5
5	98.2	25.8	7.0	2.1	1.0	.7
10	115.7	30.3	8.3	2.4	1.2	.8
15	104.2	27.3	7.4	2.2	1.1	.7
20	114.2	29.9	8.2	2.4	1.2	.8
25	108.5	27.9	7.6	2.2	1.1	.7
30	91.0	23.8	6.6	1.9	1.0	.6
35	106.0	27.8	7.6	2.2	1.1	.7
40	136.5	35.8	9.8	2.9	1.5	.9
45	169.8	44.4	12.1	3.6	1.8	1.2
50	187.1	49.0	13.4	3.9	2.0	1.3
55	198.1	51.9	14.2	4.2	2.1	1.4
60	239.0	62.7	17.1	5.0	2.6	1.6
65	143.3	37.6	10.2	3.0	1.5	1.0
70	155.9	40.9	11.2	3.3	1.7	1.1
75	265.2	69.5	19.0	5.6	2.8	1.8
80	193.5	50.8	13,9	4.1	2.1	1.4
85	267.2	70.0	19.1	5.6	2.9	1.8
90	207.4	54.4	14.8	4.3	2.2	1.4
95	292.9	76.8	21.0	6.1	3.1	2.0
100	312.5	81.9	22.3	6.8	3.4	2.1
105	375.3	98.4	26.9	7.9	4.0	2.6
110	375.7	98.5	26.9	7.9	4.0	2.6
115	202.4	53.1	14.5	4.2	2.2	1.4
120	105.7	27.7	7.5	2.2	1.1	.7
125	119.8	31.4	8.6	2.5	1.3	.8
130	308.2	80.8	22.1	6.5	3.3	2.1

In Table 32 there is a comparison of ESS for a 20% and 60% increases for all areas and for gage 29. For earlier minutes there is a tendency for the ESS to increase as the size of the area decreases, and a tendency for gage 29 to have larger values. For most other minutes there is little or no trend, with the exception of the later minutes in which there is an indication of a reversal in the previous trend. The reason for these patterns is that the probabilities

of rain for the smaller areas and for gage 29 are smaller than for the 100 mi^2 area (Table 30). For the later minutes, the effect of these probabilities are masked by the tendency for the smaller areas and gage 29 to have smaller log standard deviation values (Table 26). Thus, it cannot be concluded that the smaller areas, and gage 29, require larger ESS values than the larger areas.

Table 32. Sample size required to obtain significance for a 20% and 60% increases and for a 1-sample normal test.

Random Design, a = .05, ß = .50

ESS (effective sample size in years)

Min. from start of storm	20% Increase				60% Increase			
	Gage 29	25 mi^2	50 mi^2	100 mi^2	Gage 29	25 mi^2	50 mi^2	100 mi^2
1	—	7.6	14.5	5.5	—	1.1	2.2	.8
5	—	10.9	10.8	7.0	—	1.7	1.6	1.0
10	17.4	15.1	13.2	8.3	2.6	2.3	1.5	1.2
15	11.4	7.2	7.6	7.4	1.7	1.1	1.1	1.1
20	7.0	9.3	8.1	8.2	1.0	1.4	1.2	1.2
25	6.5	7.8	3.5	7.6	1.0	1.2	.9	1.1
30	9.5	8.4	5.4	6.6	1.4	1.3	.8	1.0
35	7.6	10.0	8.1	7.6	1.1	1.5	1.2	1.1
40	11.6	11.3	9.2	9.8	1.7	1.7	1.4	1.5
45	10.6	10.8	10.2	12.1	1.6	1.6	1.5	1.8
50	14.3	13.2	10.7	13.4	2.1	2.0	1.4	2.0
55	8.1	6.2	10.9	14.2	1.2	.9	1.5	2.1
60	4.9	9.6	16.1	17.1	.7	1.4	2.3	2.6
65	10.1	8.8	10.2	10.2	1.5	1.3	1.4	1.5
70	—	11.3	12.8	11.2	—	1.7	1.9	1.7
75	—	9.5	11.7	19.0	—	1.4	1.4	2.8
80	.3	11.1	12.6	13.9	.1	1.7	1.7	2.1
85	14.2	7.7	9.3	19.1	2.1	1.2	1.2	2.9
90	3.9	7.3	9.6	14.8	.6	1.1	1.3	2.2
95	19.0	12.2	19.0	21.0	2.8	1.8	2.8	3.1
100	7.3	16.7	19.8	22.3	1.1	2.5	3.0	3.4
105	—	8.0	11.9	26.9	—	1.2	1.5	4.0
110	—	3.7	3.9	26.9	—	.5	.7	4.0
115	3.4	11.7	17.7	14.5	.7	1.7	2.4	2.2
120	2.1	9.8	11.1	7.5	.7	1.5	1.7	1.1
125	—	16.6	10.5	8.6	—	2.5	1.4	1.3
130	—	3.8	11.7	22.1	—	.6	1.4	3.3

In Table 33 there is a comparison of ESS with NZS (the non-zero sample size of 1-minute amounts for a specific time) for a 20% increase in the various areas. Here, the effect of $P(X > 0)$ on the ESS is clearly evident. The maximum sample size before making the probability adjustment was 5.6, 8.9, 10.6, and 11.8 for gage 29 and the 25, 50, and 100 mi^2 areas, respectively. After the probability adjustment was made, these maximum values were increased to 19.1, 16.7, 19.8, and 26.9 years, respectively. To insure that one can obtain significance for each minute, the maximum number of years using the probability adjustment would be required.

Table 33. Comparison of NZS with ESS for all areas and for a 1-sample normal test using 20% increase.

Random design, a = .05, g = .50

Min. from start of storm	NZS (years)				ESS (years)			
	Gage 29	25 mi^2	50 mi^2	100 mi^2	Gage 29	25 mi^2	50 mi^2	100 mi^2
1	--	1.6	4.5	4.0	—	7.6	14.5	5.5
5	—	3.8	4.8	6.5	—	10.9	10.8	7.0
10	3.0	8.9	9.5	8.0	17.4	15.1	13.2	8.3
15	3.5	6.5	7.3	7.4	11.4	7.2	7.6	7.4
20	3.9	8.7	7.8	8.2	7.0	9.3	8.1	8.2
25	3.6	6.2	5.9	7.1	6.5	7.8	6.5	7.6
30	5.6	7.3	4.7	5.9	9.5	8.4	5.4	6.6
35	3.7	7.2	7.0	6.5	7.6	10.0	8.1	7.6
40	4.8	7.4	6.6	7.4	11.6	11.3	9.2	9.8
45	3.6	6.7	6.7	7.9	10.6	10.8	10.2	12.1
50	4.9	7.7	7.4	10.6	14.3	13.2	10.7	13.4
55	2.5	3.2	6.7	9.8	8.1	6.2	10.9	14.2
60	1.2	4.6	10.6	11.8	4.9	9.6	16.1	17.1
65	1.4	4.6	6.3	7.1	10.1	8.8	10.2	10.2
70	--	5.0	6.6	6.5	—	11.3	12.8	11.2
75	—	3.6	4.4	9.2	—	9.5	10.7	19.0
80	.1	3.8	5.6	6.7	.3	11.1	12.6	13.9
85	2.9	2.7	3.2	7.9	14.2	7.7	9.3	19.1
90	.7	2.0	3.3	4.6	3.9	7.3	9.6	14.8
95	3.3	3.4	7.2	7.9	19.1	12.2	19.0	21.0
100	.7	5.2	7.5	8.5	7.3	16.7	19.8	22.3
105	--	1.4	2.5	6.5	--	8.0	11.9	26.9
110	--	.7	.8	7.4	~	3.7	3.9	26.9
115	.8	2.8	4.9	4.5	3.4	11.7	17.7	14.5
120	.5	2.4	3.1	2.1	2.1	9.8	11.1	7.5
125	—	4.0	2.5	2.4	—	16.6	10.5	8.6
130	--	.7	2.8	6.8	—	3.8	11.7	22.1

In Table 34 there is a comparison of ESS for a 20% increase and a 20% decrease. On the average, 4.6 more years are required to obtain a 20% increase than a 20% decrease.

Table 34. Comparison of ESS for a 20% increase and 20% decrease for the 100 mi_2 area for 1-sample normal test and random design.

Min. from start of storm	Number of years	
	20% Increase	20% Decrease
1	5.5	3.7
5	7.0	4.7
10	8.3	5.5
15	7.4	5.0
20	8.2	5.5
25	7.6	5.1
30	6.6	4.8
35	7.6	5.1
40	9.8	6.5
45	12.1	8.1
50	13.4	8.9
55	14.2	9.5
60	17.1	11.4
65	10.2	6.9
70	11.2	2.7
75	19.0	12.7
80	13.9	9.3
85	19 .1	13. 8
90	14.8	9.9
95	21.0	14.0
100	22.3	14.9
105	26.9	17.9
110	26.9	18.0
115	14.5	9.7
120	7.5	5.0
125	8.6	5.7
130	22.1	12.2

What happens when other values of the type I error are selected and when more stringent requirements are imposed on the type II error? From Table 35 it is seen that for a 20% increase and for a 8 value of 0.50, the effect of varying *a* from 0.10 to 0.01 is a difference of 11.5 years. At an a value of

0.05, the number of years required to detect a 20% increase varies from 8.2 to 18.7 years as 8 is increased from 0.50 to 0.20. Hence, the degree of accuracy desired by the experimenter is an important factor in the number of years required to conduct an experiment.

Table 35. Comparison of ESS for different type I and type II errors for minute 20 and 100 mi^2 area.

1-sample test, random design

Type I error (a)	Increase	Type II error (ß) 0.50	0.20
0.10	20%	5.0	13.7
	60%	.8	2.1
0.05	20%	8.2	18.7
	60%	1.2	2.8
0.01	20%	16.5	30.6
	60%	2.5	4.6

Table 36 lists the ESS values required to detect a change in rainfall rate to uniformity within certain error bands of 0.25 inch/hour (0.00417 inch/minute). If, in a cloud seeding experiment, the seeder could produce an average uniform rate at the end of each 5-minute period which was 0.25 ± 0.10 inch/hour, it could be detected within 2.1 years. The number would be 2.6 years for a rate of 0.25 ± 0.05 inch/hour and 12.8 years for a rate of 0.25 ± .025 inch/hour. Hence, such a change (seeding model B), although perhaps more difficult to obtain than changes based on seeding model A, might be easier to detect.

Summary and Conclusions

A study was made into the feasibility of using rainfall rate as the experimental unit in a weather modification experiment. To this end, the 1-minute rainfall amounts for every 5 minutes from the start of each storm in the 29-storm sample were grouped together to form frequency distributions. This was done for the 25, 50, and 100 mi^2 areas and for gage 29. This resulted

Table 36. ESS required to detect a change in rainfall rate to a uniform rainfall rate within given error bands of 0.25 inch/hour for the 100 mi^2 area.

1-sample test, random design, a = .05, ß = .50

Min. from start of storm	Number of years		
	.25/in/hr ± .10	.25 in/hr ± .05	.25 in/hr ± .025
1	.02	.02	.02
5	.07	.07	.07
10	.67	.67	.67
15	No change required	No change required	No change required
20	"	.10	.10
25	.72	.72	.72
30	.61	.61	.61
35	2.13	2.13	2.13
40	No change required	No change required	9.05
45	"	"	12.81
50	"	"	11.22
55	"	2.57	2.57
60	1.35	1.35	1.35
65	.17	.17	.17
70	.13	.13	.13
75	.21	.21	.21
80	.18	.18	.18
85	.30	.30	.30
90	.34	.34	.34
95	.59	.59	.59
100	.73	.73	.73
105	1.65	1.65	1.65
110	.66	.66	.66
115	.17	.17	.17
120	.08	.08	.08
125	.09	.09	.09
130	.20	.20	.20

in a "typical" warm season storm for which the frequency distribution was specified for every 5 minutes. The distributions were found to be well fitted by the log-normal and gamma distributions. The log-normal distribution was then used to obtain estimates of the number of storms and years required to obtain significance for various changes in the rainfall rate regime and for three designs and two statistical tests of significance.

The resulting sample sizes certainly leave something to be desired. For a 20% increase and for a = 0.05, ß = 0.50, in the log-normal mean, 27 years are required to obtain significance; for a 60% increase, 4 years are required. To verify a change in the rainfall rate to uniformity within 0.25 *t* 0.05 inch/hour requires 2.6 years; for a rate of 0.25 ± 0.025 inch/hour, 12.8 years are required.

It is possible to reduce these sample sizes somewhat. One way would be to use a continuous seeding design which would reduce the sample size by a factor of 2.0. The use of a larger area would increase the number of storms in the sample which might decrease the sample size, provided there was not a corresponding increase in the log standard deviation. Combining the tests of significance for the different distributions, should reduce the sample size. If the correlation coefficients are large between the rainfall data in two areas which could be used in a crossover design, the sample size could then be decreased by the use of the crossover design. It is also possible that sample sizes based on the gamma distribution might be smaller.

It is concluded that useful information concerning the distribution of rainfall rates can be obtained from this study. However, the rainfall rate does not appear to be an effective unit to use in the verification of weather modification experiments unless one can produce large changes of 60% or greater in the rainfall rate regime.

PART IV

SUMMARY, CONCLUSIONS, AND RECOMMENDATIONS

OVERALL SUMMARY AND CONCLUSIONS

A 1-year research project was carried out to obtain first approximations of the natural space and time properties of rainfall rates in midwestern storms and to evaluate the potential applicability of rainfall rate measurements in the verification of cloud seeding effects. Basic data used in the research were 1-minute rainfall amounts from 50 storms sampled on two dense raingage networks in central Illinois during 1951-1953. Investigation was made of rate characteristics for point rainfall and for areas ranging from 25 to 100 mi_2 under warm season conditions. Within limits permitted by the sample size, the effects of rain type, storm type, and other meteorological parameters upon the space-time distributions of rainfall rate were evaluated. Raingage sampling requirements for the measurement of rate patterns and areal mean rates were investigated also.

Finally, statistical theory and testing procedures were employed to obtain estimates of the experimental sampling requirements for verification of cloud seeding effects when rainfall rate measurements are used as the verification tool. Three experimental designs and two statistical tests were used to define the duration of an experiment to detect various degrees of change in rainfall rate produced by seeding. Results were based upon the assumption that the rainfall rate distributions derived from the available data sample are climatologically representative.

As a first step in the research program, statistical models of the time distribution of storm rainfall were derived to aid in the definition of storm characteristics. It was concluded that application of these models as a verification tool in cloud seeding experiments is not promising at this time because the interference level from natural variability is too great for the detection of modest changes from seeding in a reasonable length of time.

Sequential variability analyses were employed to define further the absolute and relative time variability in warm season storms. Because of the large interstorm variability, it was concluded that sequential variability measurements would only be useful as a verification tool in those seeding experiments aimed at substantially changing the time distribution properties of

natural rainfall. Furthermore, the optimum use would be with experiments on relatively large target areas because of the observed property for the sequential variability to decrease with increasing sampling area.

Lag correlation analyses of 1-minute rainfall rates at a point and over an area of 100 mi^2 did not reveal the presence of any regular oscillations in the time distribution of rates. Consequently, it was concluded that these distributions could serve as one of several verification tools if periodic seeding techniques in relatively large storm systems were employed.

An investigation of the percentage distribution of storm rainfall showed that a major portion of the total storm rainfall tends to occur in a small percentage of the storm time in convective storms. This analysis suggests that substantial surface increases in rainfall from cloud seeding would occur if the treatment modestly increased the rainfall intensity during the major rain-producing period of convective storms, but the desirability of this is doubtful in naturally intense storms, otherwise, seeding success must depend upon large percentage increases in the light rates that prevail during a large portion of most storms, or upon substantial extension of the duration of the heavy intensity period.

Spatial correlation analyses revealed a rapid decay in correlation of rates with increasing distance from the point of rate measurement, and no significant improvement in correlation was achieved when 5-minute and 10-minute rates were used instead of 1-minute rates. At a distance of 1 mile from the point of rate measurement, the average correlation coefficient has decreased to 0.7, thereby explaining only 50% of the variance. Therefore, it was concluded that raingage networks with sampling densities adequate to define accurately instantaneous rainfall rate patterns for use in weather modification experiments may be beyond operational and/or economic feasibility.

Area-depth analyses were employed in defining spatial distribution characteristics. As expected, substantial variability was found in the area-depth relations from minute-to-minute within storms and between storms of similar type. With respect to application in weather modification, it can only be said that the area-depth curve is one of several useful tools that could be employed in the verification of seeding experiments. Because of the great space-time variability in natural rainfall, it is extremely doubtful that any single

precipitation parameter or measurement will uniquely define seeding effects. The area-depth curve can help answer questions regarding changes that seeding may be producing in the time distribution, tendencies for seeding to intensify or decrease rainfall gradients in treated storms, and changes in skewness of the areal distribution resulting from seeding.

In some cases, interest might be primarily in average rates over an area from minute-to-minute. Investigation of sampling errors in the measurement of storm mean rates on the 100 mi^2 network indicate that extremely dense networks would be needed to achieve the high degree of accuracy necessary to identify small percentage increases from seeding. If rainfall rate is to serve as a verification tool in weather modification, it appears more logical to turn to a combination of raingages and 10-cm radar to evaluate short-period rate properties and their changes in space and time in warm season storms.

Statistical tests of three seeding experimental designs were made. These have been used in the past and may likely be employed in the future. The designs include (1) randomization of storms over a single target area into seeded and non-seeded storms with the non-seeded storms being the control, (2) random choice of storms to be seeded over a single target area with the historical record as the control, and (3) continuous seeding on all potential storm days with the historical record being the control. The normal 1-sample and 2-sample tests were performed for log normal distributions of the data.

Results of these statistical tests, based on the average of the rainfall rates at a given minute within the storm, indicate sampling requirements that may not be acceptable operationally. For example, if seeding is producing a 20% increase in rainfall rate, there is a 50% probability that this increase will not be proven at the 95% confidence level after 27 warm seasons of seeding under design (2) described above. However, this reduces to 4 warm seasons for a 60% increase under the above specifications.

In general, it was concluded that rainfall rate, by itself, does not appear to be a very effective meteorological parameter for the verification of seeding experiments unless changes of 60% or greater can be produced in the rainfall rate regime. However, used in conjunction with other rainfall parameters, it could probably aid in solving some of the verification problems.

RECOMMENDATIONS

Despite the problems brought out in this report, time and space parameters of rainfall rate could be among the useful verification tools, provided cloud seeding causes pronounced changes in the intensity characteristics. If seeding produces a less intense, more uniform space-time distribution, the rate measurements would be very useful. Such changes have been suggested in the literature in the past. Furthermore, analyses of drop size distributions in seeded and unseeded rainstorms in the Flagstaff area by Jones (1969) indicate distinct differences in raindrop concentrations and maximum drop sizes between the two storm types.

Before the use of rainfall rate as a verification tool can be properly evaluated, more knowledge must be obtained with regard to rate changes produced by seeding. Therefore, as a first step in this direction, it is recommended that consideration be given to analyses of rainfall rate distributions from recording raingage data collected in conjunction with the Project Whitetop experiments in the 1960-1964 period.

Analyses of the rainfall rate data from daily recording raingage charts within and outside the downwind plume on operational days should provide considerable information on the magnitude of the seeding effects on rainfall rate. The daily charts can provide average 10-minute rates which should reveal any pronounced changes from seeding.

As a result of this 1-year study, it is not considered desirable at this time to extend the present studies to the 400 mi^2 network in east central Illinois for which additional 1-minute rate data could be processed from existing chart records. It is believed that only relatively small gains in seeding verification with rainfall rates would be achieved with statistical testing over the larger area.

If rainfall rate measurements are found to be desirable in seeding verification tests in the future, a combination of 10-cm radar and raingages should be employed to define more accurately the space-time patterns of instantaneous rates.

REFERENCES

Battan, Louis J., 1966 Silver-iodide seeding and rainfall from convective clouds. Journal of Applied Meteorology, 5, 669-683.

Braham, R. R., Jr., 1966: Final report of Project Whitetop, a convective cloud randomized seeding project. Part 1, Department of the Geophysical Sciences, University of Chicago, 156 pp.

Conrad, V., and L. W. Pollak, 1950 Methods in Climatology. Harvard University Press, 54-55.

Davies, Owen L., 1954: The Design and Analysis of Industrial Experiments. First edition, Hafner Publishing Company, New York, 636 pp.

Dennis, A. S., and D. F. Kriege, 1966: Results of ten years of cloud seeding in Santa Clara County, California. Journal of Applied Meteorology, 5, 684-691.

Huff, F. A., 1967: Time distribution of rainfall in heavy storms. Water Resources Research, 3(4), 1007-1019.

Huff, F. A., 1968. Area-depth curves — a useful tool in weather modification experiments. Journal of Applied Meteorology, 7(5), 940-943.

Huff, F. A., 1969: Climatological assessment of natural precipitation characteristics for use in weather modification. Journal of Applied Meteorology, 8(3).

Huff, F. A., and J. C. Neill, 1957 Rainfall relations on small areas in Illinois. Illinois State Water Survey Bulletin 44, Urbana, 61 pp.

Jones, Douglas M. A., 1969: Raindrop distributions near Flagstaff, Arizona. Final Report, U. S. Army Grant, DA-AR0-D-124-G-937, Illinois State Water Survey, Urbana, 50 pp.

Liffiefors, H. W., 1967 On the Kolmogorov-Smirnov test for normality with mean and variance unknown. Journal of the American Statistical Association, 399-402.

Schickedanz, P. T., 1967: A Monte Carlo method for estimating the error variance and power of the test for a proposed cloud seeding experiment. Unpublished Ph.D Thesis, University of Missouri, Columbia, June 1967, 113 pp. Available from University Microfilms, Ann Arbor, Michigan.

Schickedanz, P. T., S. A. Changnon, and C. G. Lonnquist, 1969: A statistical methodology for the planning and evaluation of hail suppression experiments in Illinois. Part II, Final Report on Hail Evaluation Techniques for the National Science Foundation, NSF GA-482.

Smith, E. J., E. E. Adderley, and F. D. Bethwaite, 1965: A cloud seeding experiment in New England, Australia. Journal of Applied Meteorology, 4, 433-441.

Thorn, H. C. S., 1958 A note on the gamma distribution. Monthly Weather Review, 86, 117-122.